

# eScholarship@UMassChan

## The Effect Cognate Antigen Has on T Cells Responding to Influenza Infection

Item Type	Doctoral Dissertation
Authors	Jones, Michael C.
DOI	<a href="https://doi.org/10.13028/2gnb-3h96">10.13028/2gnb-3h96</a>
Publisher	UMass Chan Medical School
Rights	Licensed under a Creative Commons license
Download date	2026-06-13 16:03:52
Item License	<a href="http://creativecommons.org/licenses/by/4.0/">http://creativecommons.org/licenses/by/4.0/</a>
Link to Item	<a href="https://hdl.handle.net/20.500.14038/32407">https://hdl.handle.net/20.500.14038/32407</a>

**THE EFFECT COGNATE ANTIGEN HAS ON T CELLS RESPONDING TO  
INFLUENZA INFECTION**

A Dissertation Presented

By

MICHAEL CHRISTOPHER JONES

Submitted to the Faculty of the  
Morningside Graduate School of Biomedical Sciences at UMass Chan Medical School in  
partial fulfillment of the requirements for the degree of

DOCTOR OF PHILOSOPHY

JUNE 3, 2022

IMMUNOLOGY AND MICROBIOLOGY

**THE EFFECT COGNATE ANTIGEN HAS ON T CELLS RESPONDING TO  
INFLUENZA INFECTION**

A Dissertation Presented By

MICHAEL CHRISTOPHER JONES

This work was undertaken in the Morningside Graduate School of Biomedical Sciences

Immunology and Microbiology Program

Under the mentorship of

Susan L. Swain, Ph.D., Thesis Advisor

The signatures of the Dissertation Defense Committee signify completion and approval  
as to style and content of the Dissertation

John E. Harris, M.D., Ph.D., Member of Committee

Jeremy Luban, M.D., Member of Committee

Lawrence J. Stern, Ph.D., Member of Committee

Matthew A. Williams, Ph.D., External Member of Committee

The signature of the Chair of the Committee signifies that the written dissertation meets  
the requirements of the Dissertation Committee

Samuel M. Behar, M.D., Ph.D.

The signature of the Dean of the Morningside Graduate School of Biomedical Sciences  
signifies that the student has met all graduation requirements of the School.

Mary Ellen Lane, Ph.D.

June 3, 2022

## ACKNOWLEDGMENTS

I would like to extend a heartfelt thank you to Dr. Susan Swain for taking me on as a student in her laboratory and for mentoring me throughout my graduate training. Suzy is a kind, thoughtful and passionate scientist who lifts all those around her. Suzy your dedication to your craft and enthusiasm for your work has inspired me throughout the years. It has been an honor and a pleasure working with you. Thank you for encouraging and mentoring me along the way, I greatly appreciate it!

I also would like to thank the members of my thesis research advisory committee Dr. Samuel Behar, Dr. John Harris, and Dr. Lawrence Stern for their guidance and support throughout my graduate training. Additionally, I would like to thank Dr. Jeremy Luban and Dr. Matthew Williams for serving on my dissertation examination committee. I appreciate your time and insights throughout this process.

The Swain lab has been like family over the years. Dr. Richard Dutton brought wonderful thoughts and perspective to lab meetings when I first joined the lab. Former lab members Dr. Esteban Rozen and Dr. Jingya Xia helped me find my footing when I joined the lab. Dr. Bianca Bautista and Dr. Allen Vong were encouraging senior graduate students who helped me learn experimental techniques and how to properly present data. Mike Perkins and Jialing Liang helped me perform several large memory experiments and kept our mouse colony in order. Catherine Castonguay is an invaluable member of the lab, wearing all the hats and keeping the lab up and running. Cate thank you for all the experimental help over the years, these large memory experiments would not have been feasible without your assistance. Olivia Kugler-Umana taught me how to be a better

scientific writer. As the two current graduate students in the lab, Olivia and I would often share in the ups and downs of graduate school. Olivia thank you for being a wonderfully positive person, for teaching me patience and kindness and picking me up when I was down. I will miss your laughter from one bay over! Dr. Priya Devarajan thank you for being my sounding board over the years. I love discussing science with you, your excitement and enthusiasm for not just your own work but the work of others is infectious. Thank you for encouraging me over the years, for helping me plan and design experiments and analyze and interpret the results. You all made the day-to-day of working in lab a wonderful experience, thank you!

I would like to thank my family for their unconditional love and support. To my parents, Lizzy and Mike, thank you for always believing in me, for pushing me to be my best self, for always having my back and for teaching and showing me the value of hard work. To my brothers Zach, Sam and Matt, thank you for always making me laugh and reminding me to not take myself too seriously. To Lily our grumpy English bulldog, thank you for the endless snuggles and kisses. To my wonderful partner Maura, thank you for being there for me through the ups and downs over the past two years. Mo your compassion and fierce nature have kept me going, thank you for encouraging me and having my back.

## ABSTRACT

The contributions of peptide antigen affinity for TCR in driving T cell memory is unclear. Effector CD4 T cells must recognize cognate antigen again at an effector checkpoint, 5-8 days post-infection, to generate an optimal memory population. In this thesis, we examined whether peptide affinity for the TCR of effectors impacts the extent of memory and degree of protection against rechallenge. We used an influenza A virus (IAV) nucleoprotein (NP)-specific TCR transgenic strain, FluNP, and generated NP-peptide variants that bind FluNP TCR with a broad range of avidity. Varying peptide avidity *in vivo* at the effector checkpoint revealed that higher affinity interactions yielded greater numbers of FluNP memory cells in the spleen and most dramatically in the lung and dLN. The major impact of avidity was on memory cell number, not cytokine production, and was already apparent within several days of transfer. These memory cells demonstrated enhanced protection against lethal IAV infection with a robust early day 5 secondary effector response in the lung. We previously showed that autocrine IL-2 production during the effector checkpoint prevented default effector apoptosis and supported memory formation. Here, peptide avidity determined the level of IL-2 produced by effectors while IL-2R expression was unaffected. However, IL-2R $\alpha$  expression by APC drove more memory cell formation, suggesting that transpresentation of IL-2 by APC at this checkpoint enhanced CD4 memory generation. Secondary memory generation was also avidity-dependent. We propose this pathway selects CD4 effectors of highest affinity to progress to memory and can instruct future vaccine design.

## Table of Contents

Acknowledgements .....	iii
Abstract .....	v
Table of Contents .....	vi
List of Figures .....	ix
List of Third Party Copyrighted Material .....	xii
Preface .....	xiii
<b>CHAPTER I: Introduction .....</b>	<b>1</b>
Overview .....	1
Influenza Viruses .....	1
A. Overview .....	1
B. Structure and Genome .....	2
C. Infection and Spread .....	3
D. Disease .....	6
Influenza Vaccination .....	7
A. Overview .....	7
B. Split or Whole Inactivated Virus .....	8
C. Protein Subunit Vaccination .....	10
D. Live Attenuated Immunization .....	10
E. Adjuvants .....	12
F. New Technologies .....	12
Immune Response to Influenza	
A. Innate and Adaptive Immunity to Influenza .....	13
B. T cell responses to Influenza .....	16
C. T Cell Memory Subsets .....	23
D. Factors that Influence T Cell Memory .....	24
Cognate Antigen Impact on Memory	
A. Impact on Effector Differentiation .....	26
B. Impact on Memory Formation and Recall Responses .....	28
<b>CHAPTER II: Materials and Methods .....</b>	<b>33</b>
Mice .....	33
Virus Stocks and Infections .....	34

NP Peptide Generation .....	34
BMDC Generation and Peptide/APC Preparation .....	35
Splenic APC Preparation and <i>In Vitro</i> Culture .....	35
Sequential Transfer Model .....	36
<i>In Vitro</i> Culture of Naïve and 6 dpi effector FluNP CD4 T cells .....	37
ELISA .....	37
Quantitative PCR (qPCR) .....	37
Flow Cytometry and Cytokine Staining .....	38
Statistical Analysis .....	39
<b>Chapter III: Peptide Avidity for TCR on CD4 and CD8 Effectors Determines the Extent of Memory Generation .....</b>	<b>40</b>
Introduction .....	40
Validation of the CD4 FluNP TCR transgenic system .....	42
Establishment of NP peptide binding frame and affinity of NP peptides for I-A <sup>b</sup> .....	52
NP peptide affinity and biological avidity for FluNP TCR .....	55
Peptide avidity at the effector phase determines the number of memory cells .....	58
Phenotype of day 21 memory FluNP cells .....	69
Immediate cytokine production from spleen day 21 memory FluNP cells .....	79
Survival & proliferation analysis of NP peptide stimulated FluNP effectors .....	82
Peptide avidity at the effector checkpoint acts by inducing more effector IL-2 ...	91
CD25 expression on APC during the effector phase promotes effector transition to memory .....	105
Peptide avidity at the effector checkpoint determines protection to influenza challenge .....	115

Increased peptide avidity at the effector checkpoint generates memory cells that respond more rapidly to IAV infection in the lung .....	115
Ag recognition by secondary effectors is required for memory generation and peptide avidity determines the size of response .....	124
Effector checkpoint Ag recognition and dose influences effector CD8 T cell memory .....	127
<b>CHAPTER IV: Discussion .....</b>	<b>134</b>
Overview .....	134
The summation of all cognate antigen signals throughout the life of a T cell .....	135
Additional potential roles of effector checkpoint cognate Ag .....	141
IL-2 as a master regulator of effector T cell survival .....	144
Implications for vaccine design .....	149
<b>CHAPTER V: References .....</b>	<b>152</b>

## List of Figures

Figure 1.1. Lung T cell kinetics in response to IAV infection .....	18
Figure 3.1. Lung kinetics of donor FluNP & host CD4 CD44 cells in response to IAV ..	43
Figure 3.2. Secondary lymphoid organ kinetics of donor FluNP in response to IAV .....	45
Figure 3.3. Day 8 lung donor FluNP and host CD4, CD44hi effector phenotype and function .....	48
Figure 3.4. Day 8 spleen donor FluNP and host CD4, CD44hi effector phenotype and function .....	50
Figure 3.5. Day 21 donor FluNP & host CD4, CD44hi spleen, dLN & lung memory subsets: tissue resident memory ( $T_{RM}$ ), effector memory ( $T_{EM}$ ) and central memory ( $T_{CM}$ ) .....	53
Figure 3.6. NP peptide binding affinity for I-A <sup>b</sup> and FluNP TCR .....	56
Figure 3.7. Functional avidity of NP peptides measured by naïve FluNP activation .....	59
Figure 3.8. Comparison of day 21 FluNP memory cell numbers generated from IAV and high avidity Ag/APC .....	62
Figure 3.9. Peptide avidity during the primary effector phase dictates the size of the memory population .....	65
Figure 3.10. Impact of peptide avidity on fold-change of memory FluNP cell number (Day 21) .....	67
Figure 3.11. CD127 expression of memory FluNP from spleen, dLN & lung (Day 21) ..	70
Figure 3.12. Memory subset characterization of memory FluNP in spleen and dLN $T_{CM}$ and $T_{EM}$ , Lung $T_{RM}$ (Day 21) .....	73
Figure 3.13. CXCR3 expression by memory FluNP in spleen, dLN and lung (Day 21) ..	77
Figure 3.14. Cytokine expression by memory FluNP in spleen (Day 21) .....	80
Figure 3.15. Peptide avidity has no influence on <i>in vivo</i> spleen effector FluNP cell number, CD25 expression, survival or proliferation 2 dpt .....	83
Figure 3.16. Peptide avidity has no impact on donor FluNP proliferation 3 days post transfer .....	86

Figure 3.17. Peptide avidity determines donor FluNP survival 3 days post transfer .....	89
Figure 3.18. Peptide avidity increases donor FluNP cell recovery 3 dpt and reflects cell survival pattern .....	92
Figure 3.19. qPCR phenotype of effector FluNP cells stimulated by different NP peptides on APC after 2d <i>in vitro</i> .....	95
Figure 3.20. Increased peptide avidity results in greater expression of transcription factors on effector FluNP cells after 2d <i>in vitro</i> .....	98
Figure 3.21. IL-2 receptor subunit expression on 6d and 3 dpt FluNP effectors .....	101
Figure 3.22. Increased peptide avidity results in more day 6 effector FluNP cytokine expression and production .....	103
Figure 3.23. Several APC subsets express CD25 4-8 days post IAV infection .....	106
Figure 3.24. Comparison of WT and CD25KO BMDC following activation .....	109
Figure 3.25. WT and CD25KO BMDC both effectively stimulate 6d FluNP effector cytokine production .....	111
Figure 3.26. CD25 expression on APC induces more effectors to become memory .....	113
Figure 3.27. Increased peptide avidity at the effector checkpoint promotes a more protective population of memory cells .....	116
Figure 3.28. Peptide avidity at the effector checkpoint increases the secondary effector FluNP response in the lung (Day 5) .....	119
Figure 3.29. Peptide avidity at the effector checkpoint enhances cytokine production from secondary effector FluNP in the spleen (Day 8) .....	122
Figure 3.30. Peptide avidity during the secondary effector checkpoint regulates the size of the secondary memory population .....	125
Figure 3.31. Cognate antigen during the effector checkpoint regulates the size of the memory CD8 population .....	128
Figure 3.32. Culture of 6d OT-I effectors reveals Ag dose and IL-2 increase IFN $\gamma$ production and decreases KLRG1 expression <i>in vitro</i> .....	131

Figure 4.1. A model illustrating how effector checkpoint cognate Ag improves effector CD4 T cell survival by a novel autocrine IL-2 signaling mechanism ..... 147

## LIST OF THIRD PARTY COPYRIGHTED MATERIAL

The following figure was reproduced from journals: no permission required.

Figure Number	Publisher
Figure 1.1	Swain, S. L., Dutton, R. W., & Woodland, D. L. (2004). T Cell Responses to Influenza Virus Infection: Effector and Memory Cells. <i>Viral Immunology</i> , 17(2), 197–209. Distributed under the terms of the Creative Commons Attribution license. ( <a href="http://creativecommons.org/licenses/by/4.0/">http://creativecommons.org/licenses/by/4.0/</a> )

## PREFACE

This dissertation is submitted to fulfill the requirement for a degree of Doctor of Philosophy at the University of Massachusetts Chan Medical School. This dissertation represents original work that I conducted under the supervision of Dr. Susan L. Swain. Parts of the introduction, results and discussion chapters, both text and figures, have been taken from the following manuscript available at [biorxiv.org](https://www.biorxiv.org) and submitted to The Journal of Immunology:

Jones, M. C., C. Castonguay, P. P. Nanaware, G. C. Weaver, B. Stadinski, O. A. Kugler-Umana, E. Huseby, L. J. Stern, P. Devarajan, and S. L. Swain. 2022. Peptide Avidity for TCR on CD4 Effectors Determines the Extent of Memory Generation. *bioRxiv*: 2022.2005.2009.491158.

Figure 3.6 was conducted in collaboration with Dr. Lawrence J. Stern's laboratory. Dr. Padma P. Nanaware performed the I-A<sup>b</sup> binding experiments and Grant C. Weaver performed the TCR affinity experiments.

Dr. Priyadharshini Devarajan and Dr. Susan L. Swain helped to edit this dissertation.

## **CHAPTER I: Introduction**

### **Overview**

As we continue to feel the negative impacts caused by a global pandemic resulting from a rapidly mutating single-stranded RNA respiratory virus, SARS-CoV-2, we are reminded of the crucial importance of T cell memory, which recognizes mostly conserved viral epitopes and hence provides broader, heterologous immunity compared to antibody. Effector and memory CD4 T cells are a crucial element to protecting against infection. During the effector phase of the immune response, effector CD4 T cells provide help to germinal center B cells (GCB) to promote a robust antibody (Ab) response and drive somatic mutation and selection of high affinity antibody-secreting B cells (AbSC) (1), as well as provide help to CD8 T cells during influenza A virus (IAV) infection to promote CD8 T cell resident memory ( $T_{RM}$ ) (2-4). After viral clearance, a cohort of CD4 effectors become memory CD4 T cells which mediate protection by multiple mechanisms that act alone or in synergy with B and CD8 T cells, against lethal infection (5-7). However, signals required for the transition of CD4 effectors to memory cells are not yet well-defined. Therefore, it is critical we identify the signals required to support an optimal transition of CD4 effectors to memory cells. Understanding these signals and processes will provide essential insights into effective future vaccine strategies that will benefit society for the rest of time.

### **Influenza Viruses**

#### **A. Overview**

Influenza viruses belong to the *Orthomyxoviridae* family of viruses. There are four genus of influenza virus, classified as influenza A virus (IAV), influenza B virus (IBV), influenza C virus (ICV) and influenza D virus (IDV) (8). All four can infect people, however IAV and IBV are the predominant influenza viruses that cause disease in humans. Both IAV and IBV have eight RNA segments, while ICV and IDV have only seven (8). IAV is known to infect waterfowl and mammals, IBV primarily infects humans but has been isolated from other mammals, ICV primarily infects children, but can also infect pigs, and IDV primarily infects cattle and pigs, although some cattle workers have recorded antibodies against the virus (8-10). In public health, IAV and IBV are of the greatest concern because these species mutate rapidly and can cause severe disease in people, while ICV and IDV pose less mutation risk and result in mild infections.

IAV classifications exist because of different variations of viral proteins, hemagglutinin (HA) and neuraminidase (NA), expressed on the surface of the virion. There are 18 HA subtypes (H1-18) and 11 NA subtypes (N1-11), however the predominant strains in humans are H1N1 and H3N2. Typical nomenclature for influenza viruses include the type (A, B, C, D) and if A include parenthetical H#N#, followed by the host if not humans, the location of isolation, the isolate number, and the year of isolation, i.e. B/Victoria/2/1987, as per World Health Organization guidelines (11).

## **B. Structure and Genome**

The influenza viruses are anti-sense, single stranded RNA, enveloped viruses made up of either eight (IAV, IBV) or seven (ICV, IDV) gene segments. IAV and IBV gene segments include HA, NA, NP, NS, PA, PB1, PB2 and M. The hemagglutinin (HA) gene

segment encodes the HA glycoprotein trimer expressed on the surface of the virion which enables viral entry into host cells and the neuraminidase (NA) segment encodes the tetrameric surface glycoprotein NA which enables viral exit from the host cell. The influenza RNA polymerase complex is comprised of proteins generated from the PB1, PB2 and PA gene segments (8). Nucleoprotein (NP) interacts with the gene segments inside the virion to protect the viral RNA from degradation. The viral ribonucleoprotein (vRNP) complex consists of one influenza RNA gene segment coated with numerous NP proteins and loaded with the polymerase complex (protein) ready for immediate transcription following infection. NP may also serve a back-up role in targeting the vRNP to the nucleus, as NP contains two nuclear homing sequences (NLS). The non-structural protein NS1 and the nuclear export protein (NEP) is encoded by the NS gene segment. The NS1 protein acts to dampen the host cell innate immune response and the NEP results from an NS splice variant and assists the vRNP in leaving the host cell nucleus following replication. The M gene segment encodes for two proteins, M1 and M2. M1 is the surface envelope matrix 1 protein which acts as the scaffold to the host-derived lipid envelope. The ion channel matrix (M2) protein is the least abundant per virion at about a 16-20 count and spans the viral envelope. The viral envelope itself is comprised of a lipid bilayer stolen from host cells and contains HA and NA on its surface while M2 acts as a trans-membrane protein.

### **C. Infection and Spread**

Influenza virus enters a new host through the respiratory tract following contact with infectious aerosols or any inhaled viral particles. The HA binds to sialic acid on host cell receptors. Many host cells express membrane-bound glycoproteins with sialic acid at

the terminal ends. Different host organisms display different versions of these sialic acid molecules and the IAVs that infect these organisms utilize different HA molecules to take advantage of these interactions. Humans have an abundance of  $\alpha(2,6)$  sialic acid while waterfowl have a greater abundance of  $\alpha(2,3)$  sialic acid (12, 13). IAVs that have evolved to infect humans contain HAs with greater affinity for  $\alpha(2,6)$  sialic acid, while IAVs that predominately infect birds have HAs that bind well to  $\alpha(2,3)$  sialic acid. Interestingly, pigs express both  $\alpha(2,6)$  and  $\alpha(2,3)$  sialic acid which makes them a great host to propagate pandemic or endemic IAV strains (13).

Influenza viruses predominately infect and replicate in lung epithelial cells (14, 15). Once HA binds to sialic acid on the host cell, the viral particle gets taken up by the host cell through endocytosis. As the endosome becomes more acidic (pH 5-6), the virus uses this to its advantage. The acidic environment induces a few key conformational changes in influenza proteins that allow for release of vRNPs into the host cell cytoplasm. Influenza HA has two key forms, a precursor HA0, and a cleaved form HA1 and HA2 linked by disulfide bonds. Cleavage of the HA0 precursor is thought to occur extracellularly, or on exit from infected host cells at the cell membrane and will be discussed below. The acidic environment of the endosome causes a conformational change in HA2 which exposes the fusion peptide without disrupting the sialic acid binding domain of HA1. The now exposed fusion peptide of HA2 inserts into the host endosomal membrane and brings the viral membrane and host endosomal membrane into contact. The acidic conditions of the endosome results in a conformational change in the M2 ion channel that opens this channel and allows for the acidification of the viral particle itself. This in turn releases the vRNP

bound to M1 and allows the vRNP to move freely. As multiple HAs form a bridge between the viral and host membrane a pore is opened into the host cell cytoplasm. The now free vRNPs move through the pore and into the host cell cytoplasm.

Once inside the host cell the next phase of the influenza life cycle involves transcription, the process by which more viral proteins are built, and replication, the process by which new viral gene segments are generated. However, both processes cannot happen until the vRNPs gain access to the host cell nucleus. The vRNP is too large to passively enter the host cell nucleus through the nuclear pore complex and instead utilize protein mediated active transport (16). All four viral proteins associated with the viral RNA segments (NP, PB1, PB2 & PA) contain nuclear localization signals (NLS) which target the vRNP for active transport into the nucleus (17-20).

Influenza has developed several sophisticated tricks to take advantage of host cell machinery, none more ingenious than “cap snatching.” Host cell mRNA contain a 3’ poly(A) tail and a 5’ methylated cap, while the vRNPs have a poly(A) tail but no 5’ cap. In order to initiate transcription of the viral RNA, the viral RNA polymerase complex associates with host cell RNA Pol II and steals the 5’ cap from nascent host mRNA strands to initiate transcription of the viral genome (21, 22). The PA subunit loads viral RNA into the active site of PB1 and PB2 and transcription is terminated by polyadenylation. Viral mRNAs exit the host cell nucleus and hijack host cell machinery for translation into protein while inhibiting host protein synthesis (23).

Viral replication requires an intermediate positive sense RNA strand and more vRNP-associated proteins NP, PA, PB1 and PB2. Following translation, these vRNP-

associated proteins traffic back to the nucleus to facilitate replication. The viral RNA polymerase complex initiates the generation of a positive sense complementary RNA strand from which the new negative sense RNA of the vRNP complex is synthesized. The nuclear export protein (NEP) allows for the active transport of newly synthesized vRNPs out of the nucleus and into the cytoplasm.

Once translated in the cytoplasm, HA and NA traffic to and insert into the host cell membrane. This is when extracellular proteases cleave the HA0 precursor into the HA1 and HA2 subunits. The M1 protein then attaches to the cytoplasmic tails of the HA and NA proteins and are loaded with newly synthesized vRNPs exported from the nucleus. Recruitment and insertion of M2 into the lipid bilayer is required for forming the spherical shape of new viral particles and for release of these new virions from the host cell membrane.

#### **D. Disease**

An accurate assessment of the global influenza disease burden is difficult to calculate due in part to a lack of systematic laboratory influenza virus diagnostic testing and the dramatic variation in circulating strains from year to year. Looking at the 1999-2015 period, an estimated 300,000-645,000 people were killed each year as a result of influenza infection (24). From 2010-2020 the United States experienced 9-45 million influenza infections per year which resulted in 4-21 million medical visits each season and an estimated death toll of 12,000-61,000 per year (25). In the United States, seasonal influenza costs the healthcare system approximately \$3.2 billion dollars each season and the total economic impact is estimated at slightly over \$11 billion dollars per year (26).

However, since the start of the coronavirus pandemic, seasonal influenza infections and related deaths have plummeted. The 2020-2021 flu season saw the fewest recorded influenza infections in the USA since data collection began in 1977 (27). This short-term influenza relief may fade as physical measures such as masking and social distancing fall out of favor. An additional headwind is that the historically low influenza infection rate makes it very difficult for the WHO to get a sense of the predominant strains in circulation, which are crucial for seasonal vaccine formulation, as discussed below.

## **Influenza Vaccination**

### **A. Overview**

In 1918 an H1N1 influenza pandemic killed an estimated 50-100 million people across the globe, one of the deadliest global events in all of human history (28). On the heels of this global catastrophe, the scientific community rallied together to study this disease, and in 1933 the first influenza virus was isolated from patients and propagated in ferrets (29). In 1937, the first influenza vaccination strategy was developed in Soviet Russia, by passaging influenza virus isolated from patients through ferrets and mice to generate a less virulent live attenuated vaccine (30). Patients inhaled this live attenuated influenza through the nose, and only 20% of subjects developed mild symptoms, allowing the authors to declare this immunization “well-tolerated” (30). Since that time, researchers have developed different vaccination strategies to reduce the incidence of adverse events in patients, while promoting satisfactory protection against lethal infection. A major challenge to influenza vaccine development is the high mutation rate of the virus, with influenza A strains developing  $1-8 \times 10^{-3}$  mutations per site per year (31, 32) while influenza

B strains demonstrate a lower mutation rate of about  $0.5 \times 10^{-3}$  mutations per site per year (32). Influenza viruses have such a high mutation rate because influenza RNA polymerase lacks any proofreading mechanism (33). Mutations that occur in HA and NA genes may result in the loss of epitopes on these viral surface proteins that are recognized by existing antibodies, and these mutations are classified as antigenic drift (33). Furthermore, antigenic shift can occur when a host becomes infected with two or more influenza viruses at the same time and viral genetic material reassorts, generating a new virus with random gene segments from the two initial viruses (33, 34). Wild migratory aquatic birds are generally accepted as the predominant host these endemic influenza strains originate from (35), although there are instances of new strains developing in mammals, most recently the 2009 H1N1 “swine flu” (36), so preventing new viruses from arising is not feasible. Since influenza viruses have such a high mutation rate, coupled with the ability to generate novel strains through antigenic shift, it is quite challenging to foster life-long influenza immunity in people. From a probabilistic perspective, vaccines that elicit the widest immune response to surface and internal influenza antigens provide the greatest chance to protect people from severe disease year after year.

### **B. Split or Whole Inactivated Virus**

When you receive your influenza vaccine one of the questions asked every year is “do you have an egg allergy?” This is because historically the inactivated influenza vaccine was prepared from virus grown in chicken eggs. Inactivated influenza vaccines (IIV) have been widely utilized since the 1940s. During the Southern Hemisphere’s flu season, the World Health Organization (WHO) typically selects three or four of the most prominent

circulating influenza strains to include in the influenza vaccine for the upcoming Northern Hemisphere flu season. These typically include two or three influenza A virus strains and one influenza B virus strain. These influenza virus strains are grown in fertilized chicken eggs, harvested, and killed by some mechanism or other (37). For whole inactivated virus vaccines, once the virus is grown and isolated from the eggs, the process moves straight to inactivation. However, split vaccines require another step of isolating the surface HA and NA viral antigens as well as pieces of internal M1 and NP proteins. The isolated whole virion is “split” using a solution with tween and either Triton X100 or di-ethyl-ether to lyse the viral particle and release all the proteins (38). The specific proteins, HA, NA, M1 and NP, are further isolated from this viral particle soup. Next, the whole virus or split virus is inactivated. The inactivation or killing methods for approved human vaccines utilize formaldehyde (formalin) or beta-propiolactone, but other methods used in laboratory studies may include heat or ultraviolet radiation inactivation.

There are several drawbacks to these vaccination approaches. The first is that of a human nature. The WHO attempts to predict what the prevalent flu strains will be in the future. Unfortunately, this is a best guess, and not time travel. Given the nature of time and viral evolution, by the time 6 months have passed and the Northern Hemisphere enters flu season, the prevailing strains may have changed over this time, so the vaccines created for that season generate protection against different strains than those in circulation. A second viral evolution problem arises from growing influenza virus in chicken eggs. For the virus to better infect the egg cells, the virus will often mutate its HA to better infect the egg cells. Since HA is one of the predominant antigens antibodies are generated against, if the virus

growing in the eggs to be used in upcoming vaccines has mutated away from the original strain to better infect its new host, the chicken egg, then the isolated strains used to make the vaccines will be different from the parent strain. To circumvent this issue, some vaccine viral stocks are grown in MDCK cells instead of chicken eggs, however this cell culture process is much more expensive than using chicken eggs and several countries around the world still rely on chicken eggs to grow their vaccine viral stocks.

### **C. Protein Subunit Vaccination**

Protein subunit vaccines, also called recombinant vaccines, are produced in insect cells using a baculovirus expression vector. These vectors use the insect cell machinery to express viral mRNA and translate them into protein in the insect cells. The protein antigens are isolated, purified and used as a vaccine. The most common influenza proteins used in subunit vaccines are HA (FluBlok), NP, M2 and NA (39). These vaccines rely heavily on adjuvants to provide adequate inflammatory signals to generate an immune response (39). These vaccines are enticing because they provide at least a three-times greater dose of specific Ag compared to IIV (40, 41), and have been shown to increase anti-HA antibody titers in the elderly (42). In a direct head-to-head comparison in humans, the protein subunit vaccine, FluBlok, elicited both a larger CD4 T cell response and anti-HA antibody response, compared to the IIVs Fluzone and Flucelvax (43). A potential downside risk to protein subunit vaccines is that if the virus mutates away from the protein subunit used in the vaccine, the immunological memory induced by these vaccines may prove useless against new variants.

### **D. Live Attenuated Immunization**

Live attenuated influenza vaccines (LAIV) were actually the first vaccines utilized to immunize workers in the Soviet Union in the late 1930s (30). These first vaccines were crudely generated by serial passage of patient isolated influenza virus through mice and ferrets, generating an attenuated virus that was “well tolerated” by subjects. Today, much more sophisticated techniques are used to generate LAIV, however the methodology remains largely the same. Cold adapted (CA) LAIV can replicate in the nose at a temperature of 25°C but cannot replicate at higher temperatures in the lung of about 37°C. Intranasal LAIV allows for modest viral replication to occur, specifically restricted to the nasal passage, but prevents replication in critical lung tissue. These vaccines better mimic conditions arising from infection because the immunogen can infect cells and replicate, in the hopes of generating an immune response comparable to a response arising from infection. In contrast to inactivated vaccines, LAIV are delivered intranasally and thus generate a local immune response at the site of influenza virus infection, the respiratory tract, compared to intramuscular inoculation with inactivated vaccines.

In a meta-analysis of clinical trial data spanning 1988-2020, there was a slight advantage of trivalent IIV over LAIV in preventing confirmed influenza infection of adult and elderly populations (44). In children however, both LAIV and adjuvanted trivalent IIV was significantly better at preventing laboratory confirmed influenza compared to trivalent IIV (44). One possibility for why LAIV work better in children compared to adults is that the LAIV may be neutralized by pre-existing antibodies better or more completely in adults with a long history of exposure to influenza, compared to children with a more naïve immune system. The LAIV may replicate better and present viral antigens for a longer

duration in kids vs. adults, thus generating a better immune response compared to IIV, while LAIV gets neutralized very quickly in adults, does not replicate to the same degree as in children and thus performs more like an intranasal IIV than a LAIV. All subjects regardless of age were better protected from laboratory confirmed influenza after receiving any vaccine compared to placebo (44).

### **E. Adjuvants**

Adjuvants are added to vaccines to boost the immune response compared to the vaccine alone. Protein antigens are broken down and cleared from hosts very quickly, so adjuvants can act to emulsify or stick to antigens and slow their degradation (45). Adjuvants also activate innate pattern recognition (PR) pathways and induce production of inflammatory molecules, such as cytokines and chemokines, to further promote the T and B cell response (46). This, in turn, can increase activation and migration of APC to the site of immunization, which helps to activate a T cell response (47). In a direct comparison of children immunized with either non-adjuvanted IIV or IIV adjuvanted with MF59, laboratory confirmed cases of influenza were reduced in the IIV MF59 compared to IIV alone (44).

### **F. New Technologies**

The COVID-19 pandemic saw the US government rapidly invest \$18 billion dollars in the development of novel SARS-CoV-2 vaccines. The “new” vaccines utilized adenovirus vector (AAV) and mRNA lipid nanoparticle (LNP) technologies to provide SARS-CoV-2 Ag to the host. DNA, RNA and AAV vaccine and gene therapy designs have been studied for years (48, 49), so it is great to see these technologies enter the mainstream

and earn FDA approval. Both AAV and mRNA vaccines induce anti-spike protein antibodies and memory T cells against SARS-CoV-2 (50, 51). In comparison to IIV, which only present Ag for 3-4 days *in vivo* (52), mRNA-LNP vaccine delivery demonstrates that the encoded protein Ag persists up to 13 days after injection (53). As an added bonus, the LNP itself is highly inflammatory, which generates the cytokines and chemokines akin to an adjuvant that activate APC (54). This long duration of Ag delivery, coupled with a robust inflammatory signal, demonstrates the promise of mRNA-LNP vaccine technology to activate the innate immune system and provide Ag for T and B cells for a significantly longer duration than IIV.

## **Immune Response to Influenza**

### **A. Innate and Adaptive Immunity to Influenza**

The overall immune response can be broken down into two key arms, the innate and adaptive response. Under homeostatic conditions, specific cellular components are contained in certain locations and in specific conformations, while influenza infection introduces viral components in locations and conformations that are outside normal cellular conditions. The innate immune response consists of the innate ability of all cells to mount some type of inflammatory response, typically utilizing pattern recognition receptors (PRR), stimulated by pathogen-associated molecular patterns (PAMPs). The adaptive immune response consists of a specialized cellular response to a pathogen, specifically in the case of influenza, B and T cell responses.

Influenza virus infects and replicates inside lung epithelial cells (14, 15). These cells possess the innate ability to detect viral components that are not normally present

under homeostatic conditions. The main contributors to the innate recognition of influenza infection are the Toll-like receptors (TLR), retinoic acid-inducible gene 1 (RIG-I) like receptors (RLR) and NOD-like receptors (NLR) (55). Each PAMP and the PRRs that trigger the innate immune response will be discussed below.

As mentioned previously, the outset of influenza infection starts when a host cell uptakes the virus into an endosome. Two of the endosomal TLRs, TLR3 and TLR7, recognize double-stranded and single-stranded RNA respectively and activation of these TLRs results in production of pro-IL-1 $\beta$ , pro-IL-18 and the type I interferons, IFN $\alpha$  and IFN $\beta$  (55–59). Since influenza is a single-stranded RNA virus, it is currently unclear how TLR3, a double-stranded RNA sensor, responds to influenza and mice that lack TLR3 actually exhibit a survival advantage and a completely normal T cell response (57, 60).

Newly replicated vRNPs are recognized by RIG-I in the cytoplasm. The cytoplasmic RIG-I receptor recognizes the 5' triphosphate of the uncapped vRNP (61, 62). This triggers a conformational change in RIG-I that enables it to interact with mitochondrial antiviral signaling protein (MAVS), which in turn results in pro-IL-1 $\beta$ , pro-IL-18 and type I interferon production (63, 64).

Lastly, the NOD-like receptor pyrin domain 3 (NLRP3) can recognize multiple viral determinants, such as viral RNA, M2-mediated acidification of the viral core, and high molecular weight PB1 complexes specifically in activated macrophages (65-67). This triggers activation of the NLRP3 inflammasome which results in caspase-1 mediated cleavage of pro-IL-1 $\beta$  and pro-IL-18 into the active and secreted forms of these cytokines.

These PRR pathways serve a semi-redundant and synergistic role in initiating the immune response to influenza. While on their own TLRs and RLRs are not required for viral control, survival or T cell mediated protection (56, 57, 60, 68), mice lacking NLRP3 or caspase-1 experienced increased mortality compared to intact mice however saw no benefit in viral control (65, 69). This suggests that cleavage of pro-IL-1 $\beta$  and pro-IL-18 are crucial for survival yet independently TLR, RLR and NLR signaling have no direct impact on viral load. IL-1 assists dendritic cells (DC) in getting to the lung draining mediastinal lymph node (dLN) while IL-18 enhances IFN $\gamma$  production from responding CD8 T cells (56, 70). Type I interferons stimulate the expression of many genes that assist in the immune response, both by viral suppression in infected cells and signaling neighboring cells to join the fight.

These PRRs and associated signaling cascades, namely through IL-1, IL-6, IL-18 and type I IFN, act to initiate the adaptive immune response. Influenza-specific antibody production from B cells begins with TLR7 activation (71-73). An important note is that whole inactivated vaccination, but not split or subunit vaccines, induces TLR7 activation and better protection (72). Implications for vaccine design will be discussed in more detail later. Alveolar macrophages and DC serve as a critical bridge between the innate and adaptive immune responses. Alveolar macrophages can become infected with influenza when they phagocytose influenza-infected dead and dying cells. Phagocytosis of these apoptotic bodies is required for viral control (74). DC are professional antigen presenting cells (APC) that prime CD4 and CD8 T cells in the dLN after picking up cellular debris

from infected lung and migrating to the secondary lymphoid organs to initiate these responses (14, 56, 75).

In the mouse, both B and T cells are capable of clearing influenza infection on their own (76-78). B cells accomplish this through the production of anti-influenza antibodies (78) while CD8 T cells kill infected cells and produce cytokines to fight infection (79, 80). Naïve CD4 T cells alone cannot clear virus well as they act in part by providing help to B cells (81). CD4 T cells have multiple roles in response to infection, such as helping B cells produce antibodies and direct cytotoxic function (6). CD4 T cells are also fewer in number compared to both B and CD8 cells. Interestingly, memory CD4 T cells can protect against influenza infection on their own (5), which sets them up as a great vaccine target to provide long-term protection with multiple mechanisms of action and to synergize with B cell antibody responses.

## **B. T Cell Responses to Influenza**

Activation of naïve T cells requires antigen recognition, costimulatory stimulation, and an inflammatory signal derived from cytokines. The innate immune response to influenza provides plenty of inflammatory cytokines that primes the adaptive immune response. Dendritic cells (DC) acquire influenza antigens through uptake of cellular debris and by direct infection (15, 82, 83) and migrate to the lung draining lymph node where the naïve CD4 and CD8 T cells reside. Antigens can also be exchanged between migratory DCs and lung resident DCs (84). These antigens are processed and presented on major histocompatibility complex class I (MHC-I) and class II (MHC-II) to CD8 and CD4 T cells respectively. CD103<sup>+</sup> DC and respiratory CD11b<sup>hi</sup> DC are the primary drivers of CD4 and

CD8 T cell activation during influenza infection (85, 86). A naïve T cell becomes activated when its T cell receptor (TCR) binds to peptide-MHC (pMHC), in conjunction with signals from costimulatory molecules such as CD28. The cytokines in the environment can further tune the T cell response.

To define what is necessary for generating immunity by either infection or vaccines, it is critical to understand these interactions and the kinetics of the primary T cell response to IAV. Both CD103<sup>+</sup> and CD11b<sup>hi</sup> respiratory DC are responsible for early priming (86), up to 4 days post infection in the lung draining lymph node (dLN), while the CD11b<sup>hi</sup> DC peak at 5 dpi in the dLN and 7 dpi in the lung (87). By 4 dpi, IAV-specific T cells have undergone a few rounds of division in response to antigen (Ag) in the dLN and begin to migrate to the lung 5-6 dpi (88, 89). The number of T cells in the lung peaks at 8-9 dpi (89-91). In our studies IAV viral titers peak day 2-3 and remain high until CD4 and CD8 effector cells migrate to lung and clear infection, mostly by 7-10 dpi, with total clearance at 10-13 dpi (Figure 1.1). The sub-lethal doses of virus are cleared 10-13 dpi, although IAV Ag are detectable through 21 dpi (92).

Cytotoxic effector CD8 T cells primarily function to kill IAV infected cells (93, 94), although the loss of perforin or FAS-L on CD8s, two molecules required for cytotoxicity, does not impair the ability of these CD8s to clear infection in the absence of neutrophils, B cells, and other T cells (95). In response to IAV infection, CD4 T cells differentiate into multiple effector fates, including Th1, Th17, cytotoxic ThCTL, T<sub>FH</sub>, and T<sub>REG</sub> (6, 96-101). Although CD4 T cell help to CD8 cells is not required for efficient CD8 effector function (95, 102), CD4 help to CD8 cells during priming is critical for the

Figure 1.1. Lung T cell kinetics in response to IAV infection

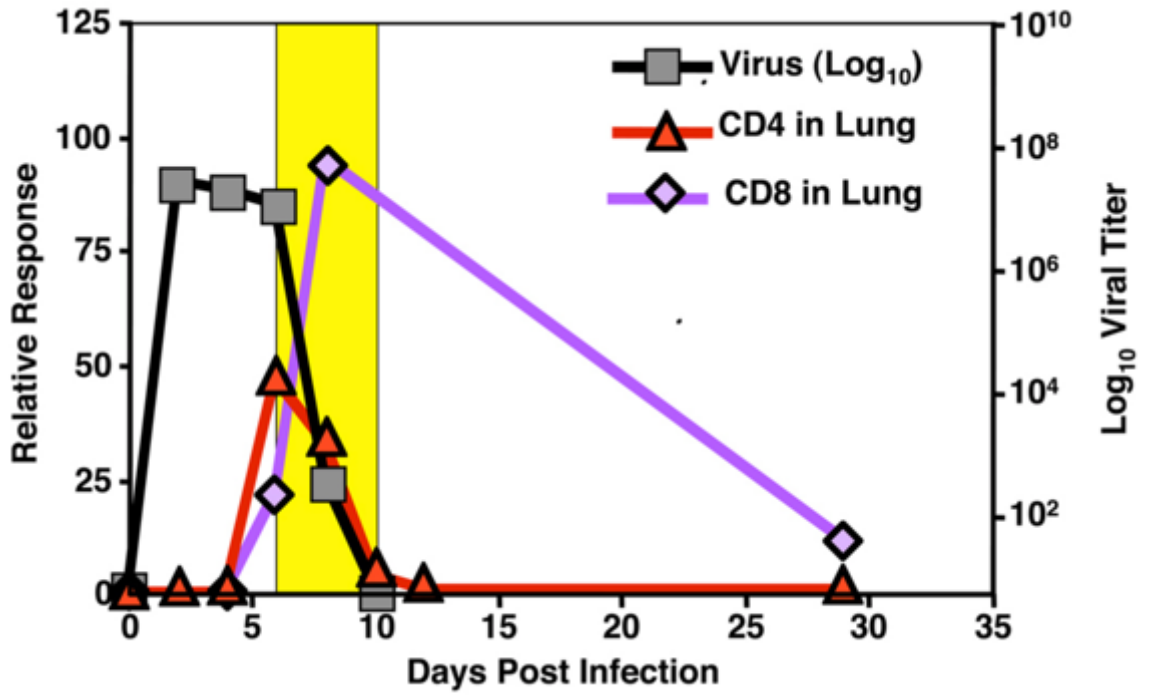


### **Figure 1.1. Lung T cell kinetics in response to IAV infection**

HA-specific T cells (CD4 and CD8) were transferred to BALB/c hosts and infected with a sub-lethal dose of PR8. Lung viral titers representing  $\log_{10}$  of virus (right y axis) are plotted together with the relative cell number response (left y axis) of HA-specific CD4 (red) and CD8 (purple) T cells in the lung.

Figure adopted from: Swain, S. L., Dutton, R. W., & Woodland, D. L. (2004). T Cell Responses to Influenza Virus Infection: Effector and Memory Cells. *Viral Immunology*, *17*(2), 197–209. Creative Commons Attribution license.

formation of CD8 tissue resident memory ( $T_{RM}$ ) cells (3, 102). Other helper functions, such as CD4 effector IL-2 production, can influence IL-10 production from CD8s (103), while CD154 expressed by CD4 effectors interacts with CD40 on DC, which inhibits the  $T_{REG}$  mediated suppression of IAV-specific CD8 effectors (104).

The CD4 effector response is dominated by Th1 cells in the spleen, dLN and lung, marked by T-bet and  $IFN\gamma$  expression (91, 105, 106). The CD4 Th1 effectors in the lung mostly produce  $IFN\gamma$  with some  $TNF\alpha$  and almost no IL-2 production, while Th1 effectors in the secondary lymphoid organs (SLO), the dLN and spleen, can produce  $IFN\gamma$ ,  $TNF\alpha$  and IL-2 (88, 91). Tissue restricted effectors ( $T_{RE}$ ) develop later in the response, 6-9 dpi, and require both signals from infection and late cognate Ag interaction (6, 96, 98). These pathways will be discussed in detail below, but briefly  $T_{FH}$  take up residence in the SLO and provide help to germinal center (GC) B cells through IL-21 and IL-4 (1, 6, 107, 108), while ThCTL occupy the lung and kill infected targets through MHC-II Ag recognition and perforin-mediated cytotoxicity (96, 97).

Once the virus is cleared at 10-13 dpi both CD4 and CD8 T cell begin to contract to memory. About 10% of IAV-specific T effectors go on to become memory, while the remaining 90% are terminally differentiated and undergo default apoptosis. Although activation induced cell death (AICD) has been implicated *in vitro* (109, 110), its role *in vivo* in response to acute viral infection is negligible (111-113). This FAS-mediated cell death seems to play more of a role in chronic LCMV infection (114), superantigen stimulation (115) and following stimulation by very high levels of IL-2 (109, 110) but is unlikely to play a major role in T cell contraction to IAV infection. Programmed cell death

is another way in which effector T cells contract. In the absence of cytokine survival factors, effector T cells undergo default apoptosis. Mechanistic details will be discussed below, but the major survival cytokines are IL-2, IL-7 and IL-15 and this pathway is mediated by pro-apoptotic Bim and anti-apoptotic Bcl-2.

Following contraction, the T cells that have survived are characterized as memory cells, because they “remember” their previous Ag encounter and have undergone epigenetic changes that allows them to respond rapidly to future infections (116-119). Memory T cells essentially have been selected to survive through cognate Ag recognition, co-stimulatory molecule stimulation and signals from cytokines throughout the course of the immune response to a pathogen. As the reader will note, these three signals are also a requirement for naïve T cell activation. As logic follows, any T cell that receives these signals may have the potential to become memory. So why do almost all effector cells die while only a small subset, about 10% of effector T cells survive to memory? Here, it is important to mention the fallacy of composition. For example, if I attended a baseball game at Yankee Stadium and I was having a hard time seeing the field, I may stand up to have a better view. Therefore, in order to have a better view anyone can stand up to see the field better. However, this premise and extrapolation becomes false if everyone at Yankee Stadium stands, now the crowd collectively is back in the same position, with everyone at the same eye level.

T cell memory development follows similar logic. Evolution has selected for the survival of enough memory cells to protect against future infection, while not blocking the view, so to speak, of other cells. There is a balance between the fraction of effector cells

that die off and those that survive to memory. Resources are scarce and generating and maintaining a memory T cell population requires time, space and energy. T cell memory formation strives for the Goldilocks scenario. If memory formation is “too cold,” the host will not be protected against future infection. If memory formation is “too hot,” those memory cells for that specific pathogen will take away resources, like energy, cytokines and space, from other memory cells or immune cells to other pathogens, and perhaps generate an over-aggressive secondary immune response causing excess pathology and potential tissue damage. Through evolution, the Goldilocks “just right” number of memory cells has been selected for. In my view, acute viral infections provide just the right amount of signals for the right amount of time and in the right place to generate ideal T cell memory populations. Therefore, using these systems to study how protective T cell memory forms can provide deep insights into the mechanisms of T cell memory development and the signals that separate terminal effector cells from those that survive to memory.

Following influenza infection, a heterogenous memory CD4 T cell population is established (120-122). These memory cells produce cytokines immediately in response to a new infection and respond more rapidly than naïve T cells, especially at the site of infection, which in the IAV setting is the lung (123). In response to new IAV infection, memory CD4 T cells provide a boost to innate immune cell inflammatory cytokine and chemokine production (124). The early and robust production of IFN $\gamma$  by memory CD4 T cells in response to IAV helps CD8 effector cells control viral load and fight infection (5). These memory CD4 T cells also enhance the anti-influenza antibody production of naïve B cells (5). Because memory CD4 T cells can enhance innate immune cell, CD8 T cell and

B cell secondary responses, they are potent protectors and a worthy target of vaccine design.

### **C. T Cell Memory Subsets**

The immunology research community really likes to subset different immune cell populations and memory cells are no different. The canonical T cell memory subsets are central memory ( $T_{CM}$ ), effector memory ( $T_{EM}$ ) and resident memory ( $T_{RM}$ ). Central memory cells are marked by expression of CD44, CD62L and CCR7 while effector memory cells are marked by CD44 expression and the lack or low expression of CD62L (125). As immunologists like to subset immune cell populations, several groups have studied the differences in  $T_{CM}$  and  $T_{EM}$  recall responses. However, there are conflicting reports regarding which memory population,  $T_{CM}$  or  $T_{EM}$ , provide essential protection. Some studies have found that CD4  $T_{EM}$  cells produce more  $IFN\gamma$  and less IL-2 than their  $T_{CM}$  counterparts (126, 127), while others found no difference in  $IFN\gamma$  production (128). Regarding CD8  $T_{CM}$  and  $T_{EM}$ , there are no differences in  $IFN\gamma$  production (128-131), however conflicting reports argue that  $T_{EM}$  are more cytotoxic than  $T_{CM}$  (129, 131), or that there are no differences in cytotoxicity between the populations (128, 130). Others have proposed that this is a temporally controlled joint effort, in that  $T_{EM}$  provide early support against infection, while  $T_{CM}$  cells take over later in the response (132). The general paradigm is that central memory cells recirculate through the blood and lymph nodes, scanning for Ag recognition, while effector memory cells traffic through the blood, lymphoid and non-lymphoid tissues (133). It is interesting to note that with time,  $T_{EM}$  have

been shown to give rise to  $T_{CM}$  and that these subsets are more closely related than they are different (130).

Tissue resident memory cells are marked by CD44 and CD69, and CD8  $T_{RM}$  express an additional marker CD103 (134, 135). Tissue resident memory cells reside in the tissue and do not re-circulate (136). These cells can also be identified by the lack of i.v. antibody labeling in memory experiments (137). Lung CD4  $T_{RM}$  can provide substantially better protection from lethal influenza infection compared to spleen CD4 memory (138). Additionally, effector CD4 T cells provide essential help to promote CD8  $T_{RM}$  formation (3, 4). In several other studies, T cell memory located in non-lymphoid tissues at the site of infection improve responses to viral (139-142), bacterial (143, 144), and parasite (145) infections. Immediate T cell memory responses at the site of infection are critical in defending the host against future infections. Understanding the mechanisms by which these memory cells are generated is critical to informing better vaccination strategies.

#### **D. Factors that Influence T Cell Memory**

Understanding the various and variable inputs that result in the survival of about 10% of effector T cells and formation of stable memory is essential to inform future vaccine strategies. I will dive into T cell priming and the contributions of pMHC-TCR engagement in T cell effector differentiation below, but briefly, signals from priming are not enough to establish protective memory. There are additional signals required throughout the immune response that must occur in the right place and at the right time to promote effector T cell survival to memory and generate a memory population that is effective in protecting the host from future infections. The majority (~90%) of effector T cells die by default once the

influenza infection is cleared and here, I will outline what we know about this death process and the signals that promote the survival of T cell memory.

As mentioned previously, activation induced cell death does not appear to play a major role in the death of effector T cells during contraction following an acute viral infection. Studying T cell contraction is complicated by the fact that genetic models knocking out apoptosis effector caspases 3 and 7 result in the death of the mice shortly after birth (146, 147). Genetic deletion of the pro-apoptotic molecule Bim results in an activated T cell population that does not contract following the clearance of viral infection (148, 149). The overexpression of the pro-survival molecule Bcl-2 results in the enhanced survival of effector T cells (150). The activation of naïve T cells results in the upregulation of many death pathways (151). There are several key cytokines that are required to overcome these death pathways and allow a small fraction of effector T cells to survive to memory. Signals from IL-2 (152), type I interferons (153) and IL-12 for CD8 cells (154) have all been implicated in the survival of effector T cells. Other cytokines IL-7 (155-159) and IL-15 (160-162) are important for the generation and homeostatic maintenance of memory T cells. Expression of CD127, the IL-7R $\alpha$ , serves as a quintessential memory T cell marker (106, 163). Studying when and how these cytokine signals promote effector T cell survival to memory is complicated, as these signals do not exist in a vacuum and they often act in an additive process over time. In the following section, I will examine how peptide Ag at specific times during T cell differentiation may impact production of these cytokines or expression of their receptors and result in survival or death fate decisions.

### **Cognate Antigen Impact on T Cells**

## **A. Impact on Effector Differentiation**

There are some key differences between CD8 and CD4 effector responses that arise from *in vivo* Ag withdrawal experiments. These experiments study the proliferation of naïve CD8 and CD4 T cells when Ag recognition is limited to the first 48 hr of the immune response. Removing cognate Ag from the system after 48 hr does not impair the number of Ag-specific effector CD8 T cells, however the number of Ag-specific effector CD4 T cells is dramatically reduced (164, 165). Another study showed that shortening the length of Ag presentation during priming does reduce the number, but not the function of effector CD8 T cells (166). Strong pMHC-TCR interactions during priming increase the proliferative capacity of CD8 T cells compared to weaker interactions (167). Others have shown that Ag persistence throughout priming is required for effector CD4 T cell responses (168). A potential explanation for this key difference between CD8 and CD4 cells is that the dominant effector CD8 T cell function is to kill infected cells, so the observation that a short duration of priming Ag recognition for 24-48 hours is sufficient to set these cells on “autopilot” to hunt for and kill infected cells fits with the dominant primary effector function of these cells. On the other hand, CD4 effector cells have a myriad of functions and differentiation pathways, and so additional cognate Ag signals are required to activate and sustain these complex pathways. From the perspective of evolution this also makes sense, as some immune response is warranted for short duration Ag encounter, but this may not pose a serious threat, so better to conserve resources and not risk potential auto-immune or unwanted tissue damage from an over-zealous T cell response to minimal Ag.

At this point, it is important to define the strength of peptide-MHC engagement with TCR. The strength of these interactions are modulated by the biochemical affinity of peptide-MHC for the TCR and the density of peptide Ag loaded onto MHC molecules on the surface of the APC (169). So therefore, it follows that in order to modulate the strength of pMHC-TCR engagement experimentally one must either use the same peptide Ag pulsed on APC at different doses to modulate Ag density, use several peptide antigens with different binding affinities for the TCR, or use different TCRs for the same peptide Ag. It is well established that, notwithstanding the impact from polarizing cytokines, increased pMHC-TCR engagement of CD4 T cells favors Th1 over Th2 differentiation (170-172).

Reports on how the strength of pMHC-TCR interactions influences T<sub>FH</sub> generation are less clear. Some have found that strong pMHC-TCR interactions favor T<sub>FH</sub> over Th1 differentiation (173-175), while other studies have found the opposite (176, 177), or that peptide avidity controls Th1 but not T<sub>FH</sub> differentiation (178). Some suggest that increased pMHC-TCR dwell time, rather than the affinity of the interaction promote T<sub>FH</sub> over Th1 differentiation (173, 179, 180). These differences may arise from the different experimental systems used, as the cumulative signals received by CD4 T cells from naïve through effector differentiation will undoubtedly be different under different infectious conditions, influencing the cytokine environment and APC activation status, as well as the amount of peptide Ag presented and the affinity of those peptides for TCR. Even pMHC-TCR signals during CD4 T cell development have the potential to shape peripheral CD4 T cell responses. Paul Allen's group used two different CD4 TCR transgenics for the same affinity peptide Ag to show that even the same peptide Ag can elicit different responses

from CD4 T cells (181) and that this tonic signaling during development can shape the differentiation pattern of effector CD4 T cells, with lower tonic TCR triggering favoring  $T_{FH}$  development while having no impact on Th1 formation (182). Using the influenza infection model, our lab has found that early day 6 effector CD4 T cells need both signals from infection and local Ag presentation at the tissue site of residence for tissue restricted effector development. For  $T_{FH}$  differentiation, these early day 6 CD4 effectors need signals from infection and local Ag presentation in the spleen and dLN (98), while ThCTL differentiation requires both infection and local Ag recognition in the lung (183). These results highlight the complexity of CD4 T cell effector differentiation and how different systems produce conflicting results. The infectious context, timing, location, and strength of cognate Ag interactions all seem to play roles in effector T cell differentiation, which makes the case that the cumulative instructions from these signals are more important than any one of these signals taken out of context.

## **B. Impact on Memory Formation and Recall Responses**

Just as the impact of cognate Ag interactions on effector T cell differentiation is complicated and conflicting, so is the impact of cognate Ag signals on T cell memory formation and recall responses. While limiting Ag to the first 48 hours of naïve CD8 T cell activation had no impact on the number of effector cells generated, this Ag restriction reduced the number of both memory CD8 and CD4 cells, however the reduced number of memory cells still mount a potent secondary effector response (164, 166). There again are conflicting reports on whether high or low avidity pMHC-TCR interactions favor memory formation and recall responses. A single CD8 T cell clone has the potential to become both

terminal effector and memory cells (184, 185). Single CD4 T cell clones also have the potential to differentiate into both T<sub>FH</sub> and Th1 fates and terminal effector and memory cells (173, 179, 186). Even CD4 T cells stimulated by the same peptide Ag with equal affinity for TCR demonstrate different memory potential based on levels of tonic signaling during development (181, 187). Weak compared to strong pMHC-TCR interactions result in earlier contraction of effector CD8 T cells, however again demonstrate no difference in the number or recall capacity of these memory cells (167). Modulating the strength of TCR ligation through Ag dose reveals that CD8 memory develops in response to both high and low Ag dose (188, 189). There are others that suggest the increased responsiveness of memory compared to naïve CD8 T cells with the same TCR reflects an avidity maturation paradigm (190, 191) and this may highlight how both low and high affinity CD8 memory cells are equally competent secondary effectors. Some suggest that continual boosting of the memory population can select for an increase in CD8 T<sub>EM</sub> over T<sub>CM</sub> (192) while low compared to high affinity interactions drive a proportional increase in CD8 T<sub>RM</sub> formation over total spleen CD8 memory, however the greatest total number of T<sub>RM</sub> in the lung are in response to high affinity Ag (193). There is also evidence from the influenza system that prolonged Ag exposure to primary CD8 effector cells generates a memory population with enhanced proliferative capabilities and secondary effector functions (194, 195).

The generation of CD4 T cell memory is also controversial. As stated above, CD4 T cells require a longer duration of Ag presentation to promote effector differentiation (164, 165, 168). One report suggests that high avidity TCR interactions during priming promote CD4 memory generation through an increase in the pro-survival molecule Bcl-2

(196). Another study suggests that high affinity CD4 TCR interactions during priming favors terminal Th1 differentiation, while lower affinity interactions promote T<sub>FH</sub> differentiation and memory formation (197). The authors went on to show that low affinity interactions during priming correlated to lower levels of CD25 and T-bet expression, and increased survival (197). However, as with CD8 memory recall responses, both CD4 memory populations arising from either high or low affinity interactions during priming, respond equally well to secondary challenge (197). Another group also found that early effector expression of CD25 was affinity dependent, with high affinity Ag stimulation during priming promoting greater CD25 expression on early CD4 effector cells (177). The logic follows that high affinity cognate Ag interactions during priming promote increased IL-2 production and CD25 expression (177, 197), and in turn, IL-2 signaling of early effector cells inhibits T<sub>FH</sub> generation (198), thus increasing Th1 effector differentiation. However, this group found no differences in the number of CD4 memory cells generated from priming with high or low affinity Ag (177). The recall response stemming from the CD4 memory cells primed with low affinity Ag was dominated by T<sub>FH</sub> secondary effectors while the recall response from the CD4 memory cells primed with high affinity Ag was dominated by Th1 secondary effectors (177).

Since the impact of pMHC-TCR affinity during priming on CD4 T cell memory formation and recall responses is not quite clear, our lab has focused on how cognate Ag interactions during the effector phase of the response influences memory formation. Mice infected with influenza present a wide diversity of Ag epitopes to T cells, that reach very high levels soon after infection and that remain high until infection is cleared (52, 199).

Infection produces very strong CD4 T cell memory, suggesting that persistent high levels of Ag, including some epitopes with high affinity, may explain the high levels of memory generated by infection. In this thesis, we specifically analyze the impact of peptide avidity for TCR at the effector phase, when both viral levels and CD4 effectors have peaked, and when CD4 effectors that fail to recognize Ag undergo contraction (200, 201). We ask if high compared with low affinity Ag drives generation of more CD4 memory cells that provide superior protection. Previously, our lab showed that CD4 effectors generated *in situ* by IAV infection need to recognize Ag during the effector phase, 5-8 days post infection (dpi), to become memory cells (200, 201). We call this temporal cognate Ag requirement the effector checkpoint because the CD4 effector cells must engage in a second cognate interaction and produce autocrine IL-2, which prevents their apoptosis, enabling their transition to memory (200-202). We ask here if the strength of pMHC-TCR interaction plays a decisive role in driving CD4 effectors to memory.

To study the impact of peptide avidity at this crucial juncture, we developed a TCR Tg mouse (FluNP) specific for NP<sub>311-325</sub>, an immunodominant, highly conserved, IAV nucleoprotein (NP) epitope in B6 mice (199). We made a truncation and single amino acid substitutions to generate a library of NP<sub>311</sub> peptides with a spectrum of functional avidities for the FluNP TCR, as measured by naïve FluNP cell activation following stimulation by NP peptide pulsed APC. We generated *in vivo* effectors from naïve CD4 FluNP cells by IAV infection in a first (1<sup>st</sup>) host, isolated 6 dpi donor FluNP effector cells and co-transferred them to a second (2<sup>nd</sup>) host (200) with peptides from a panel spanning high to low avidity for the FluNP TCR, as the only source of Ag.

We find that higher avidity Ag at day 6 (6d) of the CD4 effector response promotes a far larger CD4 memory population in the lung and dLN, and this leads to better protection. The peptide affinity and dose used to pulse APC determines the level of IL-2 produced by 6 day effectors, and levels of IL-2 correlate with prevention of default apoptosis, effector cell survival and development of memory (201). CD25, the high affinity IL-2 receptor (IL-2R $\alpha$ ), is not expressed on 6 day CD4 effectors, but is highly upregulated on APC in IAV-infected mice during the effector checkpoint, 4-8 dpi. Holding the peptide Ag constant, APC expressing CD25 generated higher numbers of CD4 T cell memory than CD25 deficient APC. We propose that IL-2R $\alpha$  expression on APC acts in concert with IL-2R $\beta/\gamma$  on the effector CD4 cells, to enhance local IL-2 signaling. We suggest at the effector phase, the level of IL-2 production, determined by peptide affinity, and efficacy of the response to autocrine IL-2, are the dominant pathways that regulate the size of the memory CD4 population and the extent of protection. We discuss the implications of this requirement for high peptide affinity at the effector stage for vaccine design with a focus on kinetics, Ag breadth and adjuvants that activate APC.

## CHAPTER II: Materials and Methods

### Mice

We use 8-12 wk old C57BL/6 (B6) mice as hosts in all experiments. Naive CD4 T cells are isolated from B6.FluNP strains, including B6.FluNP.Thy1.1<sup>+/-</sup> and B6.FluNP.Nr4a1<sup>EGFP</sup>.Thy1.1<sup>+/-</sup>. The B6.Nr4a1<sup>EGFP</sup> developed by Kris Hogquist and Steve Jameson (203) were from Jackson Laboratories. B6.FluNP TCR Tg mice were generated in collaboration with Eric Huseby's Laboratory at UMMS. Briefly, B6 mice were infected with a sub-lethal dose of PR8 (0.3 LD<sub>50</sub>) and at 21 dpi, 2 x 10<sup>7</sup> spleen and lung draining lymph node (dLN) cells were isolated and stimulated *in vitro* with irradiated spleen cells loaded with 100 ug/ml NP<sub>311-325</sub> peptide. After 5 days, responding T cells were fused with BW5147 to generate T cell hybridomas (204). T cell hybridomas with reactivity to NP<sub>311-325</sub> peptide, presented by lung APC from IAV-infected mice (A/PR8/34)-infected mice, were expanded. TCR V $\beta$ -chains were identified by staining with a set of V $\beta$ -specific Abs (BD Biosciences), and the TCR $\alpha$ -chains were identified by PCR analysis using a panel of TCR V $\alpha$  primers that collectively amplify all TCR V $\alpha$  gene families. We choose a hybridoma with V $\alpha$ 4.2 and V $\beta$ 2.1. A TCR Tg plasmid was made using cloned rearranged cDNAs for 22.B6 TCR V $\alpha$ 4.2 and V $\beta$ 2.1. Cloned products were fused with full length TCR C $\alpha$  and C $\beta$  sequences (205). All the TCR genes were sequenced, and error-free full-length cDNAs were subcloned into the human CD2 promoter transgene cassette for T cell-specific expression (206). B6.FluNP were established by injecting C57BL/6 oocytes with the TCR-Tg plasmid. BMDC were derived from B6 or B6.129S4-*Il2ra*<sup>tm1Dw/J</sup>

(CD25KO) mice obtained from The Jackson Laboratory and bred at UMMS breeding facility. Mice used in experiments were 8-12 wk of age. The Institutional Animal Care and Use Committee of UMMS approved all animal procedures.

### **Virus Stocks and Infections**

Mice were anesthetized with either isoflurane (Piramal Healthcare) or ketamine/xylazine (at a dose of 25/2.5 mg/kg by i.p. injection) before i.n. infection with 50  $\mu$ l of influenza virus diluted in PBS corresponding to a 0.2 to 0.3 (sub-lethal) medial lethal dose ( $LD_{50}$ ) for response,  $2LD_{50}$  for weight loss, and  $4LD_{50}$  for survival. Influenza virus A/Puerto Rico/8/34 (PR8, H1N1), originally from St. Jude Children's Hospital, was from our stocks grown and maintained at the Trudeau Institute. The virus was also characterized by its ability to infect eggs, and we found  $2LD_{50}$  corresponds about 10,000 EID<sub>50</sub>. Our standard dose sub-lethal  $0.3LD_{50}$ , corresponding to 25 PFU.

### **NP Peptide Generation**

In collaboration with Lawrence Stern's Laboratory at UMMS, we modified the NP<sub>311-325</sub> peptide to produce peptides of shorter lengths by deletions of amino acids (aa) on both ends to determine the best length. We used single alanine substitutions to determine the peptide-I-A<sup>b</sup> binding frame (P1=Y), then selective aa side-chain modifications, at known peptide-TCR contact positions to generate peptides likely to have lower affinities. Peptide-I-A<sup>b</sup> IC<sub>50</sub> was determined with surface plasmon resonance (SPR) using a BIAcore 3000. SPR analysis was performed using a BIAcore 3000 instrument (Cytiva). Briefly, biotinylated,

peptide exchanged MHCs were immobilized on a streptavidin chip. For the TCR, the FluNP TCR sequence was cloned into the pCDH lentiviral expression vector with a P2A site separating the alpha and beta chains. This construct was used to generate stable lines in 293S GnTI cells. TCR was then purified from supernatant with a nickel-NTA column and subsequent size exclusion. Recombinant FluNP TCR was then passed over at increasing concentrations. A5 was used as a negative control and the signal from this flow cell was subtracted from those of experimental flow cells. The resulting data points were plotted and fitted to hyperbolas to derive  $K_{DS}$ .

#### **BMDC Generation and Peptide/APC Preparation.**

APC were generated as in (200, 207) BM was harvested from B6 or CD25KO mice, washed with RPMI 1640, 1% FBS and cells plated at  $10^7$  cells/mL in RPMI with 10% FBS and 10 ng/mL GM-CSF. After 7d, CD11c<sup>+</sup> BMDC were isolated via MACS and activated with polyinosinic-polycytidylic acid (PolyI:C) at 10  $\mu$ g/mL overnight in culture or use as APC. APC were pulsed with a standard concentration of 100  $\mu$ M or dilutions thereof, of each of a chosen panel of NP peptides. For *in vivo* experiments pulsing was at 37°C for 1hr with shaking, APC were washed 3x, resuspended in PBS, and  $1 \times 10^6$  cells injected i.v. per mouse.

#### **Splenic APC Preparation and *In Vitro* Culture**

Spleen cells were harvested from uninfected B6 mice. Thy1.2<sup>+</sup> cells were depleted using MACS beads. The Thy1.2-depleted fraction was then plated at  $3 \times 10^6$  cells/ml in RPMI

containing 7.5% FBS and 10ng/ml LPS and 10ng/ml dextran sulfate. After 2 days in culture, these activated APC enriched cells were harvested and pulsed with a standard concentration of 100  $\mu$ M or dilutions thereof, of each of a chosen panel of NP peptides at 37°C for 1hr with shaking. APC were washed 3x and resuspended in appropriate media for cell culture or PBS for *in vivo* transfer.

### **Sequential Transfer Model**

We closely followed the model we developed previously (200). Splens and peripheral lymph nodes (LN) were collected from B6.FluNP.Thy1.1<sup>+/-</sup> mice. Naïve CD4 cells were isolated via negative selection with CD4 MACS (Miltenyi Biotec and washed 3x, resuspended in PBS. 0.5-1 x 10<sup>6</sup> naïve CD4 cells were transferred via i.v. injection into B6 1<sup>st</sup> hosts. 1<sup>st</sup> hosts were infected with a sub-lethal dose of PR8 the same day. Donor CD4 effectors were re-isolated from the 1<sup>st</sup> hosts at 6 dpi. Single cell suspensions were prepared from pooled spleen and dLN and donor FluNP cells were isolated via Thy1.1 positive selection by MACS (Miltenyi Biotec). Cells were resuspended in PBS and 1.5 x 10<sup>6</sup> donor FluNP cells per mouse injected into 2<sup>nd</sup> B6 hosts i.v., along with Ag/APC (peptide-pulsed). To maintain effector phenotype all steps were conducted at room temperature, except for one 15 min incubation at 4°C. This minimal protocol, without sorting, ensures that effector cells are only out of mice for a maximum of 2.5 hours

### ***In Vitro* Culture of Naïve and 6 dpi effector FluNP CD4 T cells.**

To assess functional avidity of peptides, we compared their ability to induce responses of FluNP naïve CD4 T cells, isolated as described above (sequential transfer model). Following isolation of naïve or 6d FluNP effectors and generation of Ag/APC, cells in complete RPMI 1640 media were plated at a CD4 T:APC ratio of 5:1. Following 2d in culture, plates were centrifuged, supernatant was removed for cytokine protein analysis via ELISA and cell pellets were stained for FACS analysis.

### **ELISA**

Supernatants were collected from *in vitro* culture. Plates (Nunc) were coated overnight with capture antibody (ELISAmix Biolegend). The following day plates were blocked following the manufacturer's protocol and supernatants were added neat, or diluted 1:10, 1:100, 1:1000 and left at 4°C overnight. The following day plates were washed, and detection protocol was followed per manufacturer's protocol.

### **Quantitative PCR (qPCR)**

Expression levels of several genes were analyzed using real-time, quantitative PCR as a validation of FACS experiments. Following 2d in culture, FluNP cells were isolated, RNA extracted using a RNeasy kit (Qiagen) and cDNA generated using TaqMan reverse transcriptase (Applied Biosystems). All qPCR reactions were performed using the CFX96 real-time system (BIO-RAD) and the amplifications were done using the SYBR Green PCR Master Mix (Applied Biosystems). The experiments were carried out in duplicate for each data point. The relative quantification in gene expression was

determined using the  $2^{-\Delta\Delta CT}$  method. Using this method, we obtained the fold changes in gene expression normalized to an internal control gene, Beta-actin.

### **Flow Cytometry and Cytokine Staining**

Cells were harvested, passed through a 70  $\mu\text{m}$  cell strainer and stained in FACS buffer (0.5% Bovine Serum Albumin, 0.01% sodium azide (Sigma Aldrich) in PBS. Cells were blocked with anti-FcR (2.4G2) and stained with amine reactive viability dyes (Invitrogen) to exclude dead cells. Surface proteins were stained with fluorochrome conjugated antibodies at 4°C. Antibodies used included anti: CD4 (GK1.5 and RM), CD44 (IM7), CD90.1 (OX-7 and HIS51), CD11c, CD25, CD62L, CD69, CD80, CD86, CD122, CD132, CD185 (CXCR5, SPRCL5), NKG2A/C/E, MHCII (I-A<sup>b</sup>). For CD127 staining, anti-CD127-Biotin was included in the surface stain mixture, cells were washed 3x, and a secondary fluorochrome conjugated SA was used in the second step. For cytokine staining, total splenocytes were stimulated with 10  $\mu\text{M}$  of NP<sub>311-325</sub> for 6 hr at 37°C. Brefeldin A (10  $\mu\text{g}/\text{mL}$ ) was added after 1 hr of stimulation. Following surface staining, cells were fixed in 2% paraformaldehyde for 20 min and permeabilized with 0.1% saponin buffer (1% FBS, 0.1% NaN<sub>3</sub> and 0.1% saponin in PBS (Sigma Aldrich) for 15 min. Subsequent staining for cytokines using the following antibodies: anti-IFN $\gamma$  (XMG1.2), anti-TNF $\alpha$  (MP6-XT22), anti-IL-2, anti-IL-17. For transcription factor staining cells were first surface stained then fixed and permeabilized using FoxP3 fix/perm kit (eBioscience) overnight per manufacturer's protocol and stained with the following antibodies: anti-BCL-6 (K112-91), anti-FoxP3, anti-T-bet at 4°C for 1 hour. Antibodies obtained from BD Bioscience,

Biolegend and eBioscience. Stained cells were acquired on a BD LSRII flow cytometer and analyzed using FlowJo analysis software.

### **Statistical Analysis**

Groups of at 3-5 mice were used in all experiments, and exact conditions repeated to obtain sufficient statistical power. All experiments shown were repeated 2-3 or more times. For statistical analysis an unpaired, two-tailed independent t test was used. All analysis was performed using GraphPad's Prism.

## **CHAPTER III: Peptide Avidity for TCR on CD4 and CD8 Effectors Determines the Extent of Memory Generation**

### **Introduction**

Studying the impact of pMHC-TCR interactions on the development of T cell memory poses a multitude of challenges. There are two main approaches to address this question. The first is to study the endogenous polyclonal T cell response using MHC-I or MHC-II tetramers for known immunodominant epitopes. This system is quite physiologically relevant, as no donor cell transfers are required, and naïve T cell precursor frequencies start at physiological levels. However, manipulating this system is quite challenging and limits studies to the detection of very small memory T cell populations that are very difficult to identify and analyze. The second approach utilizes a TC transgenic (tg) system in which naïve T cells all express the same TCR for the same peptide Ag. This allows the researcher to study the response of a homogeneous starting T cell population to a known Ag. The most popular TCR tg systems are the CD8 OT-I and CD4 OT-II systems. These T cells recognize specific peptide Ag from the ovalbumin (OVA) protein. Several infection and auto-immune systems have been developed to incorporate these systems and provide great insight into the T cell response. However, this system also has its flaws. First, these antigens are not derived from infectious agents and the affinity of each TCR for their respective OVA proteins are above physiological levels. The second applies more broadly to TCR tg systems, in that many donor naïve TCR tg cells must be transferred to the recipient host in order to have enough cells to track throughout the immune response, and

this starting population is much larger ( $10^5$ - $10^6$ ) than a physiologic number of naïve T cells for a specific epitope ( $10^1$ - $10^2$ ).

In my view, many of the conflicting reports regarding how peptide avidity for TCR influences effector and memory differentiation is due to the differences in the systems used to study these outcomes. There are three key derivatives to this pMHC-TCR interaction and resulting T cell differentiation puzzle. The first is the biochemical binding affinity of one pMHC molecule for the TCR. We like this type of data because we can measure the strength of this interaction as a  $K_D$  and study the dynamics of this interaction with on and off rates. The second derivative is how these interactions happen in the context of cell-to-cell interactions space. We call this peptide avidity, as it is a measure of multiple pMHC-TCR interactions that occur at the immunological synapse between APC and T cell in three-dimensional space. Peptide avidity is multi-factorial as it accounts for the summation of multiple pMHC-TCR interactions (affinity), considers the density of Ag loaded onto MHC (dose) and the dwell time which measures how long the TCR on the T cell engages with pMHC on the APC. We use T cell outcomes, such as naïve T cell activation, effector T cell cytokine production and memory T cell number recovery to measure functional avidity by changing the summation of multiple pMHC-TCR affinity interactions with altered peptides pulsed on APC at the same dose as a functional indicator. The third derivative is time or kinetics. We must consider *when* the T cell-APC interactions occur; during the priming of naïve cells, continued activation of effector cells, or re-stimulation of resting memory cells. These are only the considerations for the pMHC-TCR interaction and there are several other variables, such as the location these interactions occur, the

activation status of the APC and resulting co-stimulatory interactions between the T cell and APC, and the cytokines produced by the T cell and/or APC and therefore the resulting pro- or anti-inflammatory environment in which these interactions occur. Given all these variables, it is no wonder there are conflicting reports on how pMHC-TCR interactions from various systems influences effector and memory T cell outcomes.

### **Validation of the CD4 FluNP TCR transgenic system.**

To solve the TCR tg problem, we generated a B6 TCR tg mouse specific for an immunodominant NP core protein epitope, NP<sub>311-325</sub>, from the internal nucleoprotein (NP) of influenza PR8/34 (H1N1) presented by I-A<sup>b</sup> (MHC-II). This epitope is conserved among all dominant outbreak strains of IAV in people (199). The mouse was created by selecting T cell hybridomas specific for NP<sub>311-325</sub> from IAV-infected mice (204-206). We call the mouse FluNP. To my knowledge, this is the first CD4 TCR tg system specific for a specific influenza shared core protein Ag. This allows us to study the response of an immunodominant CD4 T cell clone and manipulate the system to ask fundamental questions.

We generated B6.FluNP.Thy1.1/Thy1.2 mice so we could readily detect donor FluNP cells after transfer to new hosts using Thy1.1 expression. To evaluate whether IAV induces a comparable response of the donor FluNP cells and polyclonal host CD4 T cells, we transferred naïve FluNP CD4 T cells into hosts and infected with a sub-lethal dose of PR8/34, an influenza A virus (IAV). We compared the kinetics of donor FluNP TCR Tg and endogenous host (CD4<sup>+</sup> CD44<sup>hi</sup>) T cell responses 4, 6, 8, 12, 21 and 63 days post infection (dpi) in the lung (Figure 3.1), draining mediastinal lymph node (dLN) and spleen

(Figure 3.2). IAV infection induced a similar pattern of expansion and contraction of donor FluNP and host CD4 T cells in the lung (Figure 3.1), spleen and dLN (Figure 3.2). To evaluate the subsets of CD4 effectors generated, we compared donor and host CD4

**Figure 3.1. Lung kinetics of donor FluNP and host CD4, CD44hi cells in response to IAV**

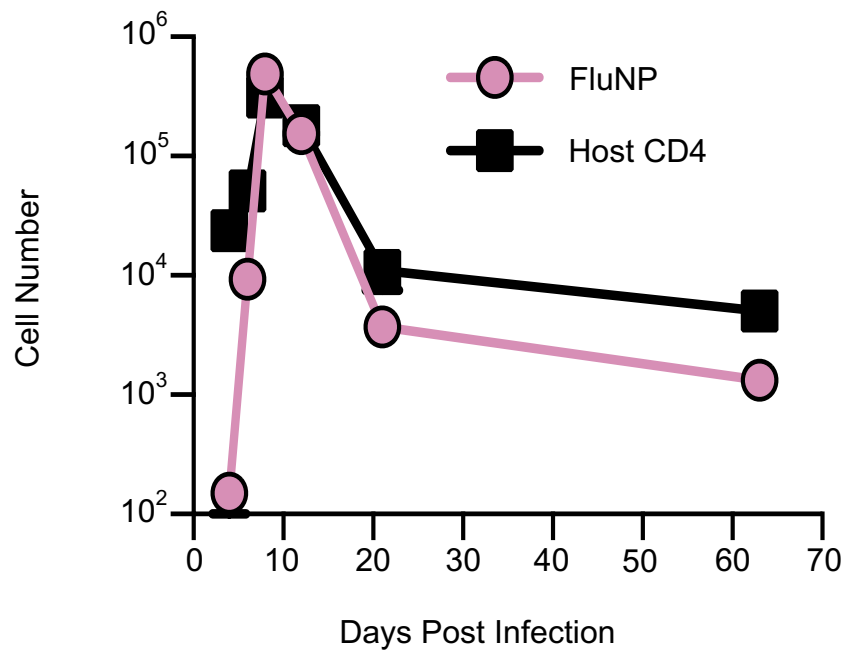


**Figure 3.1. Lung kinetics of donor FluNP and host CD4, CD44<sup>hi</sup> cells in response to IAV**

Naïve FluNP.Thy1.1<sup>+/+</sup> cells were transferred to B6 hosts, then infected with a sub-lethal dose of PR8. Lungs were collected at 4, 6, 8, 12, 21 and 63 dpi and numbers of donor FluNP and responding host CD4<sup>+</sup>, CD44<sup>hi</sup> cells were determined by FACS. Days 4, 6, 8, 21, 63 Pooled data, n = 9-10, two experiments. Day 12 one experiment n = 5. Mean +/- SEM.

**Figure 3.2. Secondary lymphoid organ kinetics of donor FluNP in response to IAV**

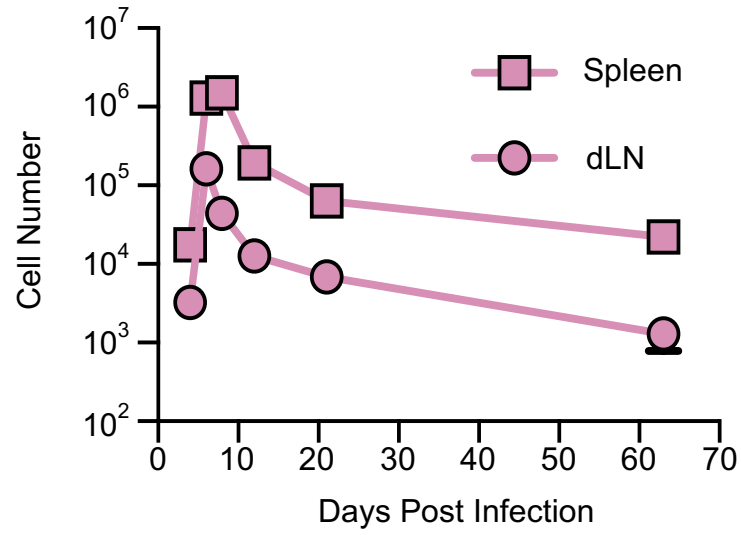


**Figure 3.2. Secondary lymphoid organ kinetics of donor FluNP in response to IAV**

Naïve FluNP.Thy1.1<sup>+/-</sup> cells were transferred to B6 hosts, that were then infected with a sub-lethal dose of PR8. Kinetics of FluNP Response (SLO) Lung draining lymph node (dLN) and spleen were collected at 4, 6, 8, 12, 21 and 63 dpi and the number of donor FluNP cells determined in each mouse by FACS analysis. Days 4, 6, 8, 21, 63 Pooled data, n = 9-10, two experiments. Day 12 one experiment n = 5. Mean

effectors at 8 dpi by examining cytokine production and phenotype markers: Th1 (T-bet, IFN $\gamma$ , TNF $\alpha$ , IL-2), Triple cytokine producers (IFN $\gamma$ , TNF $\alpha$ , IL-2), Th17 (IL-17), and T<sub>REG</sub> (FoxP3). We used NKG2A/C/E expression to detect cytotoxic CD4 (ThCTL), found only in the lung (96), and CXCR5 and Bcl-6 co-expression markers for T<sub>FH</sub> in the spleen (98). Both donor and host responses in the lung were dominated by Th1 phenotype cells (105, 106, 208), with high expression of T-bet (Figure 3.3A, E), IFN $\gamma$  and TNF $\alpha$  (Figure 3.3B, E), and little expression of IL-17 or FoxP3 (Figure 3.3B-C, E). Only a small fraction, less than 25%, of donor and host cells express IL-2 in the lung (Fig 3.3B, E) or are triple cytokine (IFN $\gamma$ , TNF $\alpha$ , IL-2) producers (Figure 3.3E). ThCTL were found in both at similar proportions (Figure 3.3D-E).

In the spleen, donor and host subset patterns were also similar. Both donor FluNP and responding host CD4 cells at 8 dpi in the spleen expressed similar levels of T-bet (Figure 3.4A, E) and IFN $\gamma$  (Figure 3.4 B, E), and at lower levels than seen in the lung (Figure 3.3E), as expected. A larger fraction, about 75%, of both donor and host cells expressed TNF $\alpha$  (Figure 3.3B, E), while about half of both populations expressed IL-2 (Figure 3.3B, E) at 8 dpi in the spleen. About one-quarter of both donor and host cells were triple cytokine producers in the spleen (Figure 3.4E), slightly greater than in the lung (Figure 3.3E). We note that the donor FluNP effector cells made more IFN $\gamma$  in the lung (Fig 3.3E) and more TNF $\alpha$  and IL-2 in the spleen (Fig 3.4E) compared to the endogenous host cells. Perhaps these subtle differences in cytokine expression reflect a difference in collective TCR affinity between the homogenous FluNP cells and the heterogeneous

**Figure 3.3. Day 8 lung donor FluNP and host CD4, CD44<sup>hi</sup> effector phenotype and function**

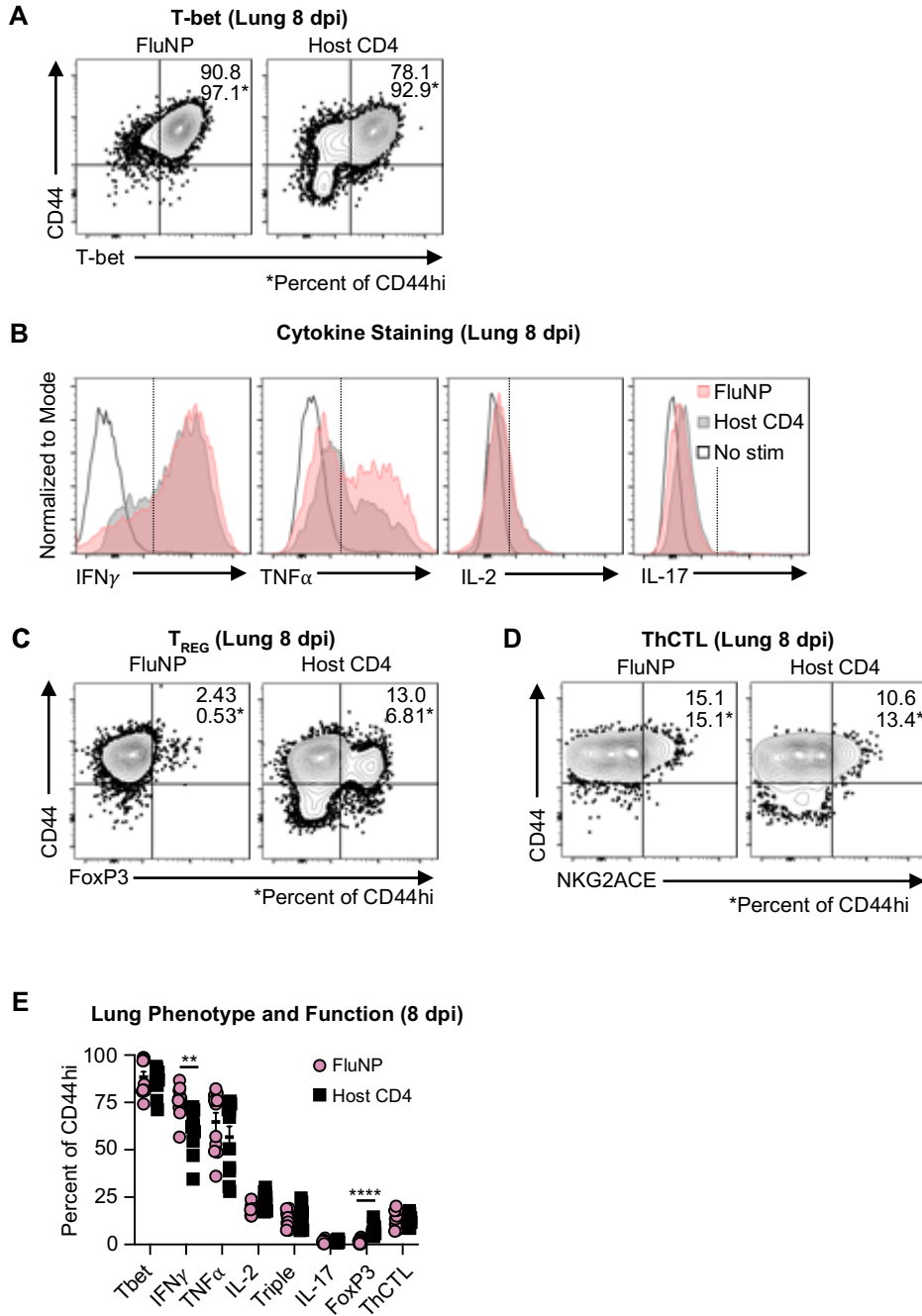


### **Figure 3.3. Day 8 lung donor FluNP and host CD4, CD44<sup>hi</sup> effector phenotype and function**

(A-E) Naïve FluNP.Thy1.1<sup>+/-</sup> cells were transferred to B6 hosts, then infected with a sub-lethal dose of PR8. Lungs were collected at 4, 6, 8, 12, 21 and 63 dpi and percent expression of effector markers on donor FluNP and responding host CD4<sup>+</sup>, CD44<sup>hi</sup> cells were determined by surface or ICCS FACS. (A-D) Representative FACS plots for effector subset analysis (8 dpi) gated on lung donor FluNP and responding host CD4<sup>+</sup>, CD44<sup>hi</sup> cells: (A) T-bet<sup>+</sup> CD44<sup>+</sup>, (B) cytokines (IFN $\gamma$ <sup>+</sup>, TNF $\alpha$ <sup>+</sup>, IL-2<sup>+</sup>, IL-17<sup>+</sup>), (C) NKG2A/C/E<sup>+</sup> CD44<sup>+</sup>, and (D) FoxP3<sup>+</sup> CD44<sup>+</sup>. (E) Expression of markers associated with subsets of CD4 effectors were analyzed at 8 dpi in lung: Th1 (T-Bet<sup>+</sup>, IL-2<sup>+</sup>, IFN $\gamma$ <sup>+</sup>, TNF $\alpha$ <sup>+</sup>), Triple positive (IL-2<sup>+</sup>, IFN $\gamma$ <sup>+</sup>, TNF $\alpha$ <sup>+</sup>), Th17 (IL-17<sup>+</sup>), Treg (FoxP3<sup>+</sup>) and lung ThCTL (NKG2A/C/E). Day 8 Pooled data, n = 9-10, two experiments. Statistical significance determined by two-tailed independent t test (\*p<0.05, \*\*p<0.01, \*\*\*p<0.001, \*\*\*\*p<0.0001).

**Figure 3.4. Day 8 spleen donor FluNP and host CD4, CD44hi effector phenotype and function**

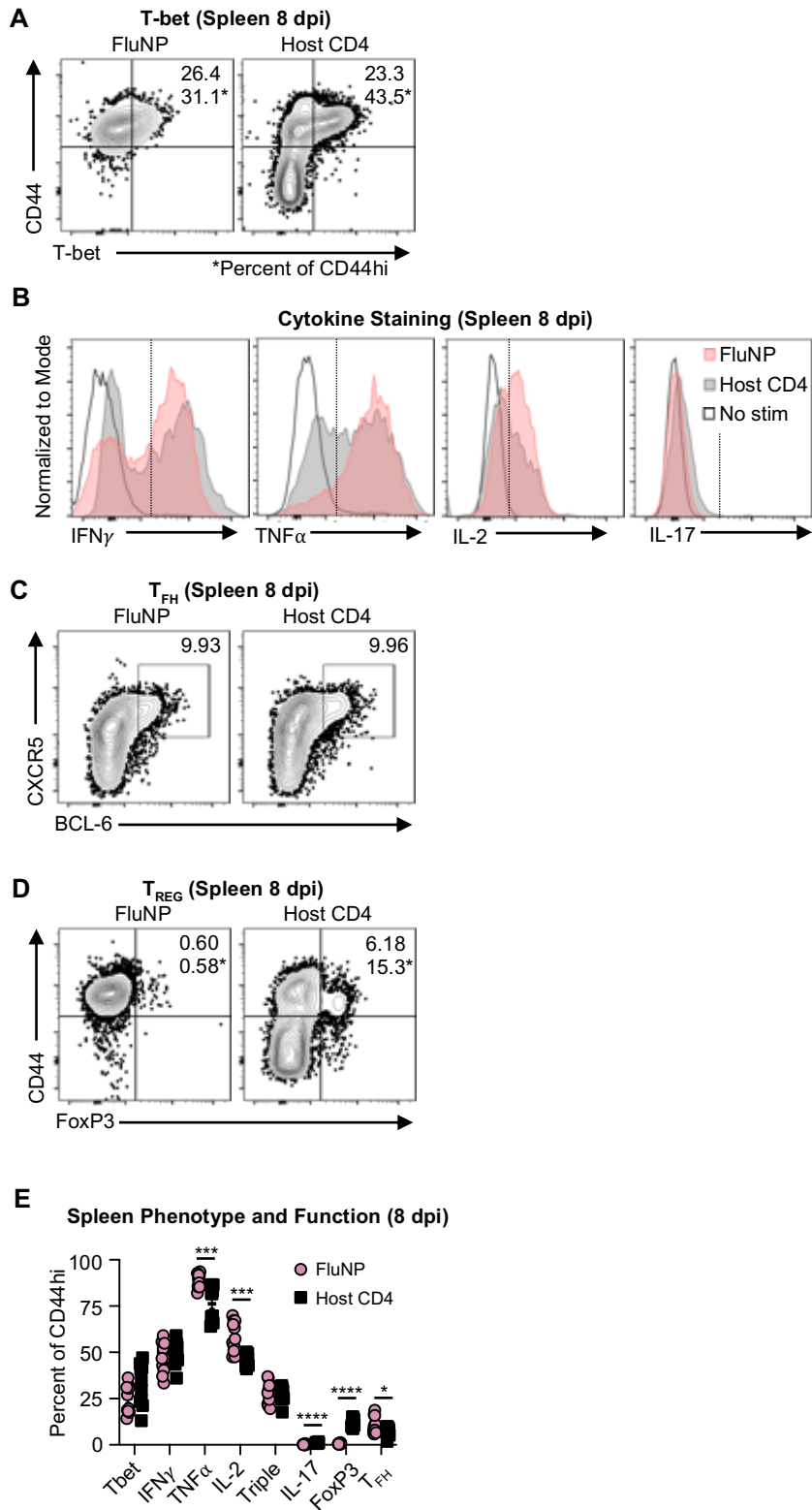


### **Figure 3.4. Day 8 spleen donor FluNP and host CD4, CD44<sup>hi</sup> effector phenotype and function**

**(A-E)** Naïve FluNP.Thy1.1<sup>+/-</sup> cells were transferred to B6 hosts, then infected with a sub-lethal dose of PR8. Spleens were collected at 4, 6, 8, 12, 21 and 63 dpi and percent expression of effector markers on donor FluNP and responding host CD4<sup>+</sup>, CD44<sup>hi</sup> cells were determined by surface or ICCS FACS. **(A-D)** Representative FACS plots for effector subset analysis (8 dpi) gated on lung donor FluNP and responding host CD4<sup>+</sup>, CD44<sup>hi</sup> cells: **(A)** T-bet<sup>+</sup> CD44<sup>+</sup>, **(B)** cytokines (IFN $\gamma$ <sup>+</sup>, TNF $\alpha$ <sup>+</sup>, IL-2<sup>+</sup>, IL-17<sup>+</sup>), **(C)** spleen T<sub>FH</sub> (CXCR5<sup>+</sup>, BCL-6<sup>+</sup>), and **(D)** FoxP3<sup>+</sup> CD44<sup>+</sup>. **(E)** Expression of markers associated with subsets of CD4 effectors were analyzed at 8 dpi in spleen: Th1 (T-Bet<sup>+</sup>, IL-2<sup>+</sup>, IFN $\gamma$ <sup>+</sup>, TNF $\alpha$ <sup>+</sup>), Triple positive (IL-2<sup>+</sup>, IFN $\gamma$ <sup>+</sup>, TNF $\alpha$ <sup>+</sup>), Th17 (IL-17<sup>+</sup>), Treg (FoxP3<sup>+</sup>) and spleen T<sub>FH</sub> (CXCR5<sup>+</sup>, BCL-6<sup>+</sup>). Day 8 Pooled data, n = 9-10, two experiments. Statistical significance determined by two-tailed independent t test (\*p<0.05, \*\*p<0.01, \*\*\*p<0.001, \*\*\*\*p<0.0001).

responding polyclonal host CD4s. Overall, the effector responses of donor monoclonal FluNP and host polyclonal CD4 to IAV were comparable.

We examined memory populations at 21 dpi, focusing on phenotypically distinct memory subsets: central memory  $T_{CM}$  (CD127<sup>+</sup> CD44<sup>+</sup> CD62L<sup>+</sup>), effector memory  $T_{EM}$  (CD127<sup>+</sup> CD44<sup>+</sup> CD62L<sup>-</sup>) in the spleen, and resident memory  $T_{RM}$  (CD44<sup>+</sup> CD69<sup>+</sup>) in the lung. We found slightly more FluNP  $T_{RM}$  in the lung on day 21 (Figure 3.5A, E), while the fraction of both donor and host spleen  $T_{CM}$  and  $T_{EM}$  were equivalent (Figure 3.5C, E). Both memory donor and host cells expressed high levels of the canonical CD4 memory marker CD127 (~75%) in all tissues (Figure 3.5B, E), although a slightly higher fraction of donor cells expressed CD127 in the lung compared to the host. These nuanced differences in lung memory may reflect that the FluNP cells have a greater propensity to take up residence in the lung compared to the polyclonal host CD4 memory and again may reflect a difference in collective TCR affinity between the homogenous FluNP cells and the heterogeneous responding polyclonal host CD4.

Taken together, the kinetics, effector response, and memory formation of the CD4 FluNP cells very closely mimics the endogenous polyclonal host CD4 response to IAV. These data support the suitability of this model to investigate the impact of peptide avidity on memory generation.

### **Establishment of the NP peptide binding frame and affinity of NP peptides for I-A<sup>b</sup>**

To study the role of peptide avidity, we generated a series of NP peptides with single amino acid (aa) substitutions that sample a broad range of abilities to stimulate the naïve FluNP response when pulsed on B6-derived activated APC. We sought to identify

**Figure 3.5. Day 21 donor FluNP and host CD4, CD44hi spleen, dLN and lung memory subsets: tissue resident memory ( $T_{RM}$ ), effector memory ( $T_{EM}$ ) and central memory ( $T_{CM}$ )**

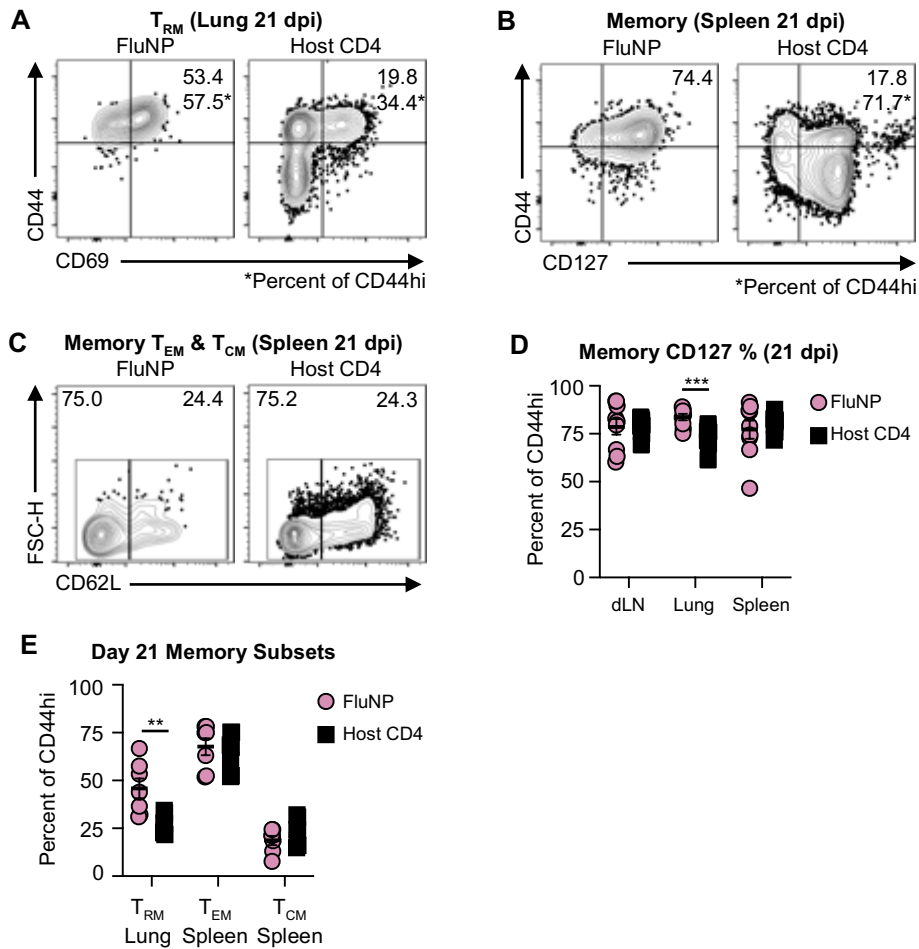


**Figure 3.5. Day 21 donor FluNP and host CD4, CD44<sup>hi</sup> spleen, dLN and lung memory subsets: tissue resident memory (T<sub>RM</sub>), effector memory (T<sub>EM</sub>) and central memory (T<sub>CM</sub>)**

(A-E) Phenotyping of memory subsets (21 dpi). Naïve FluNP.Thy1.1<sup>+/-</sup> cells were transferred to B6 hosts, then infected with a sub-lethal dose of PR8. dLN, lung and spleen were collected at 21 dpi and percent expression of memory markers on donor FluNP and responding host CD4<sup>+</sup>, CD44<sup>hi</sup> cells was determined by FACS. Representative FACS plots gated on donor FluNP and responding host CD4<sup>+</sup>, CD44<sup>hi</sup> cells: (A) Lung CD69<sup>+</sup> CD44<sup>+</sup> and (B) Spleen CD44<sup>+</sup> CD127<sup>+</sup>. (C) Representative CD62L FACS plots gated on day 21 spleen donor FluNP, CD44<sup>hi</sup>, CD127<sup>+</sup> and host CD4<sup>+</sup>, CD44<sup>hi</sup>, CD127<sup>+</sup>. (D) Percent CD127 of CD44<sup>hi</sup> donor FluNP and responding host CD4<sup>+</sup>, CD44<sup>hi</sup> cells in dLN, lung and spleen. (E) Memory CD4 subsets were analyzed at 21 dpi: lung T<sub>RM</sub> (CD69<sup>+</sup>), spleen T<sub>EM</sub> (CD127<sup>+</sup> CD44<sup>+</sup> CD62L<sup>-</sup>) and spleen T<sub>CM</sub> (CD127<sup>+</sup> CD44<sup>+</sup> CD62L<sup>+</sup>). Day 21 Pooled data, n = 7, two experiments, mean +/- SEM. Statistical significance determined by two-tailed independent t test (\*p<0.05, \*\*p<0.01, \*\*\*p<0.001, \*\*\*\*p<0.0001).

substitutions that altered TCR interaction while maintaining tight peptide-MHC interaction. First, we identified the I-A<sup>b</sup> binding frame by scanning partially overlapping 11-residue peptides that cover the full NP<sub>311-325</sub> peptide for I-A<sup>b</sup> binding, using a fluorescent peptide competition binding assay and purified recombinant I-A<sup>b</sup> carrying a cleavable linker peptide (209). I-A<sup>b</sup> binding was substantially reduced for NP<sub>313-323</sub> and lost completely for NP<sub>314-324</sub>, (Figure 3.6A) suggesting that Y<sub>313</sub> occupied the key P1 position in the I-A<sup>b</sup> binding site (210, 211). We confirmed this using alanine-scanning mutagenesis, revealing Y<sub>313</sub> as the only position where I-A<sup>b</sup> binding was substantially affected (Figure 3.6A). To identify peptides that modulate TCR interaction, we introduced other substitutions in addition to alanine at the predicted TCR contact positions P2 (Ser→Gln), P5 (Arg→Lys), and P7 (Glu→Gln). Some of these substitutions caused moderate reductions in peptide-MHC binding, up to 3.4 for Q2 (Figure 3.6A).

### **NP peptide affinity and biological avidity for FluNP TCR**

To evaluate the effect of these substitutions on FluNP TCR interaction independent of peptide-MHC effects, we measured pMHC-TCR binding using a surface plasmon resonance (BIAcore) assay with streptavidin-immobilized biotinylated I-A<sup>b</sup>-peptide complexes and recombinant soluble FluNP TCR (Figure 3.6B). FluNP TCR bound to I-A<sup>b</sup> carrying the parent NP<sub>311-325</sub> peptide or truncated NP<sub>311-322</sub> (NPT) with high affinity ( $K_D \sim 3\mu\text{M}$ ) (Figure 3.6B). The other substitutions at predicted TCR contact position caused reductions in pMHC-TCR affinity ranging from ~20-fold (for A7) to >150-fold (for Q7). The A5 substitution abrogated detectable binding.

**Figure 3.6. NP peptide binding affinity for I-A<sup>b</sup> and FluNP TCR**

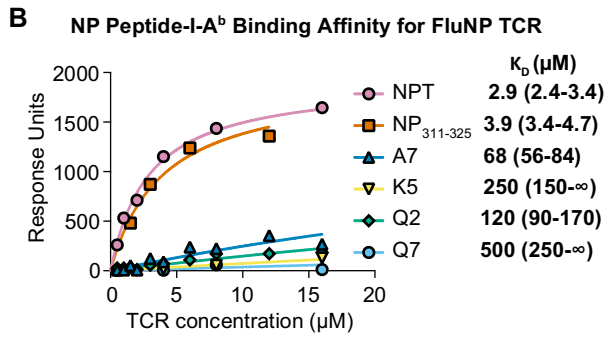
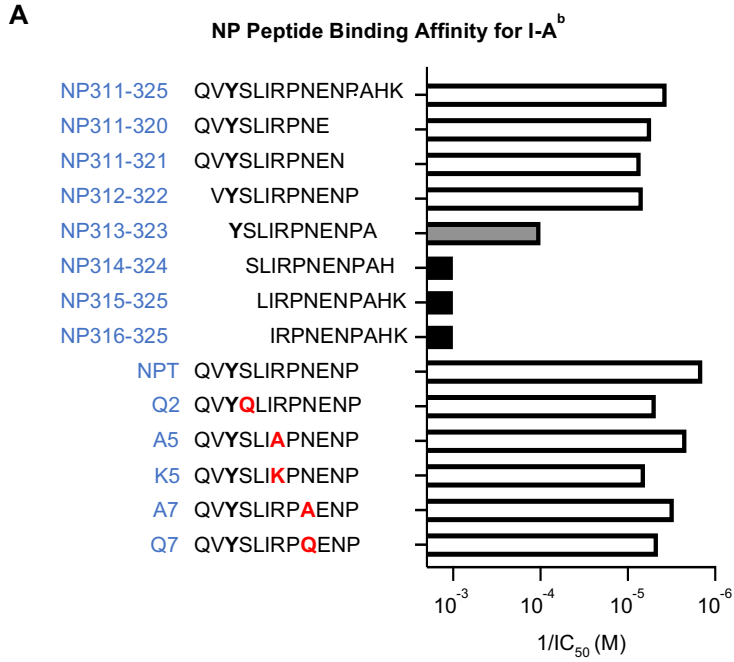


### **Figure 3.6. NP peptide binding affinity for I-A<sup>b</sup> and FluNP TCR**

(A) Peptide name, aa sequence (P1=Y, mutations in red) and the I-A<sup>b</sup> binding affinities of the NP<sub>311-325</sub> length variants and mutants were experimentally determined to identify the I-A<sup>b</sup> binding frame. The reciprocal of the IC<sub>50</sub> is shown. (B) Maximal response for a given TCR concentration was plotted for each peptide-MHC complex and nonlinear fits were generated using the equation  $Y=B_{max} * X / (K_D + X)$ . The fit was constrained to share a consistent B<sub>max</sub> and yield a K<sub>D</sub> value of <500. The resulting K<sub>D</sub> values are shown in μM with 95% confidence intervals.

Experiments conducted by Padma P. Nanaware and Grant C. Weaver (Lawrence J. Stern Laboratory).

To rank the substituted NP peptides by their ability to stimulate a biological FluNP response (functional avidity), we loaded bone marrow derived dendritic cells (BMDC) with peptides over a broad dose range and evaluated how well they stimulated naïve FluNP.Thy1.1<sup>+/-</sup>.Nurr77<sup>eGFP+/-</sup> cells *in vitro*. After 2d, we assessed induction of key markers associated with naïve T cell activation and early responses: CD69 (Figure 3.7A), CD25 (IL-2R $\alpha$ ) (Figure 3.7B) and Nurr77 (Figure 3.7C). By all three assays, FluNP CD4 T cells responded in a dose and affinity dependent manner. Thus, we could confidently rank the relative avidity of the peptide-MHC-II complex on APC for the FluNP TCR on the CD4 T cells. We classify the NPT & NP<sub>311-325</sub> as high avidity, A7 & K5 as medium (mid) avidity, Q2 & Q7 as low avidity, and A5 and unpulsed BMDC as negative controls (neg). In each assay, the high peptides (NP<sub>311</sub> and NPT) induce peak responses at doses 100-fold lower than the middle peptides (A7, K5), and the low peptides (Q2, Q7) require 10 times the dose as the two middle peptides (Figure 3.7).

From here on, we use a high dose of 10<sup>-4</sup> M to pulse APC, to minimize the contribution of peptide density and maximize the contribution of pMHC-TCR affinity. At this concentration, all 6 peptides (NPT, NP<sub>311-325</sub>, A7, K5, Q2, Q7) stimulate a measurable FluNP naïve CD4 T cell response. This gives us a panel of peptides, that when presented by MHC-II (I-A<sup>b</sup>) on APC, span a broad range of avidity for the FluNP TCR.

### **Peptide avidity at the effector phase determines the number of memory cells**

We evaluated the impact of peptide avidity on *in vivo* memory generation using a sequential adoptive transfer model, developed previously (200). The APC are short-lived and present Ag for only 48-72h (200), defining the discrete checkpoint of Ag recognition.

**Figure 3.7. Functional avidity of NP peptides measured by naïve FluNP activation**

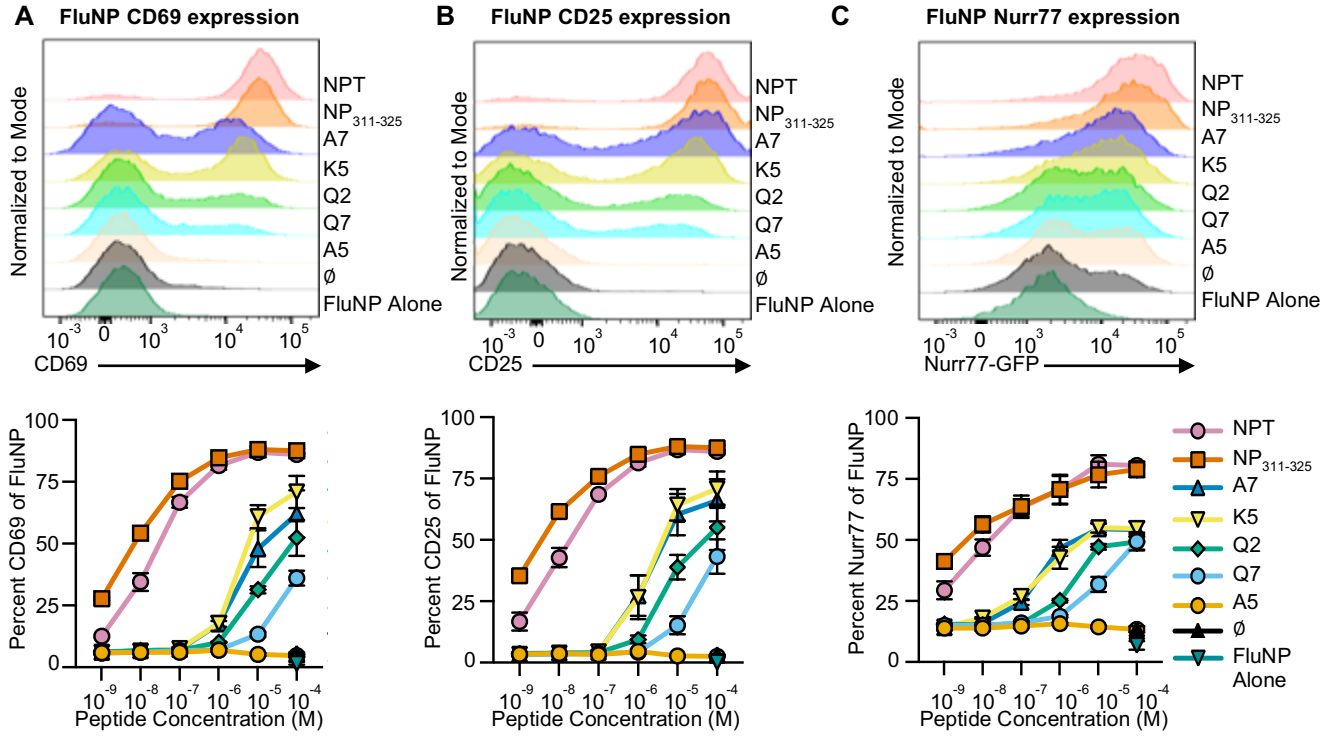


**Figure 3.7. Functional avidity of NP peptides measured by naïve FluNP activation**

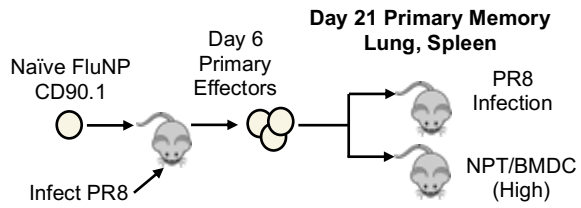
(A-C) Naïve FluNP CD4 T cells were co-cultured with BMDC pulsed with each of the NP peptides for 2d *in vitro*. Induction of markers functionally associated with TCR signal strength was measured. (A) CD69; (B) CD25; and (C) Nur77. Top histograms display level of marker expression following stimulation with Ag/APC pulsed at  $10^{-4}$  M. Bottom displays dose response curve to a broad range of peptide concentrations used to pulse APC. The rank of peptide functional avidity is shown on right. Pooled data, n = 6, two experiments, mean +/- SEM (% of FluNP).

To further validate our system, we utilized the sequential transfer model to compare the number of FluNP memory cells generated from high avidity peptide/APC stimulation at the effector phase to the number of FluNP memory cells generated from IAV infection. To do this, we transferred  $5 \times 10^5$ - $1 \times 10^6$  naïve FluNP.Thy1.1<sup>+/-</sup> cells into B6 hosts and infected them with a sub-lethal (0.3LD<sub>50</sub>) dose of PR8. We then isolated 6 dpi FluNP effectors and transferred them into either 6 dpi PR8 infection matched hosts, or into uninfected hosts along with a panel including high, mid and low avidity NP peptides pulsed on activated APC and enumerated the number of day 21 memory FluNP cells in the spleen, dLN and lung of second hosts. We first analyzed the response to the high affinity NPT/APC compared to transfer into PR8 infection matched hosts without Ag/APC (Figure 3.8A). At 21 dpi, NPT/APC stimulated FluNP effectors produced as many memory cells in spleen and lung and only slightly fewer in dLN as did PR8 infection (Figure 3.8B). Thus, a high avidity peptide/APC generates an equivalent number of memory cells from effectors as does IAV infection here (Figure 3.8B), and as seen in an equivalent model using OT-II Tg CD4 T cells responding to either Ag/APC or PR8-OVA<sub>II</sub> infection (200). This confirms our previous finding that infection is not required for optimal transition of CD4 effector cells to memory and that cognate Ag interactions delivered by APC during the effector checkpoint are sufficient (200).

As our lab has previously shown that cognate Ag interactions at the effector checkpoint, 5-7 dpi, are required for generating memory and produce an optimal number of CD4 memory cells (200, 201), we investigated how the strength of the pMHC-TCR interaction during the effector checkpoint would influence memory numbers in the 2<sup>nd</sup>

**Figure 3.8. Comparison of day 21 FluNP memory cell numbers generated from IAV and high avidity Ag/APC**

**A**



**B** Memory Donor Cell Recovery Day 21 (IAV Inf. vs. NPT/BMDC)

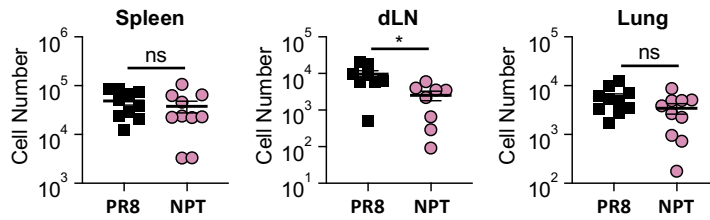


**Figure 3.8. Comparison of FluNP memory cell numbers generated from IAV and high avidity Ag/APC**

(A) Experimental design: comparison of PR8 infection to high peptide/APC memory generation. Naïve FluNP.Thy1.1<sup>+/-</sup> cells were transferred to B6 hosts, then infected with PR8. At 6 dpi, FluNP effector cells were isolated from the 1<sup>st</sup> hosts by CD90.1 MACS and 1.5x10<sup>6</sup> day 6 FluNP effectors were co-transferred with peptide Ag/APC into uninfected 2<sup>nd</sup> hosts or without APC into day 6 PR8 infection matched hosts, infected 6d previously. Fifteen days later (21 dpi) 2<sup>nd</sup> hosts were sacrificed, and donor FluNP cells were analyzed by FACS. (B) FluNP cell numbers were enumerated by FACS in the dLN, lung and spleen at 21 dpi. Pooled data, n = 10, three experiments, mean +/- SEM. Statistical significance determined by two-tailed independent t test (\*p<0.05, \*\*p<0.01, \*\*\*p<0.001, \*\*\*\*p<0.0001).

hosts using the sequential transfer model (Figure 3.9A). To do this, we generated 6 dpi FluNP effectors and co-transferred along with a panel of NP peptide-pulsed APC into uninfected second hosts and enumerated the number of day 21 memory FluNP cells in the spleen, dLN and lung of second hosts (Figure 3.9A). The impact of peptide avidity was striking (Figure 3.9B-C), with memory cell numbers clearly dependent on the rank of the functional avidity of the NP peptides established in Figure 3.7. We noted that the greatest differences in memory cell number were seen in the lung, closely followed by the dLN, and differences in the spleen were clear but not as large (Figure 3.9C). The significance of these changes between groups of peptides is illustrated by the fold change in memory cell number between each peptide compared to unpulsed (Figure 3.10A), to low peptides (Figure 3.10B) and to middle peptides (Figure 3.10C). In the lung at 21 dpi, there were 280-fold more donor memory FluNP cells in the NPT pulsed group compared to the unpulsed group (Figure 3.10A), 29 and 36-fold more compared to the low groups (Figure 3.10B) and 6 and 8-fold more donor memory cells compared to the mid groups (Figure 3.10C). A nearly identical pattern was seen in the dLN. In spleen, there were 16-fold more FluNP cells in the NPT (high) group compared to the unpulsed group (Figure 3.10A) and 5-8-fold to the mid groups (Figure 3.10C), both highly significant (Figure 3.9C). Unlike the dLN and lung, there was no significant difference in the number of day 21 donor FluNP cells in the spleen between the mid and low stimulated groups (Figure 3.9C), although both showed significant increases compared to the unpulsed group. This demonstrates that peptide avidity, especially in the mid to low range, at the effector checkpoint has a larger impact on the number of memory cells in the dLN and lung, than in the spleen. One possible

**Figure 3.9. Peptide avidity during the primary effector phase dictates the size of the memory population**

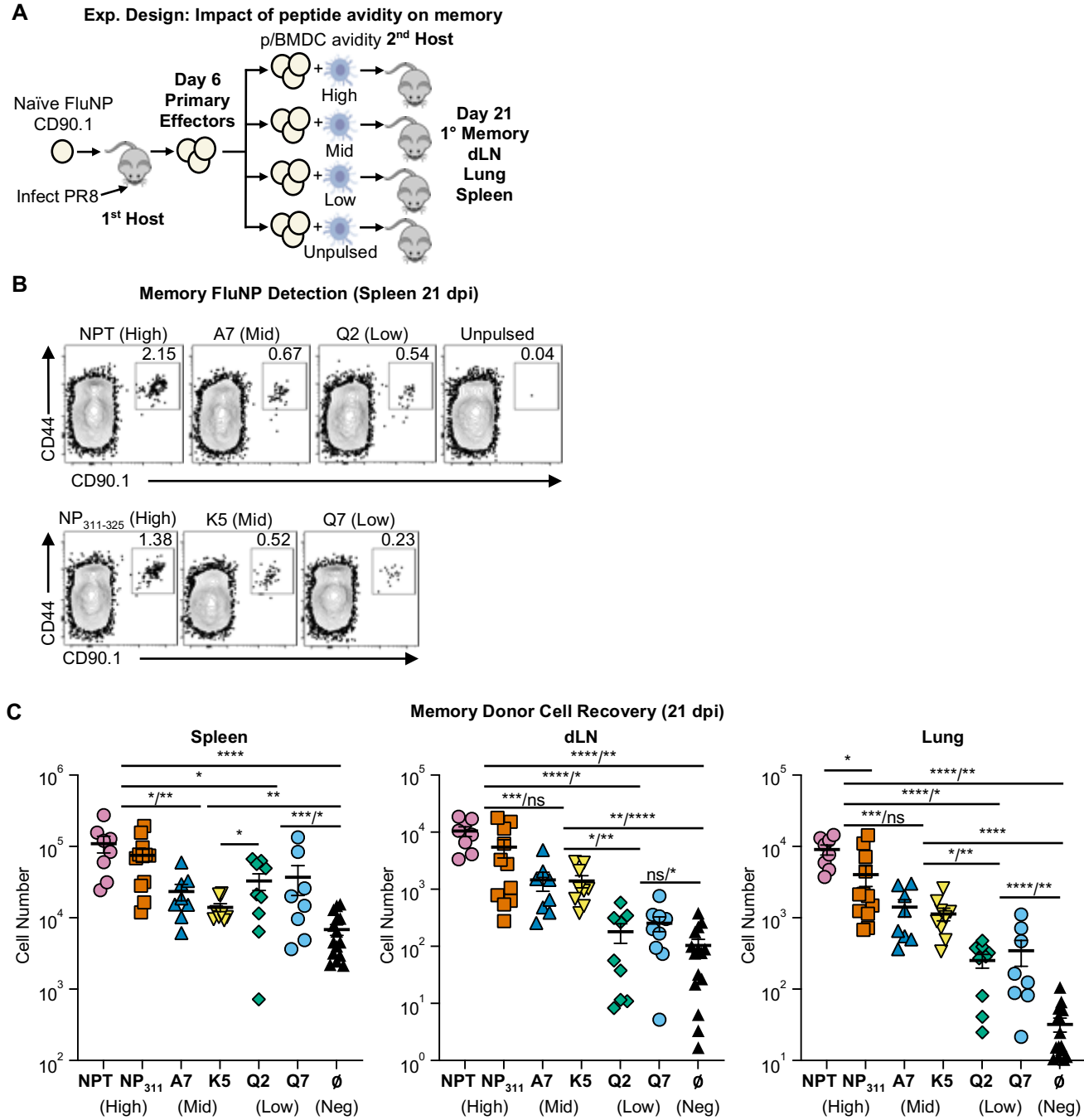


**Figure 3.9. Peptide avidity during the primary effector phase dictates the size of the memory population**

(A) Experimental design: Impact of peptide avidity on memory generation.  $1.5 \times 10^6$  6d FluNP effectors were co-transferred with Ag/APC into uninfected 2<sup>nd</sup> hosts. The panel of different peptides was used to pulse groups of activated BMDC yielding peptide/\*APC with different avidity for the TCR of the FluNP T cells. (B) Representative FACS plots showing donor memory cells by CD44 and CD90.1 expression in the spleen at 21 dpi. (C) Number of FluNP memory cells detected at 21dpi in the dLN, lung and spleen of second hosts. Spleen comparisons: highs vs. unpulsed, highs vs. lows, NPT vs. A7 / highs vs. K5; mids vs. unpulsed, K5 vs. Q2; Q2 vs. unpulsed / Q7 vs. unpulsed. dLN comparisons: NPT vs. unpulsed / NP<sub>311-325</sub> vs. unpulsed, NPT vs. lows / NP<sub>311-325</sub> vs. lows, NPT vs. mids / NP<sub>311-325</sub> vs. mids; A7 vs. unpulsed / K5 vs. unpulsed, A7 vs. lows / K5 vs. lows; Q2 vs. unpulsed / Q7 vs. unpulsed. Lung comparisons: NPT vs. NP<sub>311-325</sub>; NPT vs. unpulsed / NP<sub>311-325</sub> vs. unpulsed, NPT vs. lows / NP<sub>311-325</sub> vs. lows, NPT vs. mids / NP<sub>311-325</sub> vs. mids; mids vs. unpulsed, mids vs. Q2 / mids vs. Q7; Q2 vs. unpulsed / Q7 vs. unpulsed. Pooled data, n = 8-15, four experiments, mean +/- SEM. Statistical significance determined by two-tailed independent t test (\*p<0.05, \*\*p<0.01, \*\*\*p<0.001, \*\*\*\*p<0.0001).

**Figure 3.10. Impact of peptide avidity on fold-change of memory FluNP cell number (Day 21)**

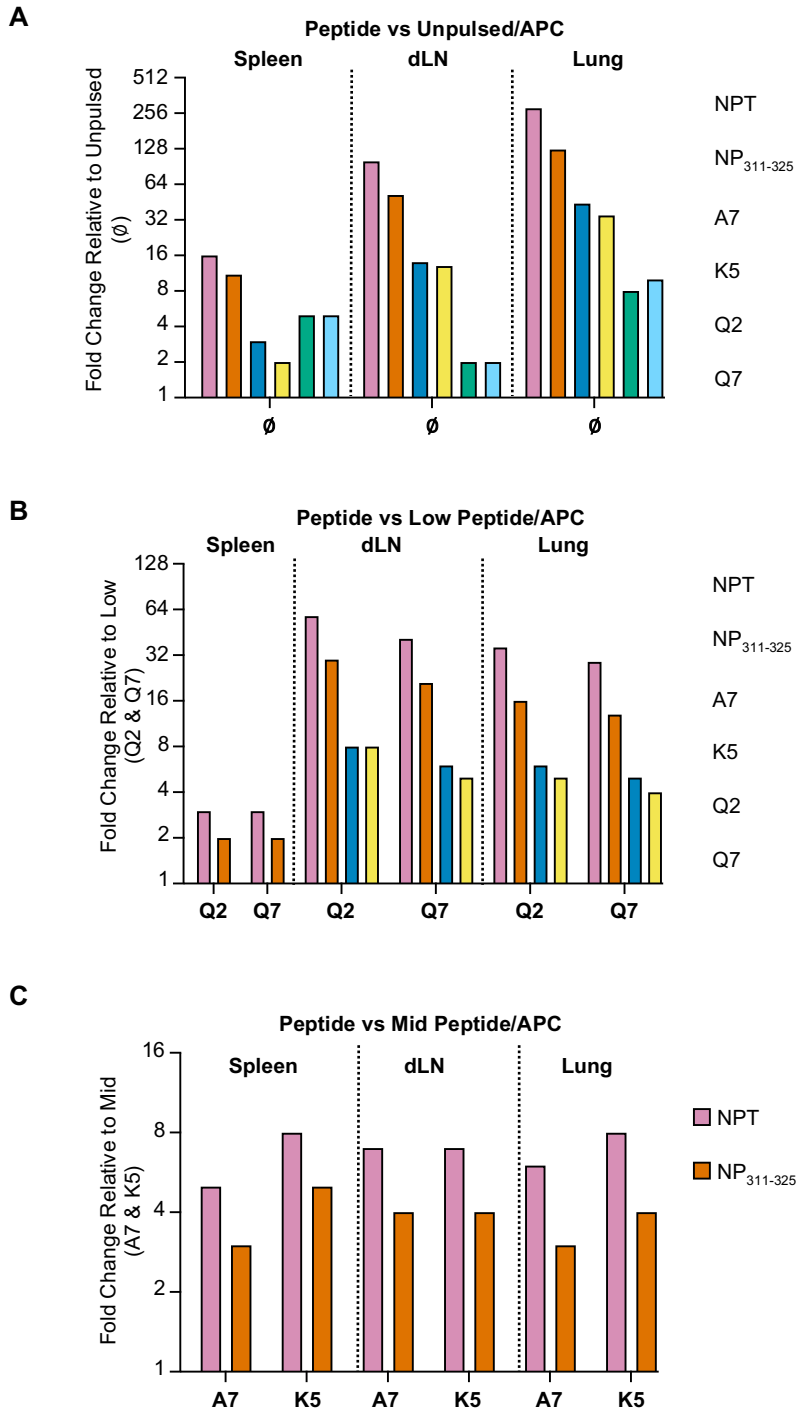


**Figure 3.10. Impact of peptide avidity on fold-change of memory FluNP cell number (Day 21)**

FluNP cell number fold change relative to unpulsed (A), low peptide-pulsed (B) and mid peptide (C) in dLN, lung and spleen 21 dpi, x-axis lists fold change denominator. Fold change calculated from cell numbers in Figure 3.8. Pooled data, n = 8-15, four experiments, mean +/- SEM.

explanation for this is that a fraction of the 6 day effectors isolated from the SLO, already have committed to memory, but need further signals to migrate to lung and dLN. These data indicate that the strength of pMHC-TCR interaction at the effector checkpoint determines the size of the memory population.

### **Phenotype of day 21 memory FluNP cells**

To demonstrate that the day 21 donor FluNP cells are memory cells, we looked for expression of the canonical CD4 memory marker CD127. The IL-7R $\alpha$  and its ligand IL-7 are needed to support CD4 memory generation in the secondary lymphoid tissues (156). The day 21 donor FluNP memory cells uniformly express high CD127 (Figure 3.11A) in all stimulated groups in the spleen and dLN (Figure 3.11B-C), while in the lung many donor FluNP cells do not express CD127 (Figure 3.11D). The percent expression of CD127 on day 21 memory donor FluNP cells in the spleen and dLN generated *in situ* in response to IAV (Figure 3.5B, C) is roughly equivalent, greater than 75%, to the FluNP memory cells generated *in vivo* in the adoptive transfer system following stimulation at the effector checkpoint by all NP peptides (Figure 3.11B-C). This is in contrast to the lung, in which day 21 memory donor FluNP cells generated *in situ* in response to IAV infection express high levels of CD127, greater than 75%, while the FluNP memory cells on day 21 in the lung following adoptive transfer and NP peptide stimulation express far less (25-50%). Since we find that peptide avidity has the greatest impact on memory FluNP cell number fold change in the lung (Figure 3.10), despite a greater percentage of the low stimulated FluNP cells expressing CD127 (Figure 3.11D), we posit that the lack or loss of CD127 expression on lung memory cells without IAV infection through the effector phase may

**Figure 3.11. CD127 expression of memory FluNP from spleen, dLN and lung (Day 21)**

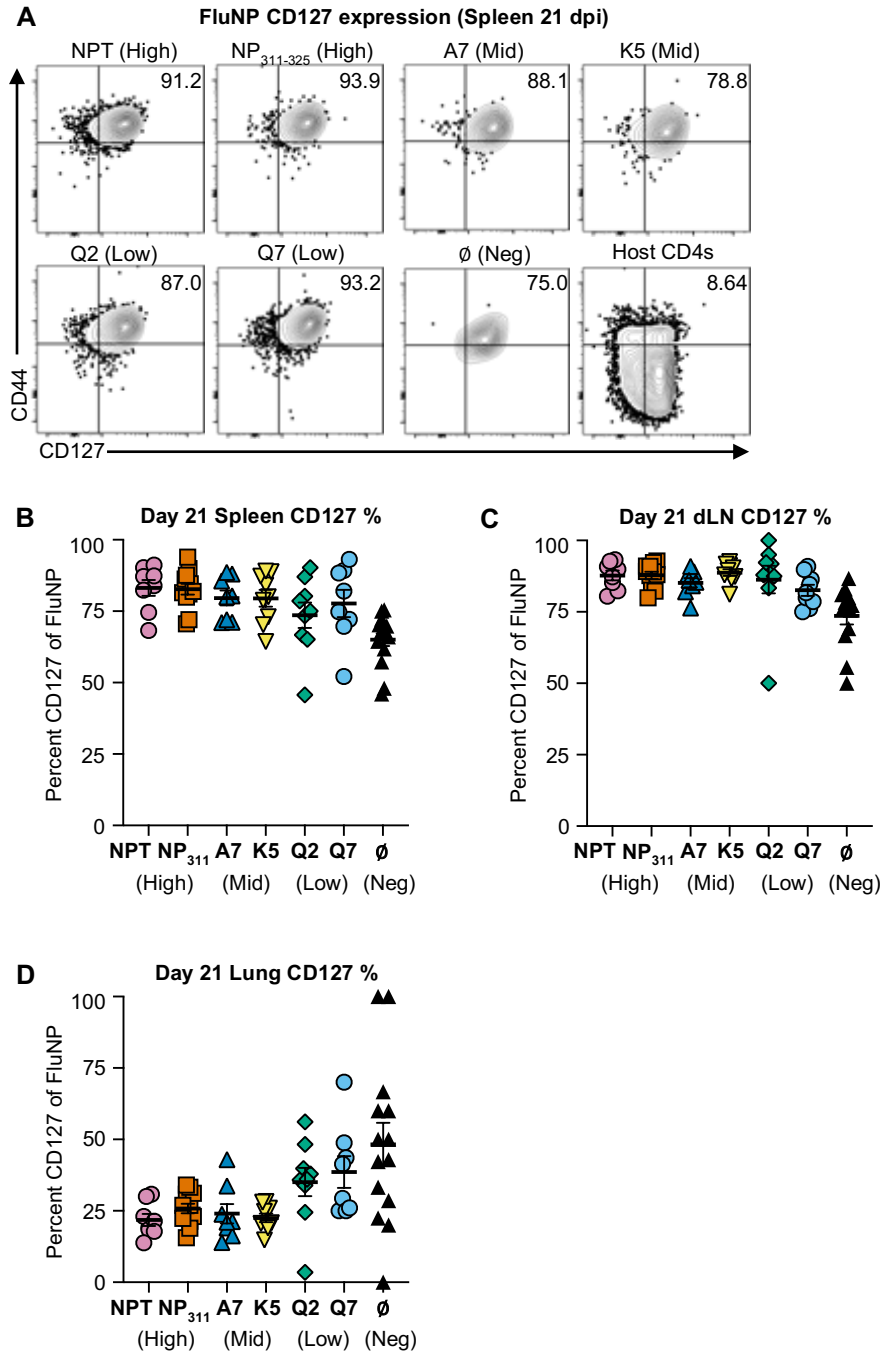


**Figure 3.11. CD127 expression of memory FluNP from spleen, dLN and lung (Day 21)**

(A) Representative FACS plots of CD44 and CD127 expression of donor FluNP. Gated on live singlets, CD4<sup>+</sup>, CD90.1<sup>+</sup> cells. (B-D) Percent of donor FluNP expressing CD127 on day at 21 dpi in (B) spleen (C) dLN and (D) lung. Pooled data, n = 8-15, four experiments, mean +/- SEM.

indicate that memory cells in the lung rely more on survival signals from other sources, such as IL-2 and IL-15, as opposed to IL-7.

We further characterized the day 21 memory donor FluNP cells by canonical memory markers: central memory  $T_{CM}$  ( $CD127^+ CD44^+ CD62L^+$ ), effector memory  $T_{EM}$  ( $CD127^+ CD44^+ CD62L^-$ ) in the spleen and dLN, and resident memory  $T_{RM}$  ( $CD44^+ CD69^+$ ) in the lung (Figure 3.12). To differentiate  $T_{CM}$  from  $T_{EM}$  memory cells in the spleen and dLN, we first gated on  $CD127^+$ ,  $CD44^+$  FluNP cells (Figure 3.11A) and then separated central memory from effector memory by  $CD62L$  expression (Figure 3.12A). We found the frequency of  $T_{CM}$  cells in the spleen (Figure 3.12B, left) and, to a slightly lesser degree, dLN (Figure 3.12C, left) equivalent between the different NP peptide stimulated groups, about 20% of all memory FluNP cells. We did find that the frequency of  $T_{EM}$  (Figure 3.12B, right) in the spleen and dLN (Figure 3.12C, right) decreased in conjunction with peptide avidity. Since  $T_{EM}$  are known to have the shortest lifespan of T cell memory populations, the reduction in frequency of  $T_{EM}$  following stimulation by lower avidity peptides might be due to the death of these cells. Alternatively, it is known that prime-boost vaccine strategies induce greater frequencies of CD8  $T_{EM}$  with each additional boost (192), so the increase in FluNP  $T_{EM}$  frequency in the spleen and dLN, resulting from increased peptide avidity, may reflect that the strength of the boost can also increase the frequency of  $T_{EM}$  cells. The proportions of *in situ* FluNP  $T_{EM}$  (~75%) and  $T_{CM}$  (~25%) induced in the spleen following IAV infection (Figure 3.5E) compared to those induced by the high peptides NPT and NP<sub>311-325</sub> on day 21 in the sequential transfer model ( $T_{EM}$  ~80%,  $T_{CM}$  ~20%) are roughly equal. This demonstrates that high avidity peptide Ag at the effector checkpoint,

**Figure 3.12. Memory subset characterization of memory FluNP in spleen and dLN T<sub>CM</sub> and T<sub>EM</sub>, Lung T<sub>RM</sub> (Day 21)**

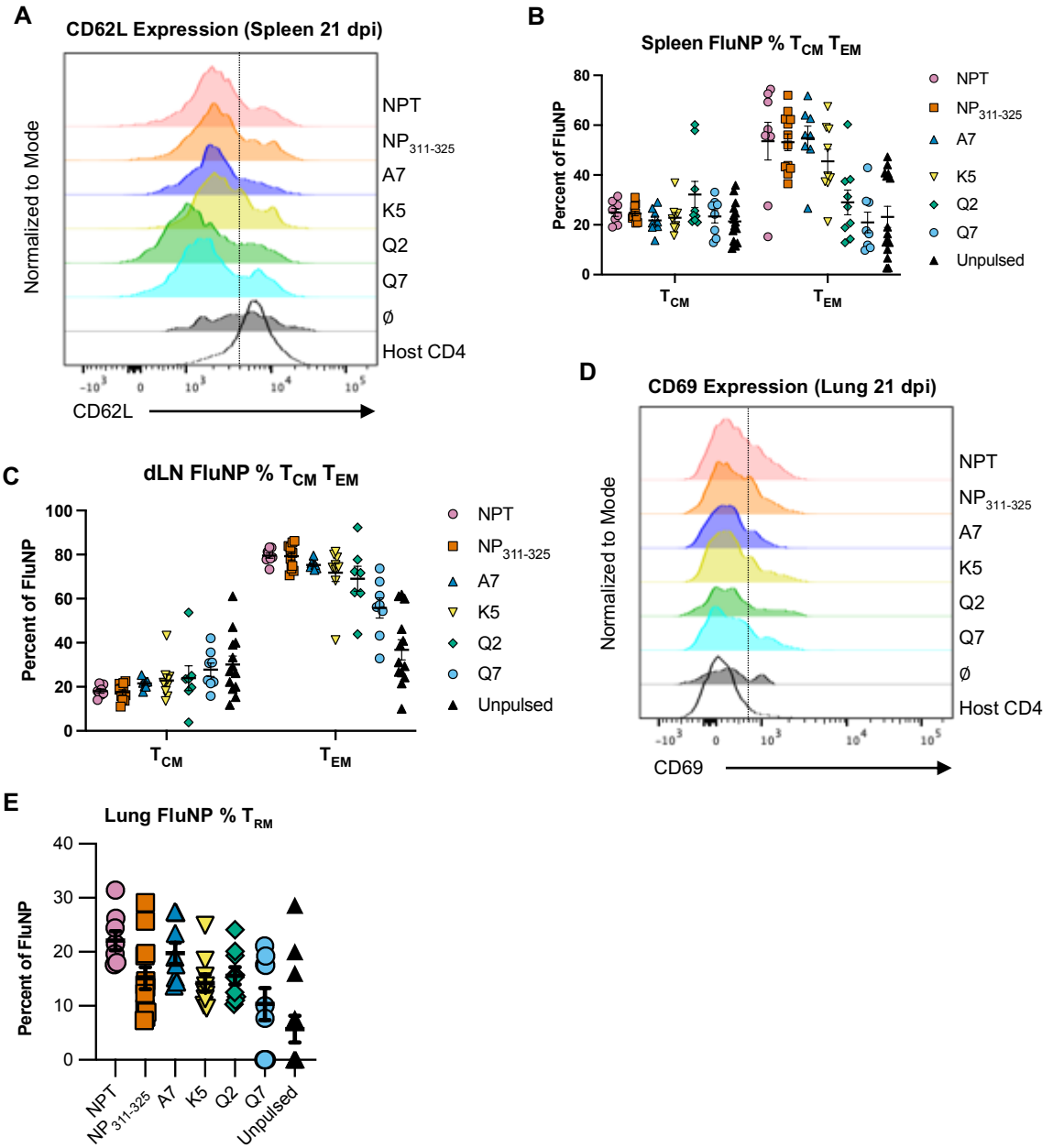


**Figure 3.12. Memory subset characterization of memory FluNP in spleen and dLN T<sub>CM</sub> and T<sub>EM</sub>, Lung T<sub>RM</sub> (Day 21)**

(A) Representative histogram of CD62L expression of spleen donor FluNP. Gated on live singlets, CD4<sup>+</sup>, CD90.1<sup>+</sup>, CD44<sup>hi</sup>, CD127<sup>+</sup> cells. (B-C) Percent T<sub>CM</sub> (CD44<sup>hi</sup>, CD127<sup>+</sup>, CD62L<sup>+</sup>) and T<sub>EM</sub> (CD44<sup>hi</sup>, CD127<sup>+</sup>, CD62L<sup>-</sup>) of donor FluNP CD44<sup>hi</sup>, CD127<sup>+</sup> cells on day at 21 dpi in (B) spleen (C) dLN. (D) Representative histogram of CD69 expression of spleen donor FluNP. Gated on live singlets, CD4<sup>+</sup>, CD90.1<sup>+</sup>, CD44<sup>hi</sup> cells. (E) Percent T<sub>RM</sub> (CD44<sup>hi</sup>, CD69<sup>+</sup>) of lung donor FluNP. (A-E) Representative and pooled data, n = 8-15, four experiments, mean +/- SEM.

without infection, can induce the same frequencies of  $T_{EM}$  and  $T_{CM}$  as IAV infection, and that as peptide avidity decreases, the total number memory FluNP cells and  $T_{EM}$  frequency of FluNP cells falls while the frequency of  $T_{CM}$  cells remains relatively stable. As all FluNP cells received signals from infection and Ag days 0-6 of the immune response, perhaps these early signals are sufficient to promote ~20-25% of the memory population to become  $T_{CM}$ , while peptide avidity and additional Ag stimulation promote a greater number of memory cells and a greater frequency of  $T_{EM}$  cells.

To distinguish  $T_{RM}$  in the lung we first gated on  $CD44^+$  FluNP cells and analyzed CD69 expression (Figure 3.12D). The  $T_{RM}$  frequency of day 21 donor FluNP memory cells in the lung increased as peptide avidity increased at the effector checkpoint (Figure 3.12D). I am cautious to call these FluNP cells true  $T_{RM}$  without further looking at i.v. antibody labeling to distinguish between cells close to the vasculature (i.v.  $Ab^+$ ) from those that are truly imbedded in the tissue and not near blood vessels (i.v.  $Ab^-$ ). If we compare  $T_{RM}$  frequencies of lung memory FluNP cells generated from *in situ* IAV infection, about 50% of day 21 lung memory FluNP cells are  $T_{RM}$  (Figure 3.5E), while from high avidity NP peptides in the sequential transfer model, about 25% are  $T_{RM}$  (Figure 3.12E), a two-fold reduction in  $T_{RM}$  frequencies. Although 6d FluNP effector cells received high avidity cognate Ag in the sequential transfer system, this did not generate as much  $T_{RM}$ , by CD69 expression, as did *in situ* IAV infection, suggesting the peptide/APC stimulation is not quite as effective as infection. We know generation of lung ThCTL and their development of tissue residence requires antigen recognition in the lung (183) and this does not occur when we introduce Ag/APC by the i.v. route, which may explain this difference.

We looked at CXCR3 expression on the day 21 memory donor FluNP cells in the spleen, dLN and lung. CXCR3 is the chemokine receptor for CXCL9 and CXCL10, which are expressed at high levels in the lung during IAV infection as a result of interferon signals (212). The chemokine receptor CXCR3 has been implicated in trafficking of CD4 cells to the lung during IAV infection (105, 213), as well as to the dLN (214). In addition, we previously noted that CXCR3 expression was increased on memory OT-II cells following cognate Ag signals at the effector checkpoint compared to donor cells that received no cognate Ag at the effector checkpoint (200). In this study, we found about a 20% increase in the fraction of day 21 donor memory FluNP cells that express CXCR3 in the spleen, dLN and lung in the NPT/APC (high) stimulated group compared to the unpulsed (Figure 3.13B). However, there was no clear pattern in CXCR3 expression between the different peptide/APC stimulated groups (Figure 3.13A-B), and the amount of CXCR3 expression, as measured by MFI of the CXCR3<sup>+</sup> day 21 donor memory FluNP cells normalized to the unpulsed group, was equivalent in the spleen, dLN and lung (Figure 3.13C). There are several possibilities as to why there is no clear pattern in CXCR3 expression on memory cells. The first is that CXCR3 expression on CD4 memory may be a digital on/off response to TCR stimulation as opposed to graded levels of expression based on peptide avidity (215). This notion fits with our data here and our previously published results (200) that show peptide stimulation compared to no stimulation at the effector checkpoint promotes more CXCR3 expression, but there are no differences between different groups stimulated by diverse peptide avidity (Figure 3.13). A second explanation is that signals during priming are sufficient to induce CXCR3 expression on 40-60% of day 21 donor memory

**Figure 3.13. CXCR3 expression by memory FluNP in spleen, dLN and lung (Day 21)**

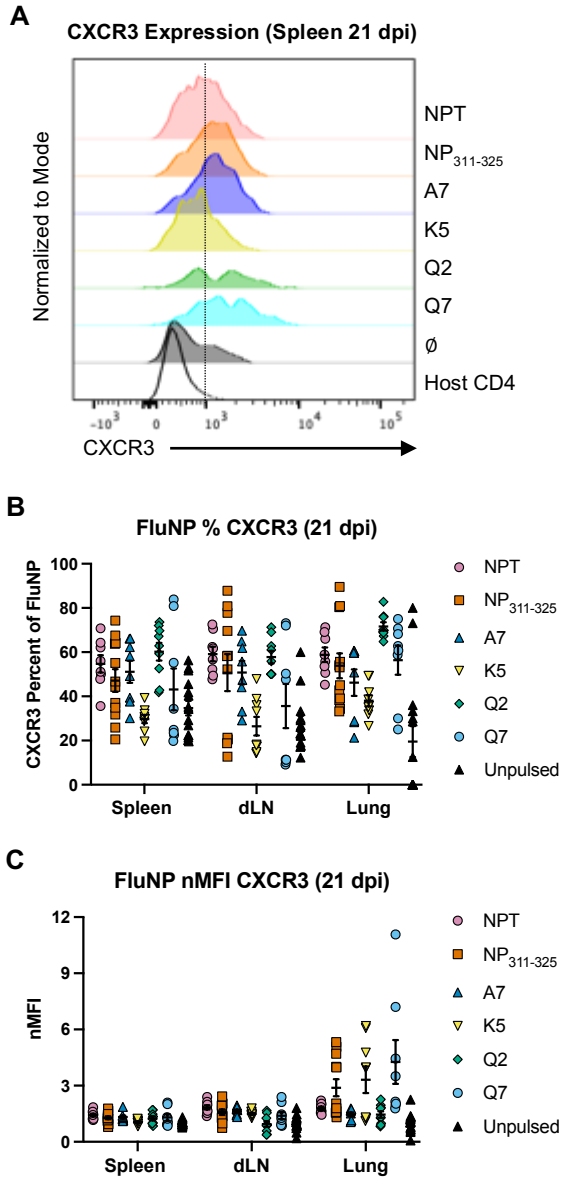


**Figure 3.13. CXCR3 expression by memory FluNP in spleen, dLN and lung (Day 21)**

(A) Representative histogram of CXCR3 expression of spleen donor FluNP. Gated on live singlets, CD4<sup>+</sup>, CD90.1<sup>+</sup>, CD44<sup>hi</sup> cells. (B) Percent CXCR3 expression of donor FluNP CD44<sup>hi</sup> cells on day 21 dpi in spleen, dLN and lung. (C) CXCR3 median fluorescence intensity normalized to unpulsed (nMFI) of CXCR3<sup>+</sup> donor FluNP CD44<sup>hi</sup> cells on day 21 dpi in spleen, dLN and lung.

FluNP cells and that cognate Ag interaction at the effector checkpoint has a limited or no role in CXCR3 induction. A third possibility is that the truth lies somewhere in the middle, that signals both during priming, and to some extent, during the effector checkpoint synergize to induce CXCR3 expression on the resultant CD4 memory cells. More work is needed to tease apart how effector checkpoint cognate Ag interactions influence CXCR3 expression on CD4 memory.

### **Immediate cytokine production from spleen day 21 memory FluNP cells**

We assessed immediate cytokine production *ex vivo* by the spleen FluNP memory cells generated from stimulation with the different avidity NP peptide-APC at the effector checkpoint by intracellular cytokine staining (ICCS) (Figure 3.14). Only one high avidity peptide (NPT) resulted in a slightly higher fraction of IFN $\gamma$ -capable memory compared to only one of the low (Q7) avidity peptides and to unpulsed APC (Figure 3.14A). Of the IFN $\gamma$ <sup>+</sup> spleen FluNP memory cells, there was no difference in the amount of IFN $\gamma$  produced, as measured by MFI (Figure 3.14A). There was no difference in the fraction of TNF $\alpha$ <sup>+</sup> spleen FluNP memory cells across the different peptide avidity groups, however TNF $\alpha$ <sup>+</sup> FluNP cells in one of the low avidity stimulated groups (Q7) produced more TNF $\alpha$  than TNF $\alpha$ <sup>+</sup> FluNP cells in one of the high avidity groups (NP<sub>311-325</sub>) (Figure 3.14B). FluNP memory cells in the NPT high avidity group had a slightly larger fraction of IL-2<sup>+</sup> cells compared to the unpulsed group, while IL-2<sup>+</sup> cells in the K5 mid avidity group produced slightly more IL-2 than FluNP cells in the Q2 low avidity and unpulsed groups (Figure 3.14C). Overall, these results reveal that all memory cells produced similar levels of IFN $\gamma$ , TNF $\alpha$  and IL-2 and thus the fewer number of FluNP memory cells that develop at lower

**Figure 3.14. Cytokine expression by memory FluNP in spleen (Day 21)**

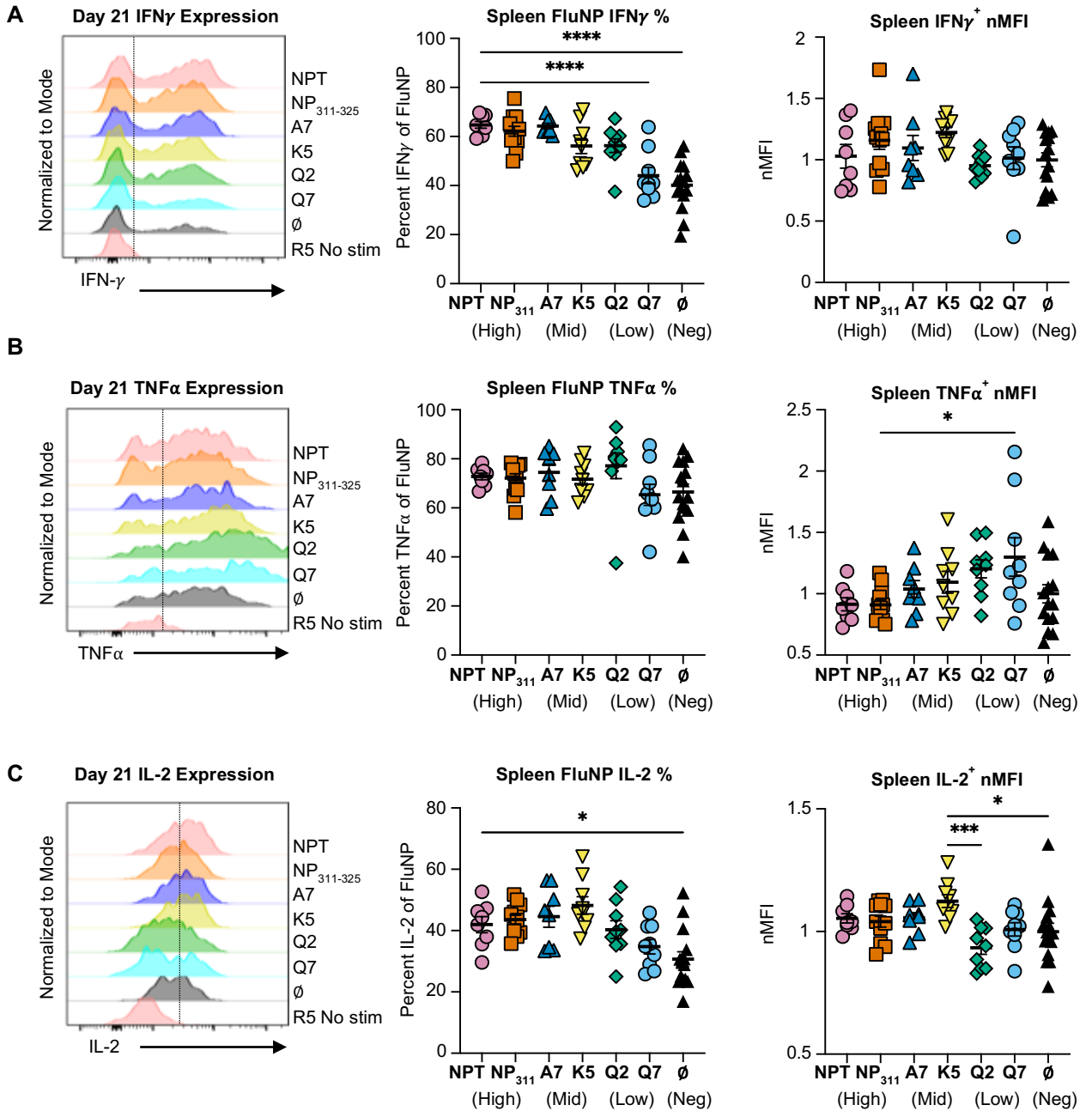


**Figure 3.14. Cytokine expression by memory FluNP in spleen (Day 21)**

(A-C) Representative histograms (left), percent expression (middle) and normalized median fluorescence intensity (nMFI) (right) of ICCS (A) IFN $\gamma$ <sup>+</sup> (B) TNF $\alpha$ <sup>+</sup> (C) IL-2<sup>+</sup>. Gated on live singlets, CD4<sup>+</sup>, CD90.1<sup>+</sup>, CD44<sup>hi</sup> cells from spleen 21 dpi. Representative data (histograms) and pooled data, n = 8-15, four experiments, mean +/- SEM. Statistical significance determined by two-tailed independent t test (\*p<0.05, \*\*p<0.01, \*\*\*p<0.001, \*\*\*\*p<0.0001).

avidity are likely functional, at least in terms of immediate cytokine release on restimulation.

### **Survival and proliferation analysis of NP peptide stimulated FluNP effectors *in vivo***

To probe the mechanisms by which peptide avidity has such a dramatic impact on memory cell recovery (Figure 3.9C), we asked if NP peptide avidity impacts FluNP effector cell proliferation, survival, or both (Figure 3A). We first asked if CD25 is upregulated, and its level determined by the strength of TCR signaling. We generated 6 dpi FluNP effectors and either co-transferred them along with Ag/APC into uninfected second hosts or transferred them alone to PR8 infection matched hosts. We used Thy-depleted splenocytes, cultured for two days and primed with dextran sulfate and LPS as APC (98, 200), instead of BMDC as in previous experiments, based on studies that they were equivalent in their ability to drive memory formation (200). At 2 dpt, the number of FluNP cells recovered from the spleen was equivalent across all groups (Figure 3.15A). We found very little CD25 expression on FluNP effector cells at 2 dpt (Figure 3.15B).

Next, to assess FluNP effector survival in the spleen 2 dpt, we stained the cells with Annexin V to label apoptotic cells, and a dead cell dye to label dead cells. The already dead cells will be double positive for the dead cell dye and Annexin V, while the apoptotic cells, committed to die but not yet dead, will be dead cell dye negative and Annexin V positive. There was no difference in double positive dead FluNP effector cells 2 dpt in the spleen between peptide avidity groups (Figure 3.15C), but we noticed a slight trend towards more apoptotic FluNP effector cells 2 dpt in the unpulsed and low peptide avidity groups compared to the PR8 infection matched group and high/mid groups (Figure 3.15D). We

**Figure 3.15. Peptide avidity has no influence on *in vivo* spleen effector FluNP cell number, CD25 expression, survival or proliferation 2 dpt**

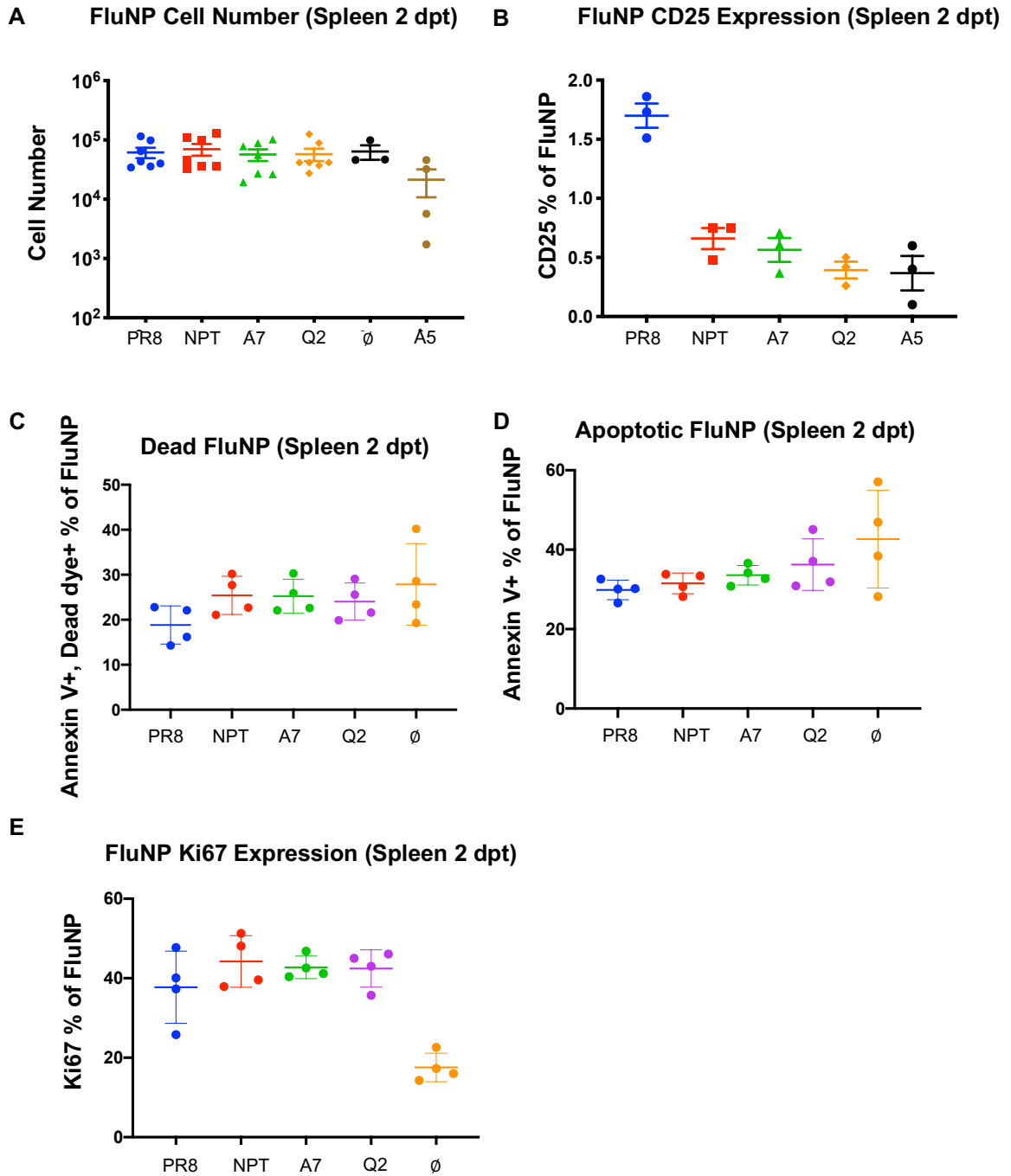


**Figure 3.15. Peptide avidity has no influence on *in vivo* spleen effector FluNP cell number, CD25 expression, survival or proliferation 2 dpt**

(A-E) FluNP effectors were isolated 6 dpi and either co-transferred along with NP peptide pulsed ( $10^{-4}$  M) APC or into PR8 infection matched hosts. After 2 dpt, spleen FluNP cells were stained by FACS. Gated on live singlets, CD4<sup>+</sup>, CD90.1<sup>+</sup>, CD44<sup>hi</sup> cells.

(A) 2 dpt spleen FluNP cell numbers gated on live singlets, CD4<sup>+</sup>, CD90.1<sup>+</sup> cells. (B) Percent CD25 expression on 2 dpt spleen FluNP cells. Gated on live singlets, CD4<sup>+</sup>, CD90.1<sup>+</sup>, CD44<sup>hi</sup> cells. (C) Percent Annexin V<sup>+</sup>, dead cell dye<sup>+</sup> (double positive) and (D) percent Annexin V<sup>+</sup> single positive FluNP cells. Gated on single CD4<sup>+</sup>, CD90.1<sup>+</sup> cells. (E) Percent Ki67 expression on 2 dpt spleen FluNP cells. Gated on live singlets, CD4<sup>+</sup>, CD90.1<sup>+</sup>, CD44<sup>hi</sup> cells.

concluded 2 dpt might not be long enough for most cell death from lack of survival factors to occur.

To analyze FluNP cell proliferation 2 dpt, we stained for intracellular expression of Ki67 as a marker of dividing cells. We observed that only the unstimulated group exhibited diminished proliferation based on Ki67 staining, while the PR8 infection matched group and all NP peptide stimulated groups showed a similar fraction (~40%) of Ki67 positive cells (Figure 3.15E). There were several challenges in this approach, so we decided to pursue a slightly different angle to assay FluNP effector cell survival and proliferation. A technical issue arose in the Annexin V staining protocol, and it was not possible to stain both Ki67 and Annexin V in the same FACS panel. Although Annexin V staining works well on cells *in vitro*, there were challenges staining cells from our *in vivo* transfer experiments. It was also interesting to note that there were no differences in FluNP cell numbers in the spleen 2dpt. This suggested that the survival or proliferation events in response to the different NP peptide avidities had not occurred yet. Therefore, we decided to change our approach to survival and proliferation readouts to address the technical issues and look out a day further in time to 3 dpt in hopes of catching differences in effector FluNP cell numbers that more reflected the memory FluNP cell numbers seen at 21 dpi.

To evaluate proliferation, we stained the 6 dpi donor FluNP effectors with cell trace violet (CTV) before transfer and examined their division *in vivo* 3d after co-transfer with Ag/APC (Figure 3.16A). In these experiments, we returned to using BMDC as the APC, to keep the experimental system as similar as possible to our previous experiments. As indicated by dilution of CTV, the spleen FluNP cells in each peptide group divided multiple

**Figure 3.16. Peptide avidity has no impact on donor FluNP proliferation 3 days post transfer**

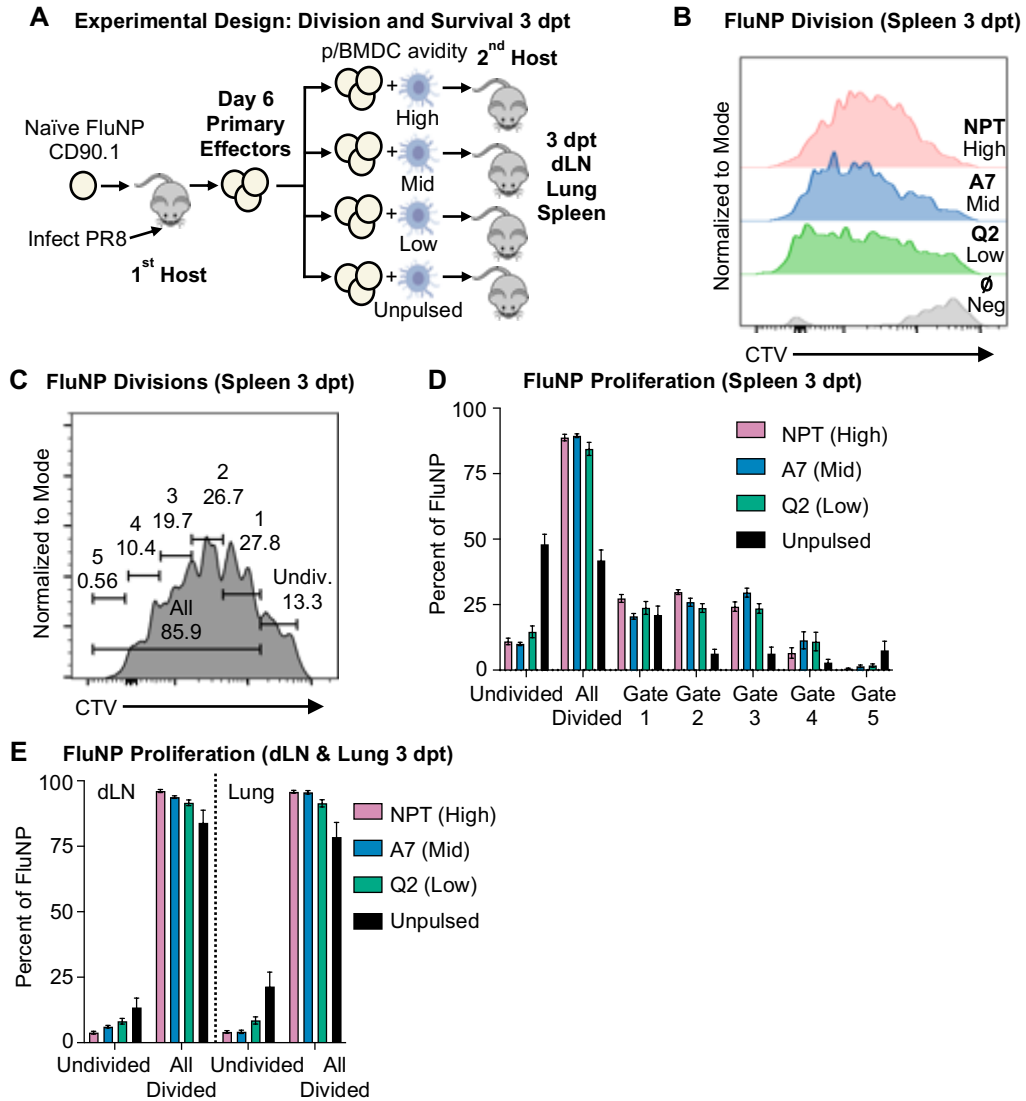


**Figure 3.16. Peptide avidity has no impact on donor FluNP proliferation 3 days post transfer**

(A) Experimental Design. Naïve FluNP CD4 T cells were transferred to B6 hosts, infected with PR8. At 6 dpi, FluNP effector cells were isolated from the 1<sup>st</sup> host, labeled with cell trace violet (CTV) and transferred to 2<sup>nd</sup> hosts given 10<sup>6</sup> APC, pulsed or not, with high, mid or low peptides. At 3 days post transfer (dpt), 2<sup>nd</sup> hosts were sacrificed and FluNP (CD4<sup>+</sup> CD90.1<sup>+</sup>) cells were analyzed. (B) Representative FACS plots of FluNP CTV dilution in spleen 3 dpt. Gated on live singlets, CD4<sup>+</sup>, CD90.1<sup>+</sup> cells. (C) Representative histogram of donor FluNP CTV dilution 3 dpt in spleen. Gates 1-5 are equally sized to undivided. (D-E) Percent of donor FluNP cells 3 dpt within gates shown in (C): (D) spleen, (E) dLN and lung.

times, while the unpulsed group barely proliferated (Figure 3.16B). Thus, proliferation of transferred cells required Ag recognition, as seen previously by Ki67 staining (Figure 3.15E), but peptide avidity did not impact the pace or extent of division in any organ (Figure 3.16C-E). Thus, the dramatic differences in memory cell numbers (Figure 3.9C), are not due to a greater rate or number of cell divisions as all avidity peptides efficiently induced proliferation.

We determined survival of FluNP effectors by measuring expression of caspase 3/7 and viability stain (Figure 3.17A-B). We replaced the Annexin V stain with FLICA caspase3/7 staining as a marker of cells on their way towards death. In the spleen, we found a much greater fraction of live, caspase 3/7 negative cells in the NPT (high) and A7 (mid) groups compared to the Q2 (low) group (Figure 3.17C), indicating there is greater apoptosis in the low avidity group compared to both mid and high groups. Most donor FluNP effector cells recovered in the unpulsed APC group were pro-apoptotic by 3d post-transfer (dpt) (Figure 3.17C), consistent with a strict requirement for Ag recognition at the effector checkpoint to prevent apoptosis (200). We did not see a clear difference in cell survival with different avidity peptides in dLN or lung, although all peptides led to higher survival than no peptide (Figure 3.17D-E). Perhaps the response kinetics are different in each organ, or the spleen is a major source of memory generation after which developing memory migrate to the lung and dLN. Therefore, we also evaluated donor FluNP effector cell recovery 3 dpt as a measure of net survival since we found no evidence that there were differences in FluNP proliferation between peptide groups. We found a clear-cut pattern with donor FluNP effector cell recovery corresponding to higher peptide avidity in the

**Figure 3.17. Peptide avidity determines donor FluNP survival 3 days post transfer**

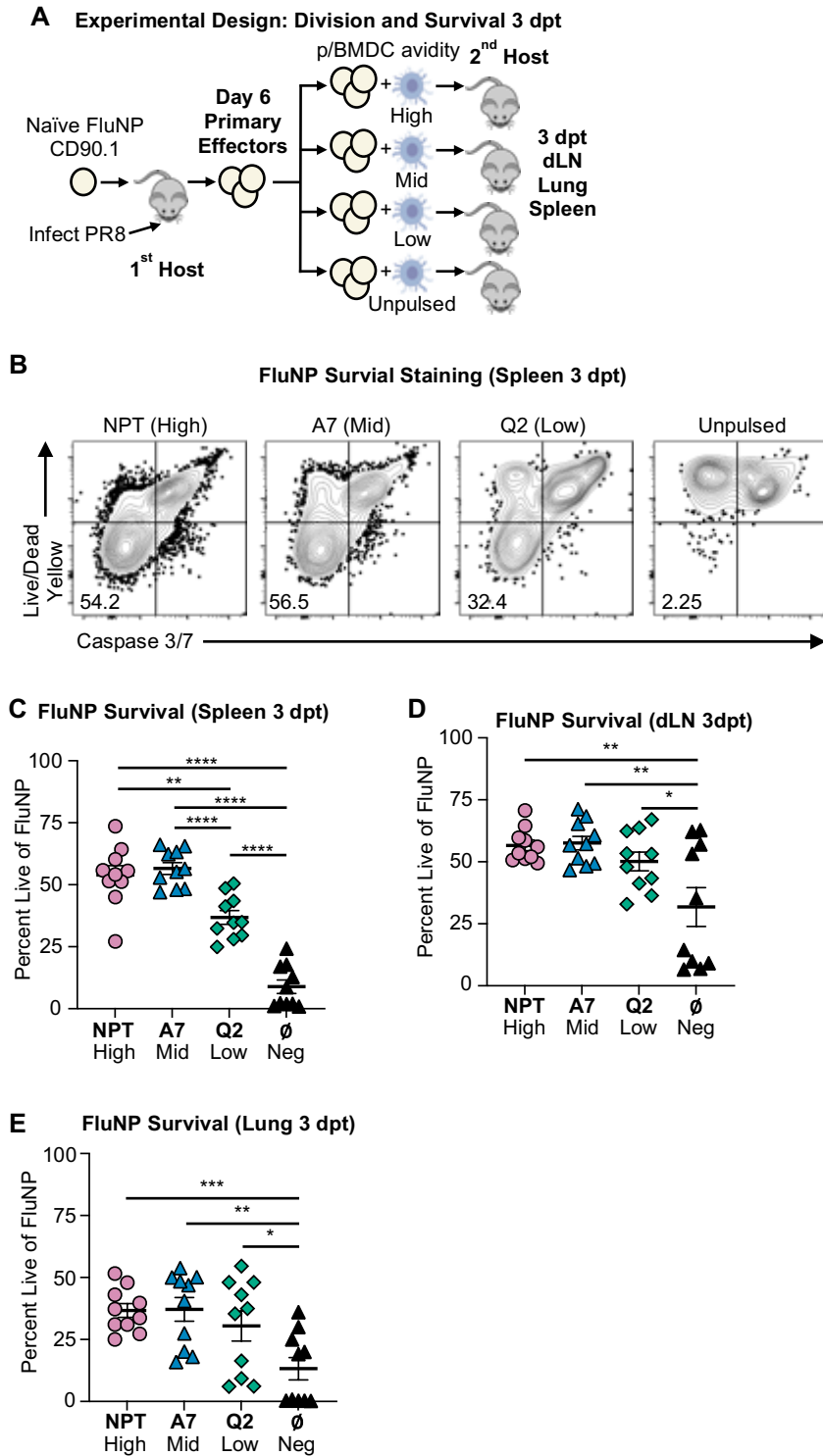


**Figure 3.17. Peptide avidity determines donor FluNP survival 3 days post transfer**

(A) Experimental Design. Naïve FluNP CD4 T cells were transferred to B6 hosts, infected with PR8. At 6 dpi, FluNP effector cells were isolated from the 1<sup>st</sup> host, labeled with cell trace violet (CTV) and transferred to 2<sup>nd</sup> hosts given 10<sup>6</sup> APC, pulsed or not, with high, mid or low peptides. At 3 days post transfer (dpt), 2<sup>nd</sup> hosts were sacrificed and FluNP (CD4<sup>+</sup> CD90.1<sup>+</sup>) cells were analyzed. (B) Representative FACS plots of donor FluNP survival by live/dead yellow and FLICA caspase 3/7 staining in spleen 3 dpt. (C-E) Fraction of live donor FluNP by FACS in the (C) spleen, (D) dLN and (E) lung.

spleen (Figure 3.18A), dLN (Figure 3.18B) and lung (Figure 3.18C) that was of similar magnitude at 3 dpt (late effector) as it is at 21 dpi (memory) (Figure 3.9C). We note that the impact of peptide avidity in regulating memory cell recovery is realized within a few days after donor FluNP effector cells encounter Ag, and it is primarily due to the fraction of effectors that survive rather than their extent of division. This focused our further experiments on determining what avidity-dependent step might be important.

### **Peptide avidity at the effector checkpoint acts by inducing more effector IL-2**

We further wanted to understand how peptide avidity at the effector checkpoint increased the survival of our transferred 6 dpi FluNP effector cells to memory. We coupled our *in vivo* approach from figure 3.15 with an *in vitro* approach to study how increasing peptide avidity influenced expression of cell surface protein mRNA expression levels and intracellular transcription factor expression on our 6 dpi FluNP effectors cultured for 2 days with NP peptide pulsed APC. To do this, we used leftover 6 dpi FluNP effectors from our *in vivo* experiment in figure 3.15 and co-cultured with irradiated Ag/APC, in this case Thy-depleted splenocytes, activated with dextran sulfate and LPS, for 2 days. We then isolated RNA from the FluNP cells and determined mRNA levels of several key molecules associated with pMHC-TCR interaction strength, Nurr77, cytokine expression (IFN $\gamma$ , TNF $\alpha$  and IL-2), PD-1 and CXCR3, and IL-2R subunit expression (Figure 3.19). We saw that as predicted from our peptide affinity measurements (Figure 3.6B) and biological naïve FluNP cell activation avidity assay (Figure 3.7), Nurr77, IFN $\gamma$  and IL-2 mRNA expression levels of our effector FluNP cells clearly reflected the relative rank of NP peptide avidity, from strongest to weakest: NPT, NP<sub>311-325</sub>, A7, K5, Q2, Q7 and unpulsed APC. TNF $\alpha$  and

**Figure 3.18. Peptide avidity increases donor FluNP cell recovery 3 dpt and reflects cell survival pattern**

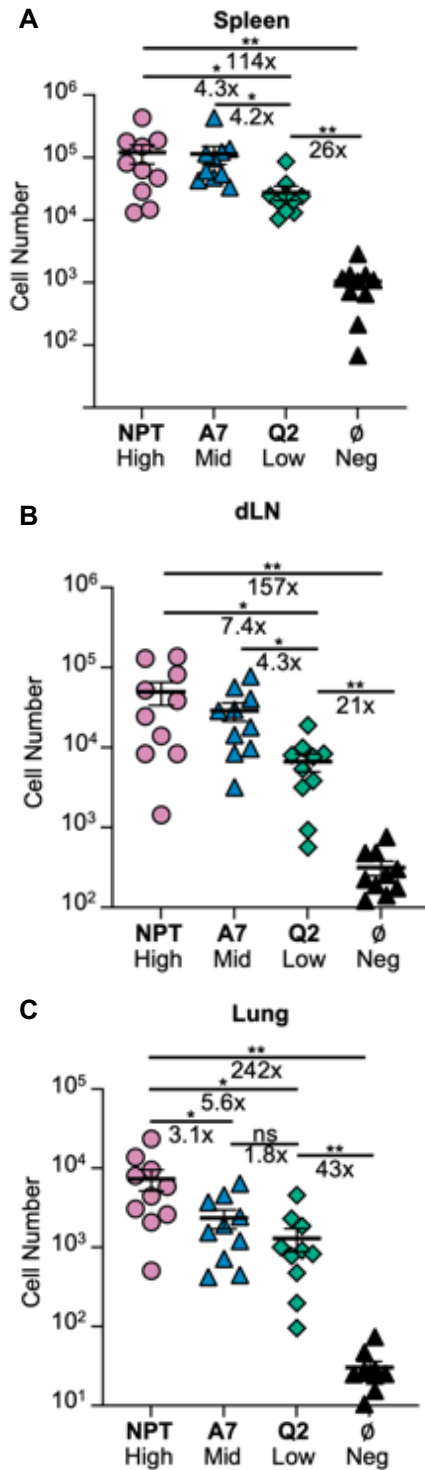


**Figure 3.18. Peptide avidity increases donor FluNP cell recovery 3 dpt and reflects cell survival pattern**

(A-C) Experimental Design. Naïve FluNP CD4 T cells were transferred to B6 hosts, infected with PR8. At 6 dpi, FluNP effector cells were isolated from the 1<sup>st</sup> host, labeled with cell trace violet (CTV) and transferred to 2<sup>nd</sup> hosts given 10<sup>6</sup> APC, pulsed or not, with high, mid or low peptides. At 3 days post transfer (dpt), 2<sup>nd</sup> hosts were sacrificed and FluNP (CD4<sup>+</sup> CD90.1<sup>+</sup>) cells were analyzed. Number of donor FluNP cells recovered 3 dpt in the (A) spleen, (B) dLN and (C) lung.

PD-1 expression mRNA levels followed this trend for the most part followed, however the low peptide Q7 seemed to induce similar levels of these molecules as the high peptides (Figure 3.19). This was interesting, as effector TNF $\alpha$  expression appeared to follow the trend established from our day 21 spleen FluNP ICCS TNF $\alpha$  measurements (Figure 3.14B), in that low peptide stimulated FluNP cells appear to make as much, if not slightly more, TNF $\alpha$  than their high signaling counterparts. The mRNA expression of CXCR3 was interesting as it reflected the inverse trend, with the greatest expression following stimulation with the low avidity peptides or unpulsed APC (Figure 3.19). We saw that CD25, the IL-2R $\alpha$  subunit, mRNA expression levels were greater following strong compared to weak avidity peptide stimulation. There was not a clear trend for CD122 and CD132 expression levels. Overall, we felt this data helped to confirm the relative avidity rank of our NP peptides and this effector data coupled nicely with our affinity (Figure 3.6B) and naïve avidity readouts (Figure 3.14B). However, it was surprising that the FluNP effectors *in vivo* 2 dpt showed very little CD25 expression (Figure 3.15B), since autocrine IL-2 is the cytokine implicated in earlier studies in supporting memory generation (201).

We also looked at transcription factor and Bcl-2 family member expression levels associated with effector and memory differentiation as well as apoptosis and survival. It is generally thought that greater Eomes expression associates with memory precursor cells, while T-bet expression is more closely associated with terminal effector cells. Similarly, Bim expression is elevated in cells that are poised to die, while Bcl-2 is a survival factor. We looked at IRF-4 expression as another way to try and confirm the avidity rank of our NP peptides, as IRF-4 expression levels correlate to TCR signal strength. After 2 days in

**Figure 3.19. qPCR phenotype of effector FluNP cells stimulated by different NP peptides on APC after 2d *in vitro***

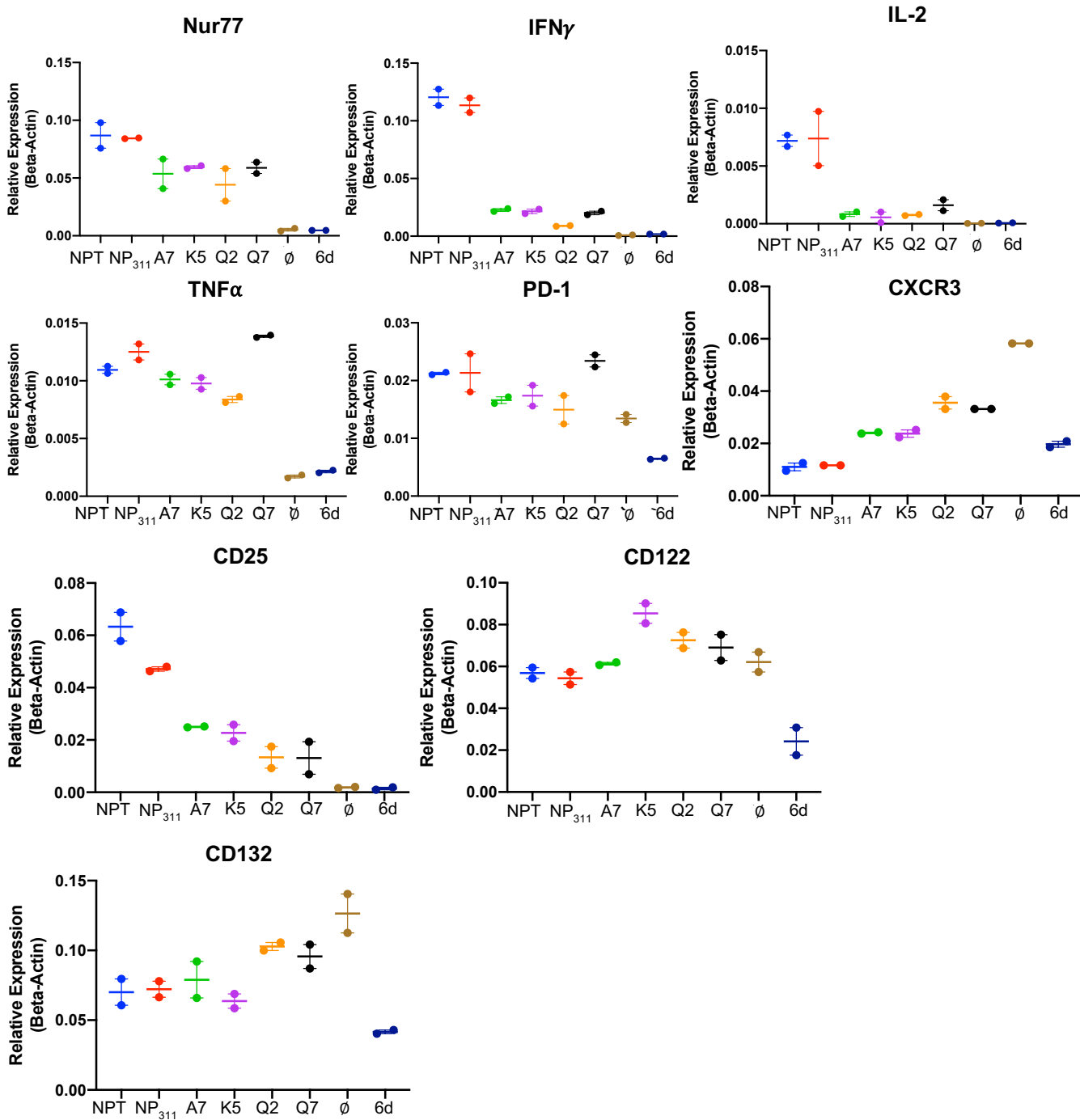


**Figure 3.19. qPCR phenotype of effector FluNP cells stimulated by different NP peptides on APC after 2d *in vitro***

FluNP effectors were isolated 6 dpi and co-cultured for 2d *in vitro* with NP peptide pulsed ( $10^{-4}$  M) irradiated APC. After 2d in culture FluNP cells were isolated and gene expression tested by qPCR relative to beta-actin expression: Nurr77, IFN $\gamma$ , IL-2, TNF $\alpha$ , PD-1, CXCR3, CD25, CD122 and CD132.

culture with Ag/APC, a greater fraction of our FluNP effector cells expressed T-bet, Eomes, Bim, Bcl-2 and IRF-4 (Figure 3.20). When we compared the ratios of Eomes to T-bet and Bim to Bcl-2 there was no obvious pattern that fit with the day 21 memory cells data (Figure 3.9C). All of the effector FluNP cells expressed more Bim than Bcl-2 (~40x) and more Eomes than T-bet (~5x) and we were unable to make any conclusions from this data, other than again confirming the affinity (Figure 3.6B) and naïve biological FluNP activation assay (Figure 3.15B) avidity rank of the NP peptides. We decided that to further decipher these nuanced differences *in vitro* was not very practical and in fact might be confounding and confusing data. We decided to turn to and rely on our *in vivo* sequential transfer model to study by what mechanism peptide avidity at the effector checkpoint increases the survival of effector cells and number of memory cells generated.

We previously established that effector phase autocrine IL-2 signaling is required for CD4 T cell memory and that autocrine IL-2 acts by downregulating pro-apoptotic Bim, which promotes the survival of CD4 effectors (200, 201). We had thought this implied that peptide Ag recognition induced IL-2R $\alpha$  expression as well, since anti-IL-2R blocked the impact of IL-2 (201). But since we saw very little IL-2R $\alpha$  expression on our FluNP effector cells 2 dpt (Figure 3.15B), we analyzed the expression of IL-2R subunits CD132 (IL-2R $\gamma$ ), CD122 (IL-2R $\beta$ ) and CD25 (IL-2R $\alpha$ ) on donor FluNP before transfer and 3d after *in vivo* stimulation with the various peptide/APC. Before restimulation, a few 6 day FluNP effectors express CD132 (15%), a fair fraction expresses low levels of CD122 (40%) but very few express CD25 (<10%) (Figure 3.21A-C, left). Following stimulation with high affinity peptide/APC *in vivo*, three-quarters of 3 dpt FluNP cells in spleen, dLN and lung

**Figure 3.20. Increased peptide avidity results in greater expression of transcription factors on effector FluNP cells after 2d *in vitro***

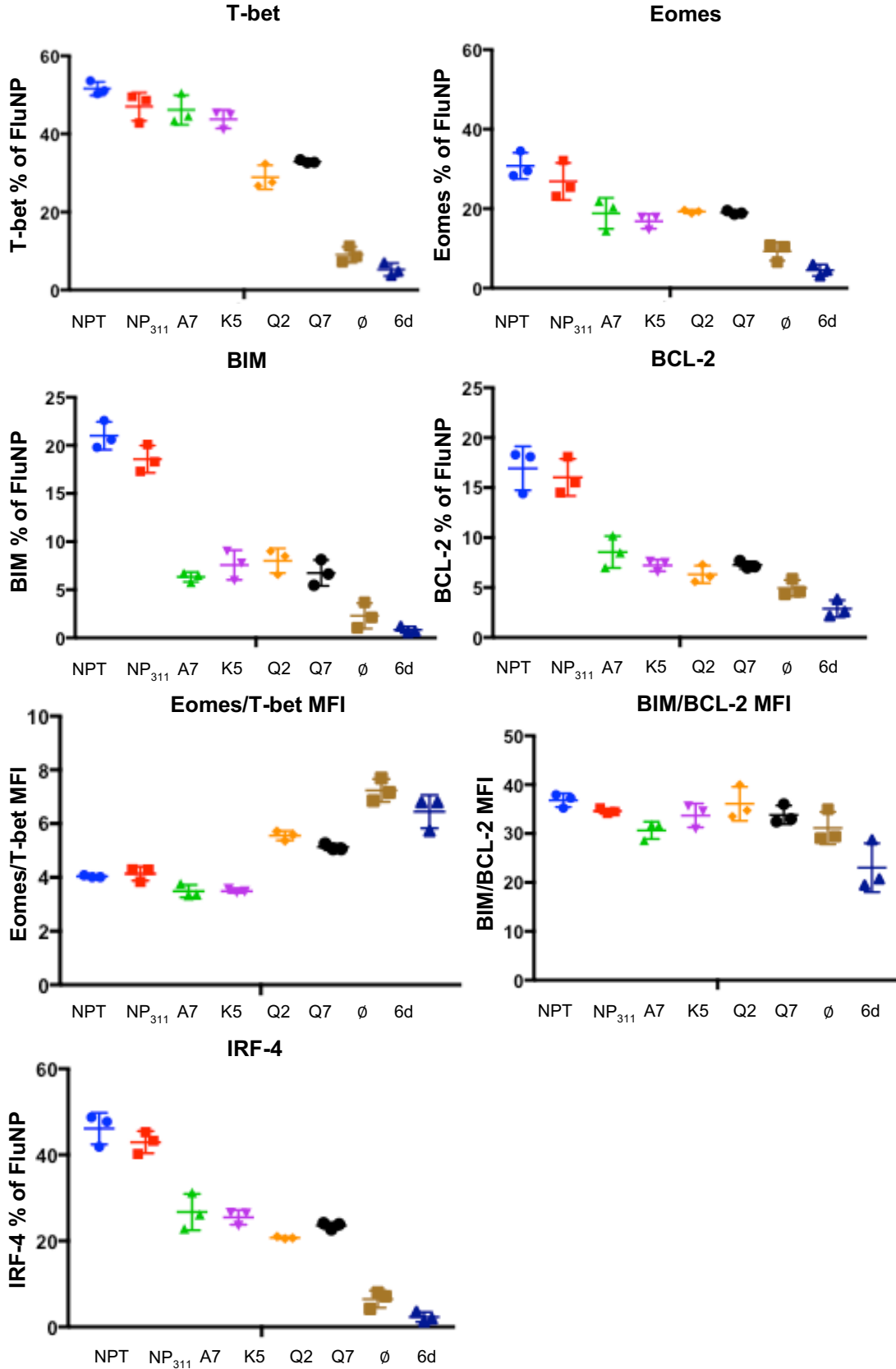


**Figure 3.20. Increased peptide avidity results in greater expression of transcription factors on effector FluNP cells after 2d *in vitro***

FluNP effectors were isolated 6 dpi and co-cultured for 2d *in vitro* with NP peptide pulsed ( $10^{-4}$  M) irradiated APC. After 2d in culture FluNP cells were isolated and transcription factors stained by FACS for T-bet, Eomes, IRF-4, BIM and BCL-2. Gated on live singlets, CD4<sup>+</sup>, CD90.1<sup>+</sup>, CD44<sup>hi</sup> cells. Median fluorescence intensity (MFI) ratios of BIM/BCL-2 and Eomes/T-bet are plotted.

strongly express CD132 and almost all express CD122 (>90%) (Figure 3.21D), but this is true regardless of peptide avidity. Moreover, we found there are few, if any, FluNP effectors that express any CD25 in spleen and lung (Figure 3.21D), and only half in the dLN (Figure 3.21A, D). In the *in vivo* setting, we found no difference in IL-2R subunit expression on 3 dpt donor FluNP cells following high, mid and low peptide avidity in any tissue, and even the unpulsed group 3 dpt effectors expressed a similar pattern (Figure 2.21D), suggesting peptide avidity does not act by inducing effector FluNP IL-2R expression, leaving unresolved how autocrine IL-2 effectively signals the effectors.

We examined the impact of peptide avidity on the level of IL-2 produced by 6 dpi effectors. We restimulated 6 dpi FluNP effectors *ex vivo* with our panel of NP peptide-pulsed APC, and quantified IL-2-producing cells by ICCS (Figure 3.22A) and levels of secreted IL-2 by ELISA (Figure 3.22B) following 2d culture. Strikingly, the fraction of IL-2-positive 6 dpi FluNP effectors corresponded closely with relative NP peptide avidity, mirroring the impact on memory (Figure 3.9C) and survival in the spleen 3 dpt (Figure 3.17C). Thus, induction of IL-2 secretion by FluNP effector cells is highly dependent on avidity of peptide Ag recognition at the effector checkpoint. Since the CD4 T cell response is also dependent on density of peptide Ag/MHC we varied the peptide concentration used to pulse APC (Fig. 3.22B). We found dose also strongly influenced IL-2 production by the 6 dpi effectors. With high avidity peptides, levels of IL-2 increased with peptide pulse concentration and were detectable even at very low dose ( $10^{-7}$  M) while mid and low peptides required much higher concentrations. We integrated the area under the curve, as a reflection of IL-2 accumulation (Figure 3.22C). This confirmed IL-2 production mirrored

**Figure 3.21. IL-2 receptor subunit expression on 6d and 3 dpt FluNP effectors**

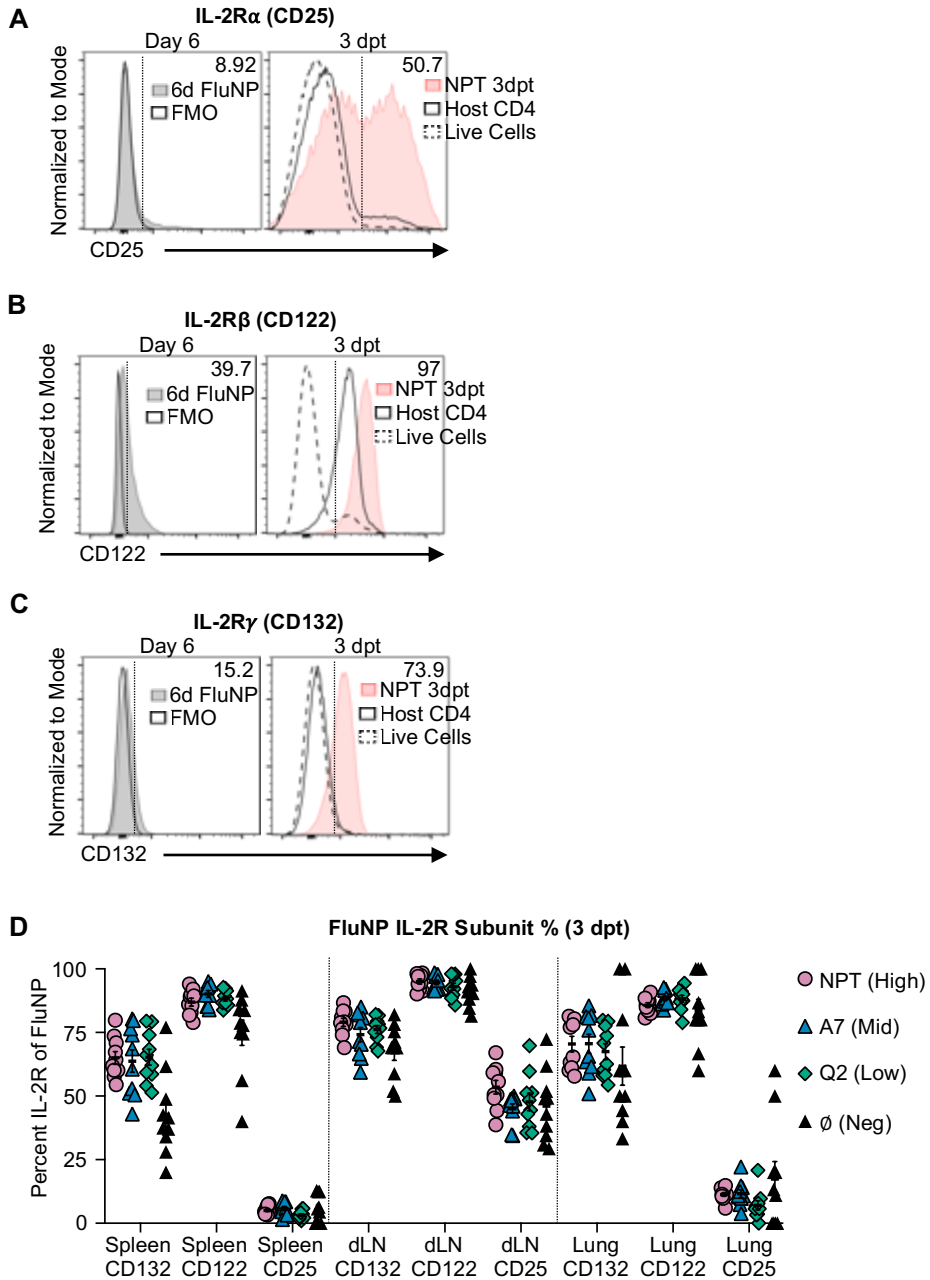


**Figure 3.21. IL-2 receptor subunit expression on 6d and 3 dpt dLN FluNP effectors**

(A-C) Effector FluNP IL-2 receptor subunit expression: (A) IL-2R $\alpha$  (CD25), (B) IL-2R $\beta$  (CD122) and (C) IL-2R $\gamma$  (CD132) expression was determined by FACS analysis of the 6 dpi effectors (left) and 3 dpt donor cells (right). (D) Percent expression of IL-2R chains by CD44<sup>hi</sup> FluNP donor cells in spleen, dLN and lung 3 dpt.

**Figure 3.22. Increased peptide avidity results in more day 6 effector FluNP cytokine expression and production**

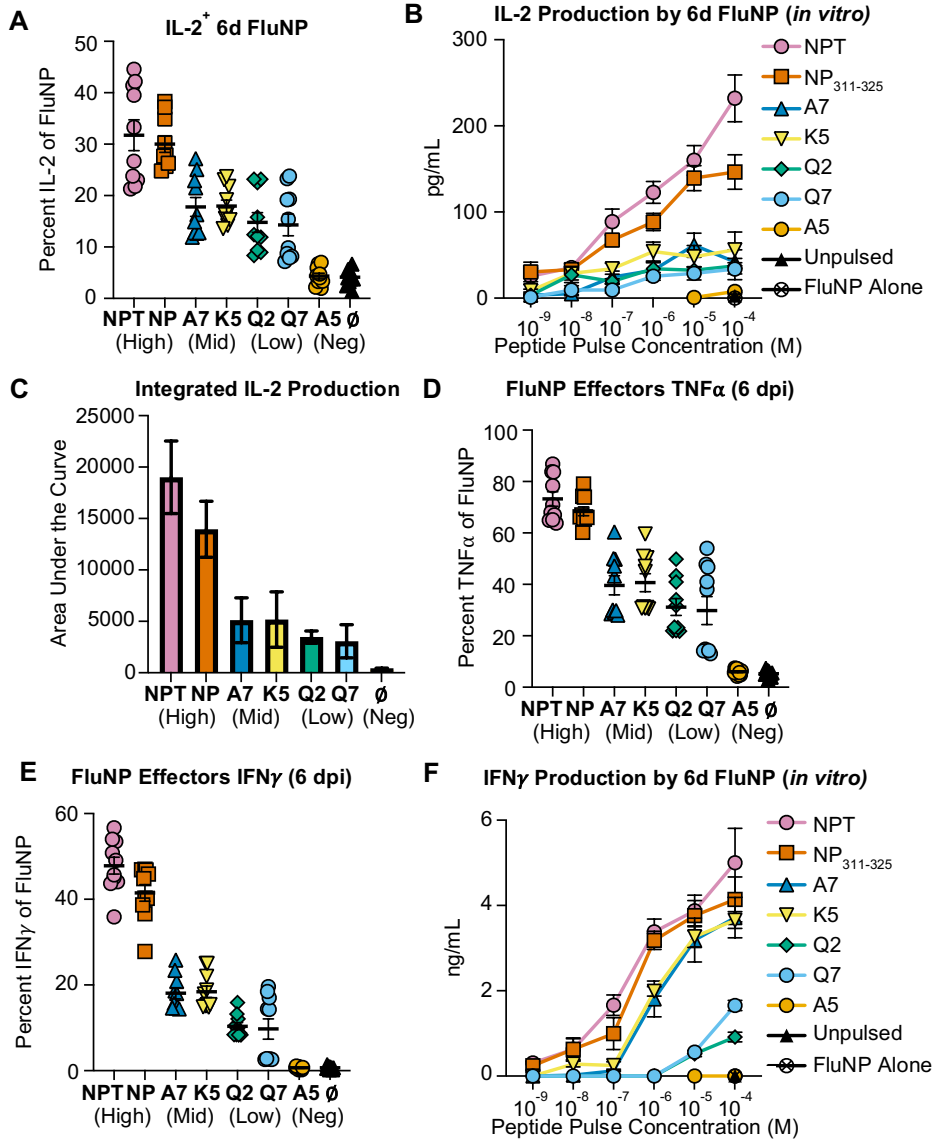


**Figure 3.22. Increased peptide avidity results in more day 6 effector FluNP cytokine expression and production**

(A, D, E) FluNP 6 dpi effectors were restimulated for 6 hours with indicated NP peptides at 10  $\mu$ M and (A) IL-2, (D) TNF $\alpha$  and (E) IFN $\gamma$  expression determined by FACS. (B, F) FluNP effectors were co-cultured with NP peptide-pulsed APC for 48 hr and (B) IL-2 and (F) IFN $\gamma$  production in the supernatant was determined by ELISA. (C) The area under the curve was calculated to quantitate impact on IL-2 production. (A-F) Pooled data, n = 3-6, two experiments, mean +/- SEM.

the rank of peptides determined by measures of affinity (Figure 3.6B) and functional avidity (Figure 3.15B). As peptide avidity determines the level of autocrine IL-2 produced, and since IL-2 availability determines their survival (201), this is likely the key pathway that translates peptide avidity to number of memory cells generated. We also noted that TNF $\alpha$  (Figure 3.22D) expression and IFN $\gamma$  expression (Figure 3.22E) and production (Figure 3.22F) was also dependent on peptide avidity and on dose, indicating the elicitation of those key effector function also is peptide avidity driven.

**CD25 expression on APC during the effector phase promotes effector transition to memory.**

When effector cells recognize peptide Ag presented by APC, they make IL-2 within several hours (216). Traditionally this autocrine IL-2 was thought to bind to the tripartite IL-2R on the same cell, since the IL-2 needs to be autocrine (201). However, since 6 dpi FluNP effectors do not express CD25 (Figure 3.21A, left), we further investigated how autocrine IL-2 might bind to effectors during this checkpoint. IL-15 shares two-thirds of its receptor (IL-2R $\beta/\gamma$ ) with IL-2 and is known to be transpresented by IL-15R $\alpha$  on APC to IL-2R $\beta/\gamma$  on T cells (217-219). Several previous studies found that IL-2 can be transpresented by APC (220-222). If IL-2 transpresentation plays a role here, IAV infection should generate CD25-expressing APC. We analyzed infection-induced APC for CD25 expression. In uninfected mice, we found no CD25 expression on MHC-II<sup>+</sup> cells but at 6 dpi a cohort of dLN CD11c<sup>+</sup>, MHC-II<sup>+</sup> cells clearly express CD25 (Figure 3.23A). At 4-8 dpi, the time when autocrine IL-2 signals are needed for CD4 T cell memory (120), substantial populations of CD11c<sup>+</sup>, MHC-II<sup>+</sup> cells (Figure 3.23B), CD11b<sup>+</sup>, MHC-II<sup>+</sup> cells

**Figure 3.23. Several APC subsets express CD25 4-8 days post IAV infection**

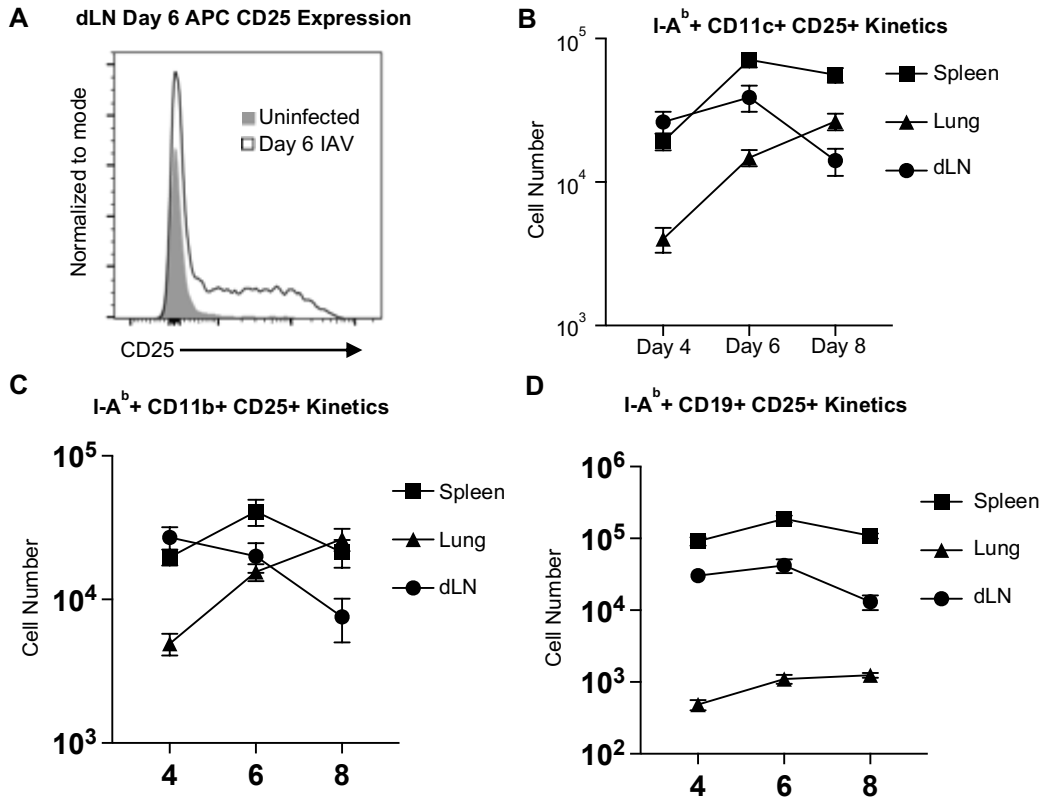


**Figure 3.23. Several APC subsets express CD25 4-8 days post IAV infection**

**(A-D)** CD25 Expression on APC *in vivo*. Mice were infected or not with PR8 influenza and sacrificed 4, 6 and 8 dpi. CD25 expression was measured by FACS staining on I-A<sup>b+</sup>, CD11c<sup>+</sup> cells in the dLN of infected (black line, no fill) or uninfected (gray) mice. **(B-D)** Kinetics in the dLN, lung, and spleen of infected mice at 4, 6 and 8 dpi of **(B)** CD25<sup>+</sup> I-A<sup>b+</sup>, CD11c<sup>+</sup> APC, **(C)** CD25<sup>+</sup> I-A<sup>b+</sup>, CD11b<sup>+</sup> APC and **(D)** CD25<sup>+</sup> I-A<sup>b+</sup>, CD19<sup>+</sup> APC.

(Figure 3.23C) and CD19<sup>+</sup>, MHC-II<sup>+</sup> cells (Figure 3.23D) express CD25 in the lung, dLN and spleen. This demonstrates that CD25 expression is induced on several APC subsets following IAV infection at the right time, 4-8 dpi, when transpresentation of IL-2 to responding CD4 effector cells might be relevant.

We analyzed whether CD25 expression on APC could play a role in CD4 effector survival to memory. To do this, we generated 6 dpi FluNP effectors and co-transferred them with WT or CD25KO activated BMDC pulsed with high and mid NP peptides into uninfected second hosts and analyzed the resultant FluNP memory cell numbers 21 dpi (Figure 3.26A). Both WT and CD25KO BMDC expressed high levels of CD11c, MHC-II, CD80 and CD86, but only WT BMDC expressed CD25 (Figure 3.24). We found that 6 dpi effectors stimulated *in vitro* for 2 days with WT vs. CD25KO peptide/APC produced equivalent amounts of IL-2 (Figure 3.25A) and IFN $\gamma$  (Figure 3.25B). This indicates that both WT and CD25KO BMDC, pulsed with the same NP peptide, activate effector FluNP cells equivalently. However, when we assessed *in vivo* generation of memory using the sequential transfer model with WT or CD25KO APC (Figure 3.26A), significantly fewer donor FluNP memory cells developed in spleen (Figure 3.26B), dLN (Figure 3.26C), and lung (Figure 3.26D), when NPT high peptide was presented by CD25KO BMDC. With the middle avidity peptide A7, there were significantly fewer donor FluNP memory cells generated with CD25KO BMDC in dLN (Figure 3.26C) and lung (Figure 3.26D). The fraction of donor memory cells that produced IFN $\gamma$  (Figure 3.26E), IL-2 (Figure 3.26F), and TNF $\alpha$  (Figure 3.26G) was equivalent. This suggests that transpresentation of IL-2 by

**Figure 3.24. Comparison of WT and CD25KO BMDC following activation**

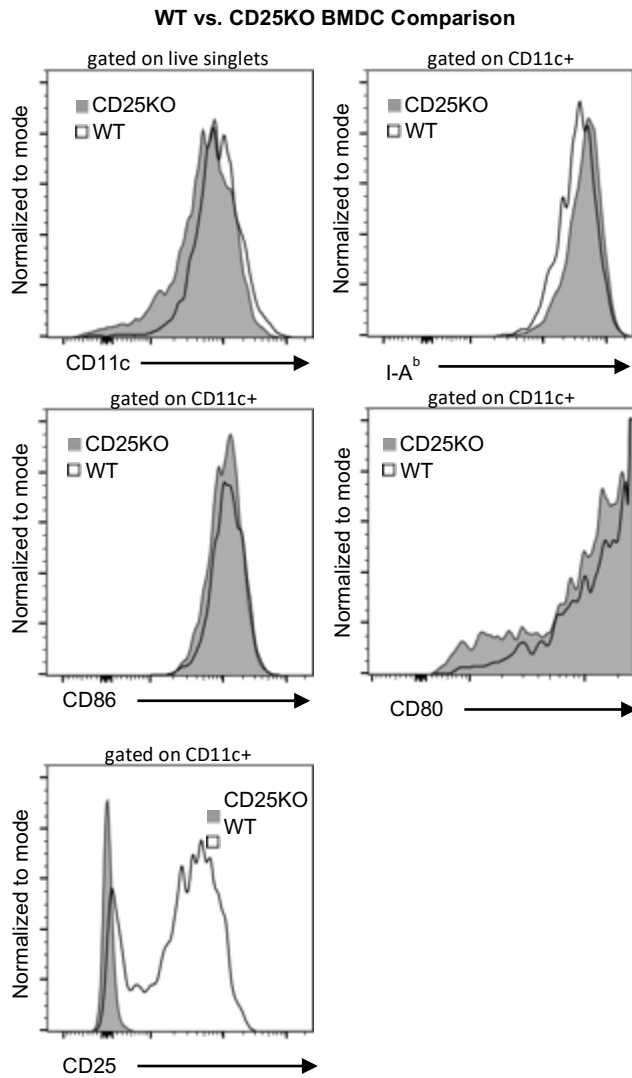
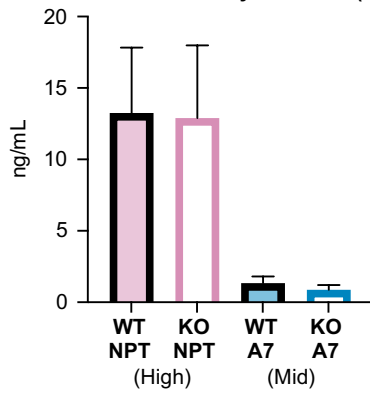


**Figure 3.24. Comparison of WT and CD25KO BMDC following activation**

Histograms of CD11c, I-A<sup>b</sup>, CD86, CD80 and CD25 expression on BMDC prepared from WT and CD25KO mice.

**Figure 3.25. WT and CD25KO BMDc both effectively stimulate 6d FluNP effector cytokine production**

**A IL-2 Production by 6d FluNP (*in vitro*)**



**B IFN $\gamma$  Production by 6d FluNP (*in vitro*)**

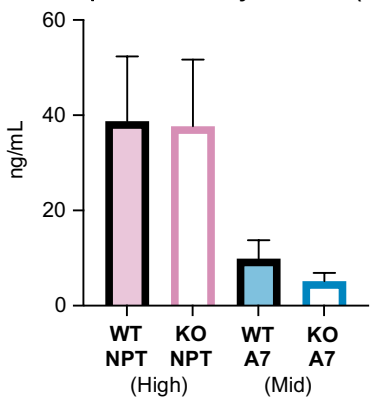


**Figure 3.25. WT and CD25KO BMDC both effectively stimulate 6d FluNP effector cytokine production**

(**A-B**) FluNP 6d effectors were stimulated with WT or CD25KO APC pulsed with NPT (high) or A7 (mid) NP peptide for 6 hr and production of (**A**) IL-2 and (**B**) IFN $\gamma$  determined by ELISA.

**Figure 3.26. CD25 expression on APC induces more effectors to become memory**

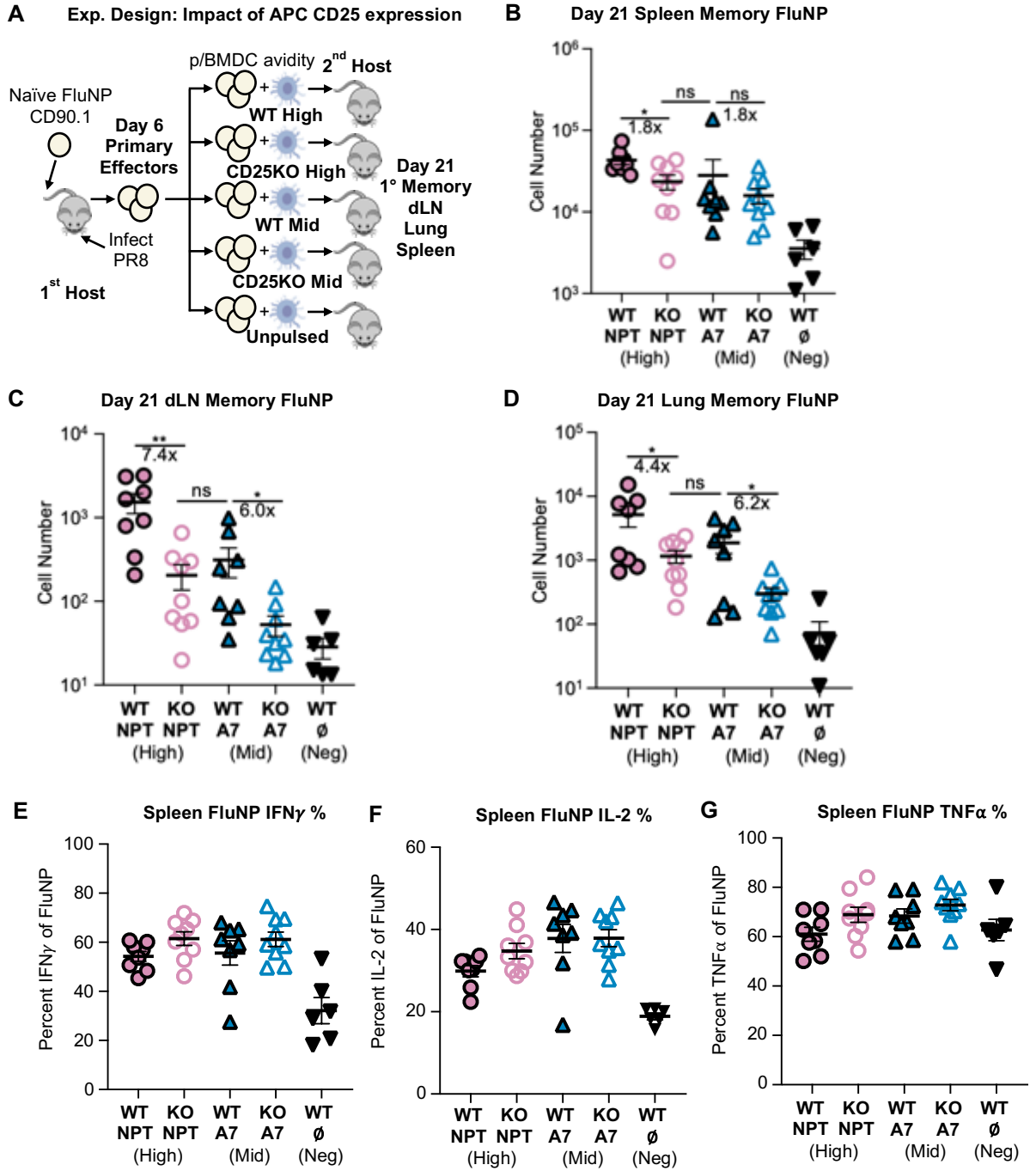


**Figure 3.26. CD25 expression on APC induces more effectors to become memory**

(A) Experimental Design. 6 dpi FluNP effectors were co-transferred with peptide-pulsed WT or CD25KO BMDC to uninfected 2<sup>nd</sup> hosts. 2<sup>nd</sup> hosts were sacrificed 15 dpt (21 dpi), and donor memory cells were analyzed by FACS. Number of memory FluNP cells determined by FACS analysis in (B) spleen, (C) dLN and (D) lung. (E-G) Spleen cells were re-stimulated with 10 $\mu$ M of NP<sub>311-325</sub> for 6 hours *ex vivo* and percent expression of 21 dpi FluNP (G) IFN $\gamma$ , (H) IL-2 and (G) TNF $\alpha$  determined by ICCS. Gated on live singlets, CD4<sup>+</sup>, CD90.1<sup>+</sup>, CD44<sup>hi</sup>.

APC serves to amplify the IL-2 signal to the CD4 FluNP effectors, leading to generation of more memory cells.

**Peptide avidity at the effector checkpoint determines protection to influenza challenge.**

We asked if mice which received higher avidity peptide were better protected from rechallenge with IAV. We generated memory from FluNP effectors co-transferred with high or low Ag/APC (Figure 3.27A). After 21 dpi, we challenged the mice with a sublethal dose of PR8 and analyzed their weight loss (Figure 3.27B). The high avidity group recovered weight significantly faster than the low group, and both recovered more rapidly than the unpulsed group (Figure 3.27B). When we challenged hosts with a higher, lethal dose of PR8 and analyzed survival, more animals in the two high groups (>80%) survived compared to their two low signaling counterparts (50-60%) and these were better protected than unpulsed APC (20%) (Figure 3.27C). Thus, higher avidity peptide at the effector phase promoted a more protective donor memory FluNP population and the degree of protection increased with the size of the memory population.

**Increased peptide avidity at the effector checkpoint generates memory cells that respond more rapidly to IAV infection in the lung**

To analyze whether the increased protection (Figure 3.27C) was due primarily to the increased donor FluNP memory cell numbers following stimulation with high avidity peptides at the effector checkpoint (Figure 3.9C), or if there were qualitative differences between the secondary effectors that could be responsible for greater protection, we studied

**Figure 3.27. Increased peptide avidity at the effector checkpoint promotes a more protective population of memory cells**

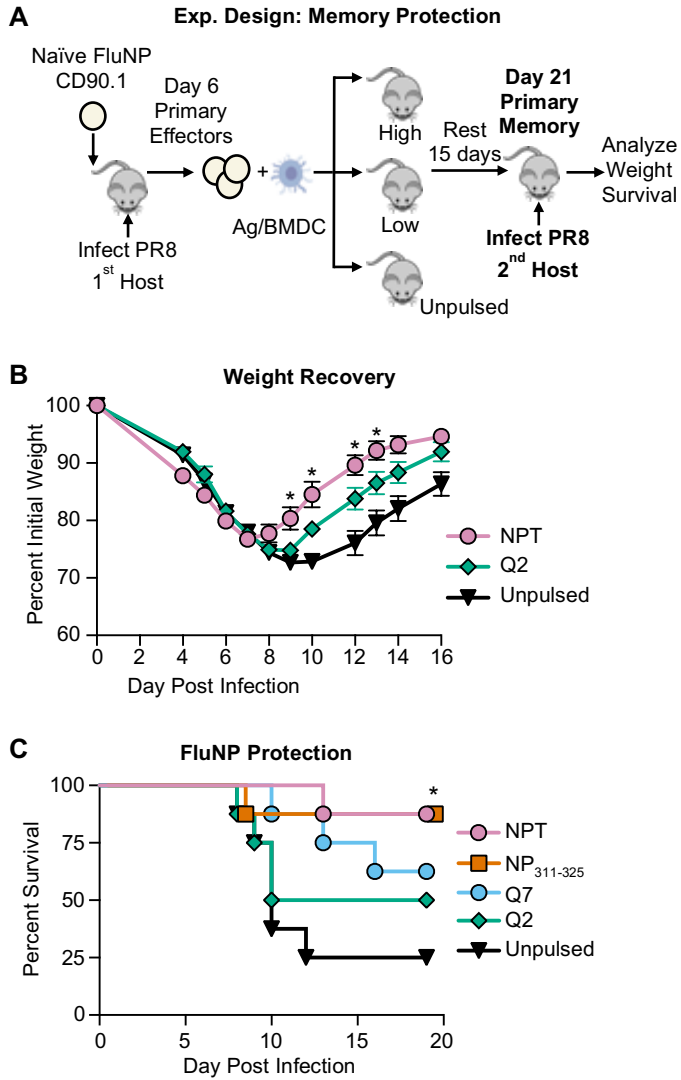


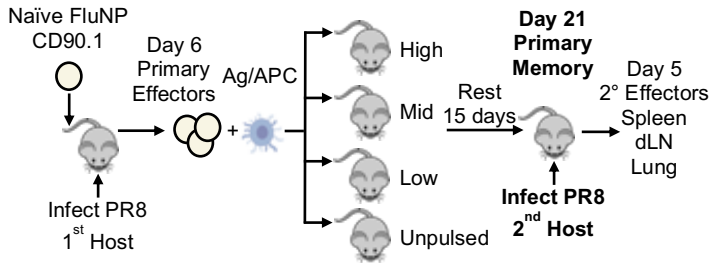
**Figure 3.27. Increased peptide avidity at the effector checkpoint promotes a more protective population of memory cells**

(A) Experimental design: FluNP effector cells (6 dpi) were co-transferred with peptide-pulsed APC into uninfected 2<sup>nd</sup> hosts and rested for 15 d (21 dpi). At 21 dpi, 2<sup>nd</sup> hosts were challenged with PR8. (B) Weight loss was determined following 2LD<sub>50</sub> PR8 challenge. Statistical significance determined by two-tailed independent t test (\*p<0.05). (C) Survival was measured following 4LD<sub>50</sub> PR8 challenge. Statistical significance determined by log-rank (Mantel-Cox) test (\*p<0.05). (B) Pooled data, n= 10-15, two experiments, mean +/- SEM. (C) Pooled data, n= 8, two experiments. (E-G) Pooled data, n= 8-9, two experiments, mean +/- SEM.

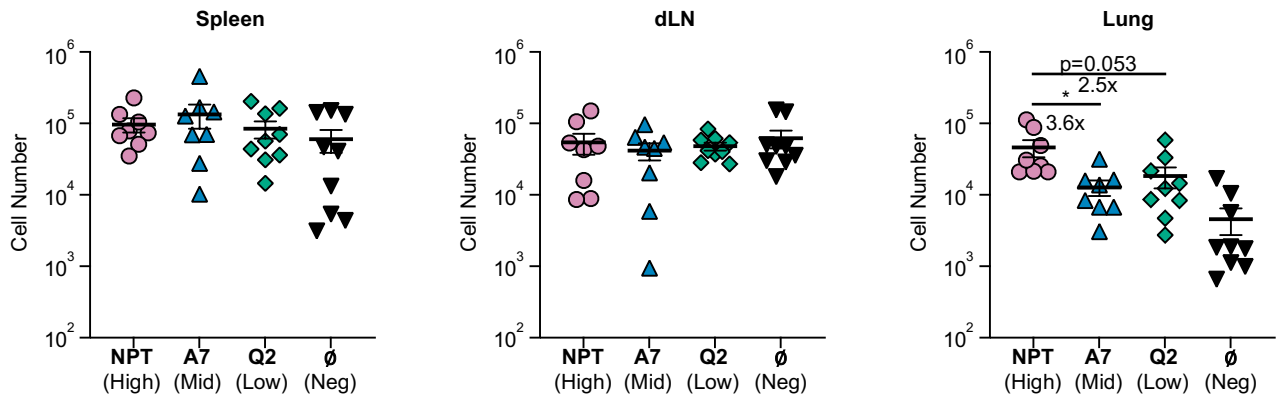
the secondary FluNP effector populations at 5 and 8 days after challenge. We hypothesized that some of the secondary FluNP effectors generated from memory cells might develop earlier (123) than during the primary response which peaks at 8 dpi (Figure 3.1, 3.2). As in earlier experiments, we generated 6 dpi FluNP effectors *in vivo* and co-transferred them along with three different NP peptide-pulsed \*BMDC (high, mid, low) into naïve second hosts. We let the donor FluNP cells become memory and after 21 days (15 dpt) we infected the second hosts with a sub-lethal dose of PR8 and looked at the resultant secondary effectors in the dLN, lung and spleen at 5 (Figure 2.28A) and 8 dpi (Figure 3.29A). We found no difference in FluNP numbers on day 5 in the spleen of dLN, however the lung contained more secondary effectors in the NPT (high) group compared to the A7 (mid) and unpulsed groups, while the Q2 group just missed the cutoff for significance but demonstrated a 2.5-fold difference in number (Figure 3.28B). Since we saw a difference in day 5 lung FluNP secondary effectors, we looked for differences in percentages of ThCTL, by NKG2A/C/E expression, and Th1 differentiation by T-bet expression. We found a significant increase in the fraction of ThCTL, and amount of NKG2A/C/E expressed by NKG2A/C/E<sup>+</sup> FluNP cells in the high compared to unpulsed group (Figure 3.28C). We also saw an increase in the percent of T-bet expression on FluNP cells in the high and mid stimulated groups compared to unpulsed, and an increase in the amount of T-bet expressed by T-bet<sup>+</sup> FluNP cells in the high and mid stimulated groups compared to unpulsed and in the high compared to low group (Figure 3.28D). This suggests that the enhanced protection seen in the high compared to low stimulated groups (Figure 3.27C) might be due to a more rapid secondary FluNP effector response in the lung, both in terms of more FluNP cells in

**Figure 3.28. Peptide avidity at the effector checkpoint increases the secondary effector FluNP response in the lung (Day 5)**

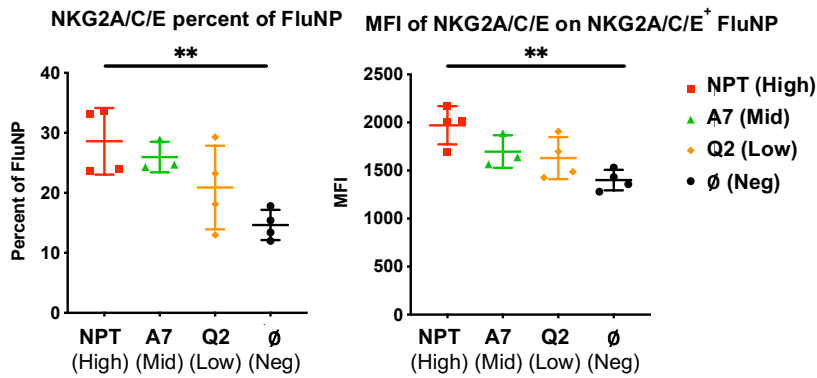
**A Analysis of 5 dpi Secondary Effectors**



**B Evaluation of Secondary Effectors (5 dpi)**



**C NKG2A/C/E expression on 2° FluNP Effectors (Lung 5 dpi)**



**D T-bet expression on 2° FluNP Effectors (Lung 5 dpi)**

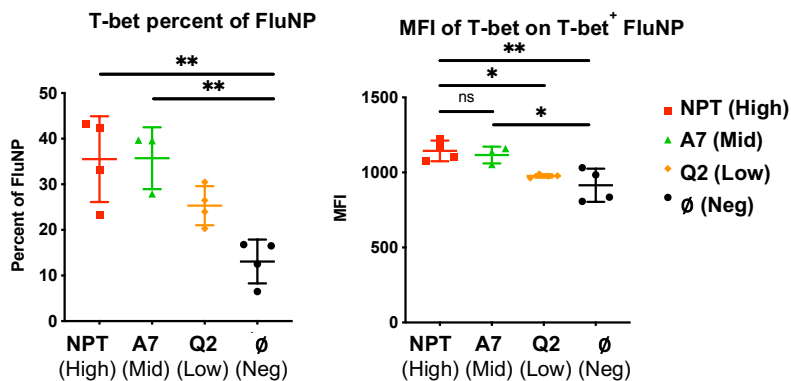


**Figure 3.28. Peptide avidity at the effector checkpoint increases the secondary effector FluNP response in the lung (Day 5)**

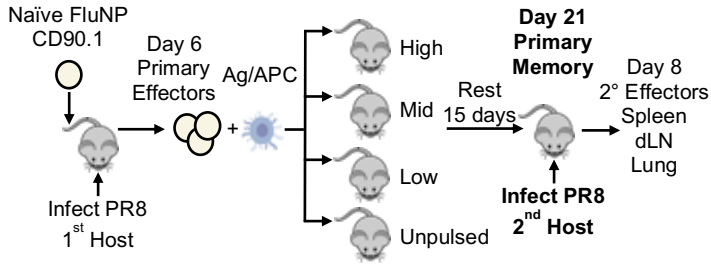
(A) Experimental Design. FluNP effector cells (6 dpi) were isolated and co-transferred with peptide-pulsed APCs into uninfected 2<sup>nd</sup> hosts. At 21 dpi, 2<sup>nd</sup> hosts were infected with a sub-lethal dose of PR8. (B-D) Secondary effector evaluation. The response of secondary FluNP effectors was determined by FACS 5 dpi. (B) Numbers of FluNP in the spleen, dLN and lung 5 dpi. Pooled data, n = 8-9, two experiments, mean +/- SEM. Statistical significance determined by two-tailed independent t test (\*p<0.05). (C-D) Lung FluNP secondary effector phenotyping. (C) Percent NKG2A/C/E expression of 5 dpi lung FluNP secondary effectors (left) and MFI of NKG2A/C/E<sup>+</sup> lung FluNP cells (right). (D) Percent T-bet expression of 5 dpi lung FluNP secondary effectors (left) and MFI of T-bet<sup>+</sup> lung FluNP cells (right). (C-D) Representative data, n = 3-4, one experiment, mean +/- SEM. Statistical significance determined by two-tailed independent t test (\*p<0.05, \*\*p<0.01).

the lung at day 5 (Figure 3.28B), and increased ThCTL (Figure 3.28C) and Th1 (Figure 3.28D) effector functions.

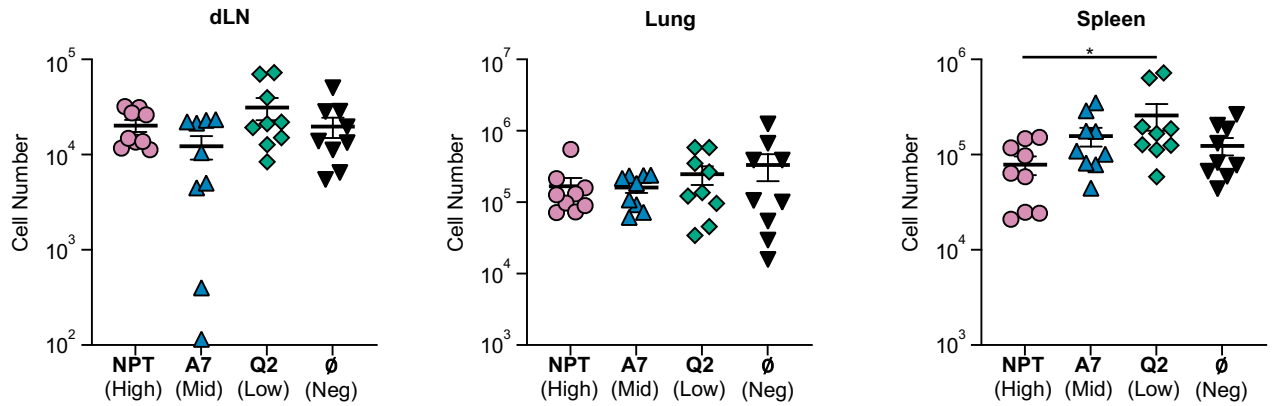
By day 8, the donor FluNP secondary effector cell numbers had equalized in the lung and remained equivalent in the spleen and dLN (Figure 3.29B). Therefore, the numerical advantage conferred by high avidity peptide interaction back at the primary effector checkpoint was significant in the effector populations in the lung but not SLO and only at 5 dpi. We next analyzed the ability of the day 8 donor secondary FluNP effectors to make effector cytokines IFN $\gamma$  and TNF $\alpha$ , as an indicator of their potential for mediating anti-viral effects. We found that a similar fraction of day 8 spleen secondary FluNP effectors were IFN $\gamma$ <sup>+</sup>, however when looking at the amount of IFN $\gamma$  made by the IFN $\gamma$ <sup>+</sup> day 8 FluNP effectors, we did find that day 8 secondary effectors made more IFN $\gamma$  in the NPT (high) group compared to A7 (mid) and Q2 (low) (Figure 3.29C). We found an increase in the fraction of TNF $\alpha$ <sup>+</sup> day 8 FluNP effectors in the NPT (high) group compared to A7 (mid) and that the TNF $\alpha$ <sup>+</sup> FluNP effectors in the NPT group also made more TNF $\alpha$  compared to A7 (Figure 3.29D). Taken together, this data demonstrates that increased peptide avidity at the effector checkpoint promotes a more protective memory population mainly by generating a greater number of memory cells. In addition, when memory cells were generated from the highest effector phase TCR signal strength, the resultant secondary effectors make a bit more IFN $\gamma$  and TNF $\alpha$ . Even though increased peptide avidity dramatically influences the number of memory cells, those that do form when encountering lower avidity peptides are nearly as competent on a per cell basis. We note that all the FluNP memory cells generated have the same TCR, with the same affinity for

**Figure 3.29. Peptide avidity at the effector checkpoint enhances cytokine production from secondary effector FluNP in the spleen (Day 8)**

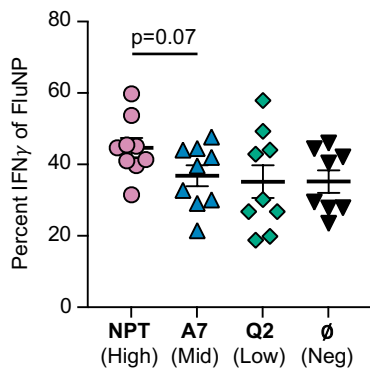
**A Analysis of 8 dpi Secondary Effectors**



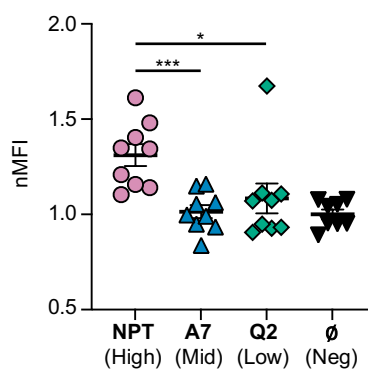
**B Day 8 Secondary Effectors**



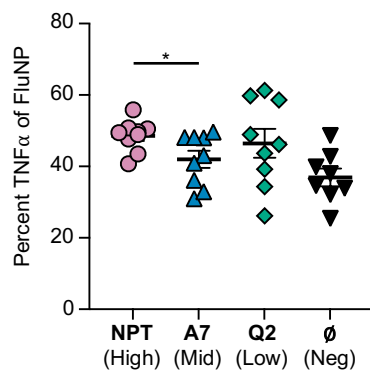
**C Day 8 Spleen IFN $\gamma$**



**Day 8 Spleen FluNP IFN- $\gamma$ +**



**D Day 8 Spleen TNF $\alpha$**



**Day 8 Spleen FluNP TNF $\alpha$ +**

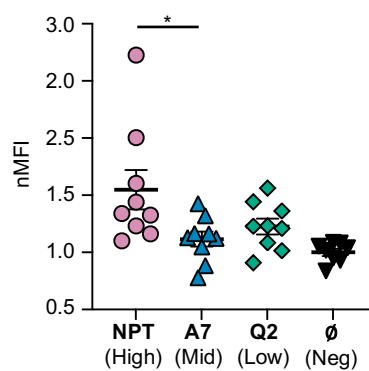


**Figure 3.29. Peptide avidity at the effector checkpoint enhances cytokine production from secondary effector FluNP in the spleen (Day 8)**

**(A)** Experimental Design. FluNP effector cells (6 dpi) were isolated and co-transferred with peptide-pulsed APCs into uninfected 2<sup>nd</sup> hosts. At 21 dpi, 2<sup>nd</sup> hosts were infected with a sub-lethal dose of PR8. **(B-D)** Secondary effector evaluation. The response of secondary FluNP effectors was determined by FACS 8 dpi. **(B)** Numbers of FluNP in the spleen, dLN and lung 8 dpi. **(C-D)** Spleen FluNP secondary effector cytokine expression. **(C)** Percent IFN $\gamma$  expression of 8 dpi spleen FluNP secondary effectors (left) and MFI of IFN $\gamma$ <sup>+</sup> spleen FluNP cells (right). **(D)** Percent TNF $\alpha$  expression of 8 dpi spleen FluNP secondary effectors (left) and MFI of TNF $\alpha$ <sup>+</sup> spleen FluNP cells (right). (B-D) Pooled data, n = 8-9, two experiments, mean +/- SEM. Statistical significance determined by two-tailed independent t test (\*p<0.05, \*\*p<0.01, \*\*\*p<0.001).

the NP of influenza so this avidity for influenza does not change, and this does not in any way evaluate if memory of higher affinity would be more effective, which we predict it would.

**Ag recognition by secondary effectors is required for memory generation and peptide avidity determines the size of response.**

Memory T cells have less stringent requirements than naïve for peptide Ag dose and costimulatory interactions (223), and they become more protective secondary effectors (123). Memory T cells to influenza accumulate with age in adult humans due to multiple exposures, through both influenza infections and vaccinations (224-226) and thus may dominate responses. We asked whether secondary (2°) effectors generated from memory cells, also require Ag recognition at the secondary effector checkpoint to become secondary memory. We generated primary memory cells from 6 dpi FluNP effectors with high peptide/APC in the 2<sup>nd</sup> host to maintain the otherwise naïve state and generate the same number of primary memory cells as IAV infection (Figure 3.8). At day 21, we infected second hosts with a sub-lethal dose of PR8 and isolated 6 dpi donor FluNP 2° effectors. We then co-transferred 2° 6 dpi FluNP effectors along with high, mid and low avidity peptide pulsed APC or unpulsed APC (Figure 3.30A) into 3<sup>rd</sup> hosts and enumerated 2° memory FluNP after 21 days in the spleen, dLN and lung (Figure 3.30B). In each organ, memory generation was dependent on Ag recognition, with the high peptide NPT producing 14.4-fold more memory in spleen, 40-fold more in dLN and 34-fold more in lung compared to APC with no peptide Ag (Figure 3.30B). As in the primary response, the

**Figure 3.30. Peptide avidity during the secondary effector checkpoint regulates the size of the secondary memory population**

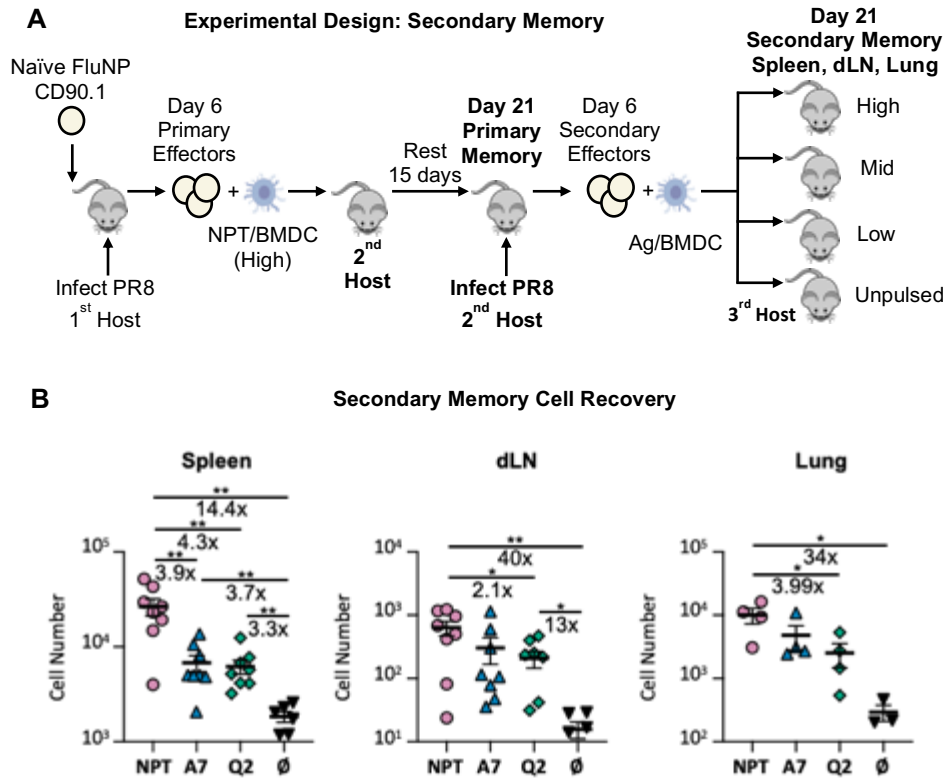


**Figure 3.30. Peptide avidity during the secondary effector checkpoint regulates the size of the secondary memory population**

**(A)** Experimental design. Primary 6 dpi FluNP effectors were generated and  $1.5 \times 10^6$  co-transferred to 2<sup>nd</sup> hosts with  $10^6$  NPT (high) peptide-pulsed BMDCs. At the memory stage, 21 dpi for the donor cells, 2<sup>nd</sup> hosts were infected with PR8 influenza ( $0.3 \text{ LD}_{50}$ ) and secondary 6 dpi effectors were isolated via CD90.1 MACS and co-transferred to uninfected 3<sup>rd</sup> hosts. Fifteen days later 3<sup>rd</sup> hosts were sacrificed, and donor secondary memory cells were analyzed by FACS. **(B)** Number of secondary memory donor FluNP cells determined FACS analysis in the spleen, dLN and lung. Spleen and dLN pooled data,  $n = 6-8$ , two experiments, mean  $\pm$  SEM. Lung representative data  $n = 6-8$ , two experiments, mean  $\pm$  SEM. Statistical significance determined by two-tailed independent t test (\* $p < 0.05$ , \*\* $p < 0.01$ ).

number of memory cells was also reduced when lower affinity peptides were used for pulsing APC. Thus, CD4 memory cells, like naïve cells, need to recognize Ag again as secondary effectors, to form optimal secondary memory and peptide avidity again determines how many secondary memory cells are formed.

### **Effector checkpoint Ag recognition and dose influences effector CD8 T cell memory**

Our lab has extensively focused on the role of late cognate Ag interactions in effector and memory fate decisions for CD4 T cells, and we wondered if this intrinsic requirement held true for CD8 T cells. To test this, we utilized the OT-I CD8 TCR tg system in the sequential adoptive transfer model, like our previously published results for OT-I CD4 T cells (200). In this model, we transferred naïve OT-I CD8 T cells into first hosts and infected with a sub-lethal dose of PR8-OVA<sub>I</sub>. The PR8-OVA<sub>I</sub> virus is a PR8 strain that expresses the OVA peptide recognized by the OT-I TCR. We then isolated 6 dpi effector OT-I cells and transferred them into PR8-OVA<sub>I</sub> (infection and Ag), PR8 (infection alone) infection matched, or uninfected (negative control) second hosts. Since we know that CD8 T cells take longer to contract to stable memory than CD4 T cells (Figure 1.1), we determined the number of OT-I cells 7 and 36 dpt (Figure 3.31A). We then enumerated the number of donor OT-I cells in each mouse by CD8 and Thy1.1 expression (Figure 3.31B). On 7 dpt (13 dpi), we found 10-fold more OT-I cells in the spleen and dLN, and 82-fold more in the lung of PR8-OVA<sub>I</sub> infected mice compared to PR8 or uninfected groups and (Figure3.31C). When we looked at 36 dpt (42 dpi), we found 350 and 280-fold more OT-I cells in the spleen and dLN respectively, and strikingly 1000-fold more in the lung of PR8-OVA<sub>I</sub> infected mice compared to PR8 or uninfected groups and

**Figure 3.31. Cognate antigen during the effector checkpoint regulates the size of the memory CD8 population**

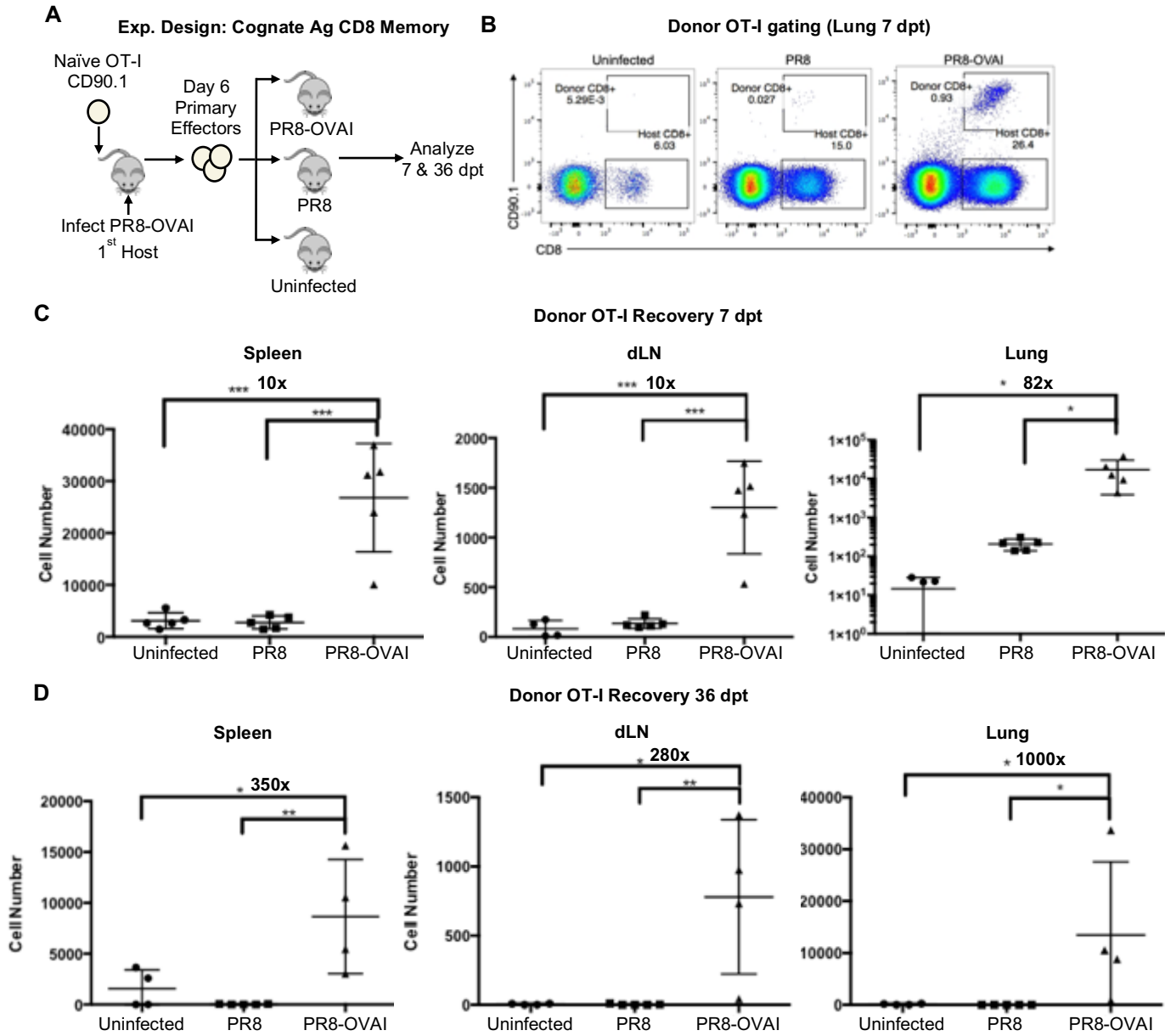


**Figure 3.31. Cognate antigen during the effector checkpoint regulates the size of the memory CD8 population**

**(A)** Experimental Design. Naïve OT-I.Thy1.1<sup>+/-</sup> cells were transferred to B6 hosts, then infected with a sub-lethal dose of PR8-OVAI. At 6 dpi, OT-I effector cells were isolated from the 1<sup>st</sup> hosts and transferred into either uninfected, day 6 PR8, or day 6 PR8-OVAI infection matched hosts (infected 6d previously). 7 and 36 days later (13 & 42 dpi) 2<sup>nd</sup> hosts were sacrificed, and donor OT-I cells were analyzed by FACS. **(B)** Representative FACS plots of lung donor and host CD8 cells 7 dpt. **(C-D)** Donor OT-I cell numbers were enumerated by FACS in the dLN, lung and spleen at **(C)** 7 and **(D)** 36 dpt. Representative data, n = 4, one experiment, mean +/- SEM. Statistical significance determined by two-tailed independent t test (\*p<0.05, \*\*p<0.01, \*\*\*p<0.001).

(Figure 3.31D). We concluded that indeed CD8 effector T cells required to see Ag again at the effector phase of the immune response in order to promote optimal memory CD8 T cell numbers in the spleen, dLN and lung.

We were curious to test if Ag dose or IL-2 signaling enhanced memory CD8 T cell formation in this system. Instead of using the different affinity SIINFEKL peptides recognized by OT-I cells, we decided to try pulsing APC with different doses of the SIINFEKL peptide. From previous work we know that CD8 effector cells can be classified as terminal effector cells by KLRG1 expression and as memory precursor cells by CD127 expression (227, 228). We generated 6 dpi OT-I effector cells as above and co-cultured them *in vitro* with Ag/APC, pulsed at various Ag doses, with and without exogenous IL-2 in the media. After 2 days in culture we assayed OT-I effector function by analyzing the amount of IFN $\gamma$  produced in the supernatant by ELISA. We found that, as expected, 6 dpi OT-I effector cells produced IFN $\gamma$  in an Ag dose-dependent manner (Figure 3.32, left). We also noticed that the addition of exogenous IL-2 in the culture media (10 ng/mL) helped to slightly boost IFN $\gamma$  production (Figure 3.32, right), presumably by keeping more OT-I cells alive in culture, although we do not have evidence of this. We also looked by FACS at KLRG1 expression on these OT-I cells after 2 days in culture as a measure of terminal effector status. Interestingly, we saw that as Ag dose increased, the effector OT-I cells expressed less KLRG1, as there appeared to be an increase in KLRG1<sup>lo</sup> cells (Figure 3.32, left). We also noticed that with exogenous IL-2 in the media, we saw diminished KLRG1 expression on OT-I cells stimulated compared with the same Ag dose without exogenous IL-2 in the media (Figure 3.32, right). Looking specifically at the IL-2 treated group, we

**Figure 3.32. Culture of 6d OT-I effectors reveals Ag dose and IL-2 increase IFN $\gamma$  production and decreases KLRG1 expression *in vitro***

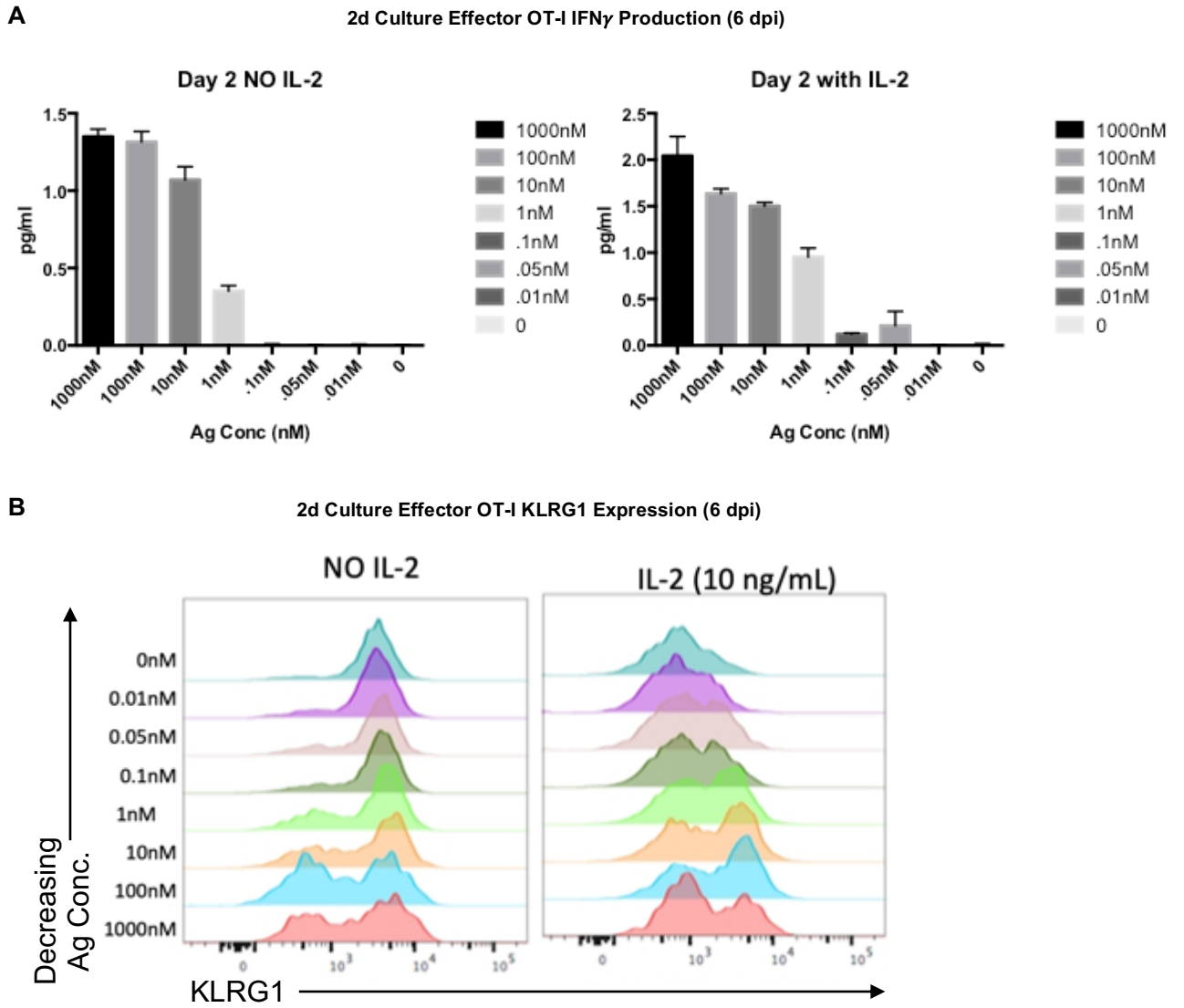


**Figure 3.32. Culture of 6d OT-I effectors reveals increasing Ag and IL-2 increase IFN $\gamma$  production and decreases KLRG1 expression *in vitro***

**(A-B)** Naïve OT-I.Thy1.1<sup>+/-</sup> cells were transferred to B6 hosts, then infected with a sub-lethal dose of PR8-OVAI. At 6 dpi, OT-I effector cells were isolated from the 1<sup>st</sup> hosts and co-cultured with SIINFEKL pulsed Ag/APC for 2d *in vitro*, with and without exogenous IL-2 (10 ng/mL) in the media. **(A)** IFN $\gamma$  production in the supernatant was determined by ELISA. **(B)** Representative KLRG1 histograms of OT-I cells after 2d *in vitro* with Ag/APC with and without exogenous IL-2 (10 ng/mL).

saw that Ag dose actually increased the KLRG1 expression on the OT-I effector cells (Figure 3.32, right). We found these results of particular interest for two reasons. The first is that in the absence of IL-2, increasing Ag dose results in an increase in KLRG1<sup>lo</sup> cells, suggesting increased TCR engagement at the effector checkpoint results in a decrease in terminal effector OT-I CD8 T cells. This fits nicely with our data showing that late Ag in the sequential transfer system increases the size of the memory CD8 T cell population (Figure 3.31). The second interesting piece here is that exogenous IL-2 reduces KLRG1 expression and thus may be important for effector CD8 T cell survival to memory as well. These results are preliminary, and more work must be done to tease apart the impact effector checkpoint Ag recognition has on the formation of CD8 memory.

## CHAPTER IV: Discussion

### Overview

In this thesis I examined the impact of peptide avidity for the FluNP TCR, delivered at the CD4 effector checkpoint (200, 201), on memory formation. The goal of this work was to build on our previous findings that both cognate Ag interactions (200) and autocrine IL-2 signaling (201) were required at the effector checkpoint, 5-8 dpi, for the optimal generation of CD4 memory that protect against future IAV infection (120, 229). We continually observed that CD25 (IL-2R $\alpha$ ) was not expressed by our 6 day CD4 effectors and we wondered how this mechanism of late cognate Ag interaction and autocrine IL-2 influenced memory outcomes. We hypothesized that peptide avidity for TCR *in vivo* might influence both IL-2, and other cytokine, production by our 6 day effectors and IL-2R subunit expression on the same cells. We recovered the greatest number of CD4 memory cells after 6 day FluNP effectors were stimulated with the highest avidity peptide, with 200-fold more in the lung compared to no peptide, and 20-50-fold more compared to low avidity peptide. Higher peptide avidity drove higher levels of autocrine IL-2 production, which promoted greater effector survival and donor FluNP cell recovery in the late effector phase, laying out the mechanisms likely to be responsible. The importance of autocrine IL-2 in memory formation was emphasized by the fact that optimum levels of memory generation required that activated APC express IL-2R $\alpha$  during the cognate interaction with CD4 effectors. This fit with our observation that 6 day CD4 effectors expressed almost no CD25, while maintaining some expression of CD122 (IL-2R $\beta$ ) and CD132 (IL-2R $\gamma$ ). The CD4 FluNP memory cells generated by both high avidity peptides led to increased

protection from lethal rechallenge. Secondary CD4 effector cells, generated from primary memory that were formed following stimulation with high avidity peptide at the primary memory checkpoint, also required Ag recognition again at the secondary effector checkpoint to form secondary memory and were again favored by high avidity peptide. To increase CD4 T cell memory, we suggest vaccine strategies must supply a second round of high avidity antigen and pattern recognition signals shortly after initial immunization during the effector T cell response.

### **The summation of all cognate antigen signals throughout the life of a T cell**

Previous studies varied Ag avidity at the initiation of the immune response and found that both increased dose and peptide avidity could lead to greater effector and memory T cell numbers, however the recall responses from these different memory populations were equivalent (177, 180, 186, 188, 189, 196, 197, 230). Extending the period of Ag presentation also promoted enhanced CD4 and CD8 memory formation (165, 166, 168, 194, 195, 200, 201). The pathways responsible were not determined and no studies restricted Ag to the effector checkpoint, that we know is strictly required for memory generation (120, 200, 201). The work here in this thesis is the first to analyze the effect of a broad range of peptide avidity during the effector checkpoint on CD4 T cell memory. Our results indicate that at the effector checkpoint, 6 days after initial infection, peptide/MHC-II avidity for the TCR on the CD4 effectors during cognate interaction determines the magnitude of memory by regulating the level of effector production of autocrine IL-2. In turn, this determines how many effectors survive over the next few days and progress to memory. In the polyclonal situation, this likely selects for CD4 memory

cells which are of the highest affinity for the pathogen Ag they recognize. Our preliminary data suggests that CD8 T cells also require late cognate Ag interactions at the effector checkpoint to form a larger memory population. We found that both increased peptide avidity and addition of exogenous IL-2 increased the fraction of KLRG1<sup>lo</sup> effector CD8 T cells *in vitro*.

There is evidence that even pMHC-TCR signals during CD4 T cell development have the potential to shape peripheral CD4 T cell responses. During development, CD4 T cells stimulated by the same peptide Ag with equal affinity for TCR demonstrate different memory potential based on levels of tonic signaling (181, 187). This data indicates that even the same affinity peptide Ag can elicit different responses from CD4 T cells (181) and that this tonic signaling during development can shape the differentiation pattern of effector CD4 T cells, with lower tonic TCR triggering favoring T<sub>FH</sub> development while having no impact on Th1 formation (182). T cell responses are educated by cognate Ag signals not just during priming. If cognate Ag signals before priming can shape peripheral T cell responses, then can cognate Ag signals after priming also instruct T cell responses?

I return here to my view that acute viral infections, particularly influenza, provide a Goldilocks “just right” amount and duration of inflammatory and Ag signals to promote high quality and effective T cell memory. Vaccine immunization, on the other hand, is the “too cold” scenario, in which for too short of a duration, too few inflammatory and Ag signals elicit mild T cell memory. Chronic infection creates the “too hot” scenario, in which inflammation and Ag signals persist for too long and drive T cell exhaustion. We must consider how signals from inflammation and Ag instruct T cell responses in different tissue

locations at different times during an immune response. This poses quite the challenge in understanding T cell memory because there are simply too many variables to control for here, and it is easy to recognize how memory studies can provide conflicting reports about how TCR triggering and peptide Ag affinity influences memory T cell responses.

I find several aspects of the work presented here of critical importance to this idea that Ag signals from development, priming, and the effector phase can instruct T cell memory fate decisions. In all the memory experiments conducted in this thesis, naïve FluNP cells were primed *in vivo* from day 0-6 of IAV infection. Using a CD4 TCR tg specific for a physiologically relevant, high affinity immunodominant IAV NP epitope allows for the natural development of effector cells, with the caveat that these cells started from a greater number ( $5 \times 10^5$ - $1 \times 10^6$ ) of naïve cells, of which there is only 10% engraftment reported during intravenous cell transfer (231), than what is physiologically relevant for an individual T cell clone of about 10-100 cells/ $10^6$  naïve cells (232, 233). When these 6 day effector FluNP cells are transferred into an uninfected second host along with unpulsed, activated APC, they still form a memory population on day 21 of about 50 cells in the lung, 100 cells in the dLN and 10,000 cells in the spleen (Figure 3.9C, black triangles) and these memory cells produce cytokines immediately on restimulation (Figure 3.14). Even though these high affinity FluNP memory cells were generated day 0-6 from IAV infection, established memory in the lung, dLN and spleen of second hosts and exhibited immediate cytokine production on re-stimulation, they still failed to protect the second host from lethal IAV challenge (Figure 3.27C). Just because memory cells can be detected in key tissues does not mean they can, or will, provide adequate protection against subsequent infection.

There appears to be a certain threshold of memory numbers required for adequate protection, and this threshold is not reached in the absence of cognate antigen recognition at the effector checkpoint.

In trying to understand how the memory FluNP cells generated from high peptide avidity stimulation at the effector checkpoint provided this enhanced protection, I hypothesized that it was either due to the dramatic fold increase in the number of these memory FluNP cells in the lung, dLN and spleen (Figure 3.10) or that increased peptide avidity at the effector checkpoint generated a better-quality memory cell. There was no striking difference in immediate cytokine production from spleen FluNP memory cells generated across all effector checkpoint peptide avidities, although about 1.5x more of the high NPT stimulated FluNP cells were IFN $\gamma$ <sup>+</sup> (60%) compared with the low Q7 and unpulsed stimulated FluNP cells (~40%) (Figure 3.14). On a per cell basis, the FluNP memory cells generated from low Q7 effector checkpoint peptide Ag produced slightly more TNF $\alpha$  than their high NP<sub>311-325</sub> stimulated counterparts (Figure 3.14). We have seen these results before in the OT-II system, where memory cells generated from effectors that received cognate Ag signals at the effector checkpoint produce more IFN $\gamma$  and less TNF $\alpha$ , while memory cells generated in the absence of effector checkpoint cognate Ag produce more TNF $\alpha$  and less IFN $\gamma$  (200). Production of TNF $\alpha$  by CD8 T cells in the lung has been shown to disrupt uninfected lung epithelial cells, cause severe tissue damage and is associated with severe influenza in humans (234-238). Additionally, expression of a TNF $\alpha$  inhibitor in the lung reduced tissue damage following influenza infection (239). Perhaps the increase in immediate TNF $\alpha$  production from our low peptide avidity generated

memory FluNP cells is enough to disrupt lung epithelial cells early during IAV challenge and increase the observed mortality seen in these mice (Figure 3.27) or exacerbate lung pathology during the secondary response. In future experiments, it will be critical to look at the cytokine profiles of these early secondary effector cells in the lung.

I studied the secondary effector response of the memory FluNP cells to further parse out if enhanced protection was due to either the dramatic fold increase in the number of memory FluNP cells in the lung, dLN and spleen (Figure 3.10) or that increased peptide avidity at the effector checkpoint generated a better-quality memory cell. Since we know that secondary effector responses demonstrate slightly more rapid kinetics than primary responses (123), We looked at the secondary FluNP effector response at 5 dpi, to catch potential early effector differences, and at 8 dpi, the peak of the effector response (Figure 3.1-2). We found an increase in the number of day 5 secondary FluNP effectors, following high avidity peptide stimulation at the effector checkpoint, in the lung, while there was no difference in FluNP numbers in the spleen or dLN (Figure 3.28B). It is unclear if the increase in day 5 secondary FluNP effectors in the lung stems from the pre-existing increase in number of day 21 memory cells in the lung (Figure 3.9C), increased or more rapid proliferation of these secondary effectors, or enhanced migration to the lung. On day 21, there are about  $10^4$  memory FluNP cells in the lung of the high NPT stimulated group (Figure 3.9C), and on day 5 of the secondary response we see almost  $10^5$  FluNP cells in the lung (Figure 3.28B), suggesting that 10-fold proliferation, recruitment from other tissues, or some combination of the two result in this secondary FluNP effector cell number increase. One could test proliferation by including BrdU in the drinking water of the second

host memory mice, and then compare BrdU labeling of day 5 secondary FluNP effector cells in the lung between the different peptide groups to look for increased frequencies of proliferating cells in the high compared to low groups. Testing migration may prove more challenging as these memory cells may rely on several different receptors to mediate movement to the lungs and particularly tricky for T<sub>EM</sub> cells as they do not express CD62L or CCR7, but one may try blocking migration to the lung with anti-CXCR3 antibody in conjunction with blocking egress from the dLN with FTY720.

We also found that, not only were there more day 5 secondary FluNP effector cells in the lung, but a greater fraction of these cells expressed the ThCTL marker NKG2A/C/E (Figure 3.28C) and the Th1 transcription factor T-bet (Figure 3.28D). Perhaps increased peptide avidity at the effector checkpoint not only increases the number of memory cells, but also enhances the capacity of these memory cells to differentiate into ThCTL and Th1 effectors more fully or more rapidly upon challenge. In future experiments it will be interesting to see if the increase in percent of ThCTL and Th1 markers of day 5 lung secondary FluNP effectors also shows increased cytotoxicity of NP-pulsed targets and diminishes or controls lung viral titers better than their low peptide avidity stimulated counterparts.

In adult humans, with a long history of exposure to influenza viruses, many responses likely stem from existing memory cells (224-226). We find that efficient generation of secondary memory also requires effector checkpoint Ag recognition and is increased by high peptide avidity interactions (Figure 3.30). This contrasts with observations that memory responses in general are less dependent on Ag dose and

costimulation than primary responses (123). We suggest that secondary effector functions, stemming from primary memory cells, have a lower activation threshold than their naïve counterparts (123) are more easily achieved in part due to the poised epigenetic landscape at effector gene loci (116-119), but when forming new secondary memory, stringent regulation is again in place to avoid the generation of unnecessary memory cells and select only those with high affinity for persistent Ag in the context of infection.

#### **Additional potential roles of effector checkpoint cognate Ag**

In our studies, the impact of effector checkpoint peptide avidity on memory was consistently more dramatic in lung and dLN, compared to the spleen. One likely explanation for this is that higher avidity peptide also promotes effector migration from the spleen to the lung, so the impact of peptide avidity is less apparent in the spleen. We and others have shown that effector checkpoint Ag recognition and strong Th1 skewing promote greater expression of CXCR3 by effector cells, promoting their trafficking to tissue sites (105, 200, 212, 213). The results are particularly striking here, because in the 2<sup>nd</sup> host there is no infection or inflammation in the lung to attract FluNP effectors. Thus, we suggest peptide avidity at the effector checkpoint also regulates migration to the tissues.

We looked at CXCR3 expression on day 21 memory FluNP cells generated from high, mid, low and no peptide avidity stimulation back at the effector checkpoint and found that high avidity compared to unpulsed increased the fraction of CXCR3<sup>+</sup> memory FluNP cells in the spleen, dLN and lung by about 2-fold (Figure 3.13B), consistent with our previous findings in the OT-II system (200). However, we saw no clear or obvious pattern comparing the fraction of CXCR3<sup>+</sup> memory FluNP cells in the spleen, dLN and lung

between high, mid and low avidity stimulated groups. There are several possibilities as to why there is no clear pattern in CXCR3 expression on memory cells. The first is that CXCR3 expression on CD4 memory may be a digital on/off response to TCR stimulation as opposed to graded levels of expression based on peptide avidity (215). This notion fits with our data here and our previously published results (200) that show peptide stimulation compared to no stimulation at the effector checkpoint promotes more CXCR3 expression, but there are no differences between different peptide avidity groups (Figure 3.13). A second explanation is that signals during priming are sufficient to induce CXCR3 expression on 40-60% of day 21 donor memory FluNP cells and that cognate Ag interaction at the effector checkpoint has a limited or no role in CXCR3 induction. A third possibility is that the truth lies somewhere in the middle, that signals both during priming, and to some extent, during the effector checkpoint synergize to induce CXCR3 expression on the resultant CD4 memory cells. More work is needed to tease apart how effector checkpoint cognate Ag interactions influence CXCR3 expression on CD4 memory.

Another area of key interest is to what extent does effector checkpoint cognate Ag and peptide avidity impact  $T_{CM}$  and  $T_{EM}$  in the spleen and dLN, and  $T_{RM}$  formation in the lung. We found the frequency of  $T_{CM}$  cells in the spleen and dLN equivalent between the different NP peptide stimulated groups, about 20% of all memory FluNP cells (Figure 3.12). We observed that the frequency of  $T_{EM}$  in the spleen and dLN decreased in conjunction with peptide avidity (Figure 3.12). A previous report has shown that prime-boost vaccine strategies increase frequencies of CD8  $T_{EM}$  with each additional boost (192), so the increase in FluNP  $T_{EM}$  frequency in the spleen and dLN, resulting from increased

peptide avidity, may reflect that the strength of the boost, in this case mediated by effector checkpoint cognate Ag, can also increase the frequency of  $T_{EM}$  cells. The frequencies of *in situ* FluNP  $T_{EM}$  (~75%) and  $T_{CM}$  (~25%) induced in the spleen following IAV infection (Figure 3.5E) compared to those induced by the high peptides NPT and NP<sub>311-325</sub> on day 21 in the sequential transfer model ( $T_{EM}$  ~80%,  $T_{CM}$  ~20%) are roughly equal. This demonstrates that high avidity peptide Ag at the effector checkpoint, without infection, can induce the same frequencies of  $T_{EM}$  and  $T_{CM}$  as IAV infection, and that as peptide avidity decreases, the total number memory FluNP cells and  $T_{EM}$  frequency of FluNP cells falls while the frequency of  $T_{CM}$  cells remains relatively stable. As all FluNP cells received signals from infection and Ag days 0-6 of the immune response, perhaps these early signals are sufficient to promote ~20-25% of the memory population to become  $T_{CM}$ , while peptide avidity and additional Ag stimulation promote a greater number of total memory cells and a greater frequency of  $T_{EM}$  cells.

The  $T_{RM}$  frequency, as measured by CD69 expression of day 21 donor FluNP memory cells in the lung, increased following stimulation at the effector checkpoint with peptides of increasing avidity (Figure 3.12D). To call these FluNP cells true  $T_{RM}$ , we must further characterize their lung tissue residence by using i.v. antibody labeling to distinguish between cells close to the vasculature (i.v. Ab<sup>+</sup>) from those that are truly imbedded in the tissue and not near blood vessels (i.v. Ab<sup>-</sup>). Comparing the  $T_{RM}$  frequencies of lung memory FluNP cells generated from *in situ* IAV infection (~50%) (Figure 3.5E) to memory FluNP cells generated from high avidity NP peptides in the sequential transfer model (~25%) (Figure 3.12E), we notice a two-fold reduction in  $T_{RM}$  frequencies in the absence

of continuing infection through the effector checkpoint. Although 6 day FluNP effector cells received high avidity cognate Ag in the sequential transfer system, this did not generate as much  $T_{RM}$ , by CD69 expression, as did *in situ* IAV infection. This suggests that both IAV infection from day 0-6 and high avidity peptide stimulation at the memory checkpoint is not sufficient to generate the same frequency of  $T_{RM}$  as the full duration acute IAV infection.

### **IL-2 as a master regulator of effector T cell survival**

We found previously that Ag presentation to effector CD4 T cells at the effector checkpoint induces autocrine IL-2 signaling, which prevents their default apoptosis and thus supports formation of memory cells (200, 201). In this thesis, we show that increased peptide avidity at the effector checkpoint does not impact the proliferation of 6 day FluNP effectors *in vivo* 3 dpt (Figure 3.16) or 2 dpt (Figure 3.15E), but does increase the amount of IL-2 produced by these FluNP effectors (Figure 3.22A-C) and leads to a dramatic increase in short term effector survival (Figure 3.17). In each organ, comparing the high avidity peptide stimulated group to the unpulsed group, there was more than a 100-fold increase donor FluNP effector cells recovered 3 dpt and very few total number of donor FluNP cells recovered in the unpulsed groups (spleen  $\sim 10^3$ , dLN  $\sim 500$  and lung  $\sim 50$ ) (Figure 3.18). At this timepoint 3 dpt in all tissues, even the low avidity peptide results in 20-40-fold more effector FluNP cells recovered compared with unpulsed APC (Figure 3.18). We find that the number of FluNP effectors recovered 3 dpt (Figure 3.18) is proportional to the size of the memory population at day 21 (Figure 3.9C). The observed increase in IL-2 production by 6 day FluNP effectors with increasing avidity and dose of

Ag (Figure 3.22A-C), clearly links the effect of effector checkpoint peptide avidity to IL-2 production, rescue of effectors 3 dpt and thus increased memory formation by day 21.

However, CD25 was either transiently expressed or not expressed on most CD4 effectors (Figure 3.21), raising the possibility that optimum autocrine IL-2-mediated survival of effectors might be regulated by something in addition to IL-2 binding to IL-2R complex on the CD4 T cell. The IL-2R has two forms, the low affinity IL-2R, comprised of CD122 (IL-2R $\beta$ ) and CD132 (IL-2R $\gamma$ ), and the high affinity IL-2R, comprised of CD25 (IL-2R $\alpha$ ), CD122 (IL-2R $\beta$ ) and CD132 (IL-2R $\gamma$ ). The affinity of IL-2 for IL-2R $\alpha$  alone ( $K_D \sim 10^{-8}$  M) (240, 241), IL-2R $\beta/\gamma$  ( $K_D \sim 10^{-9}$  M) (242) and the high affinity IL-2R $\alpha/\beta/\gamma$  ( $K_D \sim 10^{-11}$  M) (243) increases by 10-100 fold as the full tripartite receptor is assembled. IL-2 signaling is mediated by the cytoplasmic tails of the IL-2R $\beta$  and IL-2R $\gamma$  (244, 245), while IL-2R $\alpha$  contains no signaling domain and its main role is to increase the affinity of the high affinity IL-2R $\alpha/\beta/\gamma$  (246). Another interesting aspect of the high affinity IL-2R $\alpha/\beta/\gamma$  is that the IL-2R $\alpha$  appears to make no contacts with IL-2R $\beta/\gamma$  (247), instead IL-2R $\alpha$  binds to free IL-2 and this IL-2R $\alpha$ -IL-2 complex concentrates at the cell surface and engages the IL-2R $\beta/\gamma$  signaling domain (248).

Another survival cytokine, IL-15, which shares IL-2R $\beta/\gamma$  with IL-2, is presented *in trans* when bound to IL-15R $\alpha$  on APC while signaling through IL-2R $\beta/\gamma$  on the T cell (217-219). The affinity of IL-15 for the IL-15R $\alpha$  is about  $10^{-10}$ - $10^{-11}$  M (249-252), which is roughly equivalent to the high affinity of the IL-2R $\alpha/\beta/\gamma$  complex for IL-2. Interestingly, the IL-15R $\alpha/\beta/\gamma$  complex demonstrates the same affinity for IL-15 as the IL-15R $\alpha$  alone

(253). By comparison, IL-2R $\alpha$ -IL-2 affinity ( $K_D \sim 10^{-8}$  M) is 100-1000-fold lower than IL-15R $\alpha$ -IL-15 ( $K_D = 10^{-10}$ - $10^{-11}$  M).

Previous studies reported that activated APC can express CD25 in both mice and humans (220, 254). We found that several subsets of activated APC in mice infected with IAV 4-8 d earlier (Figure 3.23) and the activated BMDC we use as APC all express high levels of CD25 (Figure 3.24). There are also various reports in the literature which suggest IL-2 might be presented *in trans* by the IL-2R $\alpha$  (220-222). I hypothesized that CD25 (IL-2R $\alpha$ ) expression on APC at the effector checkpoint might increase the local affinity of IL-2R $\beta/\gamma$  on effector FluNP cells for the IL-2 these cells produce in response to peptide Ag, therefore increasing effector FluNP survival to memory. We tested CD25 deficient APC and found they drove less memory formation compared to WT APC *in vivo* (Figure 3.26). This suggests that Ag/APC transpresent autocrine IL-2 to the interacting CD4 T cells, increasing IL-2 availability at the time CD4 effectors do not express CD25, and driving greater effector survival and memory formation (Figure 4.1). Thus, we suggest infection provided pathogen recognition (PR) signals that activate APC, enhancing their CD25 expression, as well as MHC-II and costimulatory ligands, so they efficiently present both peptide Ag and CD4 effector-produced IL-2. We suggest this mechanism evolved to require that infection provide high avidity Ag at a high dose, and APC activation by PR signals, to promote optimum effector transition to memory, especially in the lung, the site of infection. This mechanism would restrict memory generation to situations where virus is still replicating and providing PR signals at the effector stage. Thus, effective vaccine

**Figure 4.1. A model illustrating how effector checkpoint cognate Ag improves effector CD4 T cell survival by a novel autocrine IL-2 signaling mechanism**

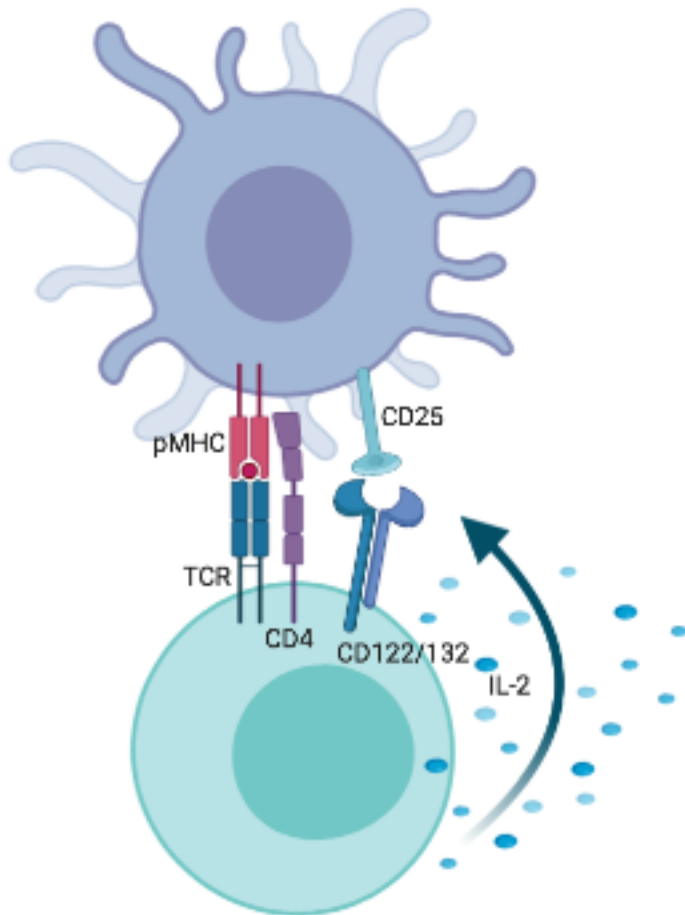


**Figure 4.1. A model illustrating how effector checkpoint cognate Ag improves effector CD4 T cell survival by a novel autocrine IL-2 signaling mechanism**

An effector CD4 T cell (green) engages Ag/APC (blue) through pMHC-TCR interaction.

The CD4 T cell produces IL-2 in response to TCR engagement in a peptide avidity-dependent manner, with strong interactions resulting in more IL-2 production. Activated APC express CD25 (IL-2R $\alpha$ ) at this time and acts to present IL-2 *in trans* to IL-2R $\beta/\gamma$  (CD122/CD132) expressed on the surface of the effector CD4 T cell. This interaction promotes the survival of this effector cell to memory.

strategies likely need to provide high dose, high avidity Ag and PR signals again during the T cell effector phase.

### **Implications for vaccine design**

The impressive impact of Ag avidity for TCR in determining the size of the memory pool from both primary (Figure 3.9C) and secondary (Figure 3.30) CD4 effectors indicates that both a high dose of available peptides and CD4 effectors bearing TCR with high affinity for some of those peptides are strictly required for robust memory generation. Because of the heterogeneity of human class-II, only a fraction of total potential viral epitopes will be immunodominant in each individual, which also argues for vaccines expressing a breadth of proteins. This implies immunization with a wide range of viral proteins, including those with known immunodominant CD4 epitopes, will be more effective in inducing memory than single proteins or epitopes. A broader repertoire of high affinity memory CD4 T cells also should lower the likelihood that escape variants, which arise by random mutations and selection, will have the opportunity to develop and escape a broad CD4 T cell response so they can be passed on, since this would require multiple mutations. Many of the immunodominant T cell epitopes, such as the FluNP NP<sub>311</sub> used here, are in core proteins of viruses, not in the viral surface proteins that B cells recognize, thus it follows that vaccines should include both core and surface protein epitopes, to elicit both T and B cell immune memory, including heterosubtypic determinants which may escape recognition by antibodies to external surface proteins that are known to mutate, like influenza HA.

Since more memory is generated when CD25 is expressed by activated APC, our studies re-affirm that vaccines need to provide continuing PR signals that directly activate APC. Our results predict that in polyclonal responses, the requirement for high avidity of TCR for Ag/APC will serve to select a spectrum of memory cells of higher affinity than the effector population. This should result in more effective protection in the real-life polyclonal situation. An advantage of vaccines is that they can supply these signals in a less dangerous context than infection. Additional studies are needed to support these later implications in detail, but we suggest that the overall purpose of the requirement for a high avidity interaction at the effector stage is to provide more memory cells with higher affinity for the infecting virus, while not allowing memory when virus does not persist at high levels into the effector stage, or there is no replicating infectious entity.

Because mRNA-LNP vaccines provide both inflammatory signals that may better activate APC (54), and demonstrate the ability to provide Ag for a longer duration through the effector checkpoint (53), they are an exciting new approach to lower the risks of infectious diseases. The immune system relies heavily on redundant mechanisms to achieve desirable outcomes. A clear example of this is how T and B cells work in conjunction to clear primary infections and provide life-long immunity. However, a glance at any clinical vaccine trial highlights that all primary outcome measures, the information that informs FDA approval decisions, reflect the antibody response. Policy makers must consider the fault in excluding T cell data from these decisions.

Using the conclusions drawn from this thesis and many other excellent studies, I propose a new paradigm in vaccine strategy. Since mRNA-LNP vaccines provide both

signals to activate APC fully and long duration of available Ag, and have demonstrated the ability to promote both T and B cell responses and protection, they are an excellent technological tool to provide life-long immunity to patients. However, we must be very strategic in how we design mRNA payloads, as immunizing against a single protein or epitope may not be the most effective strategy. It is important to include a wide breadth of potentially immunodominant Ag to avoid selecting for escape mutants. In the current prime on day 0 and boost on day 21 model, the effector checkpoint is entirely missed. We have quickly accepted the need to return to the clinic for a three-week follow-up booster shot. I propose that following day 0 intramuscular immunization with mRNA-LNP, we boost with an intranasal LAIV at day 6, followed by another mRNA-LNP boost at day 21. Following the first dose, a practitioner can send the patient home with an inhalable LAIV to be taken with a telehealth appointment, mitigating any need to return to the clinic. This second dose provides both local Ag and inflammation at the site of infection at the right time required for optimal T cell memory. This strategy may provide both strong inflammatory signals to fully activate APC to express CD25 and provide effector checkpoint cognate Ag interactions to responding primary effector and already established memory T cells, as both primary and secondary effectors demonstrated that high avidity effector checkpoint Ag induced optimal T cell memory. Future experiments may study how modulating functional avidity at the effector checkpoint, by using peptides with different affinities for TCR or the same affinity but with different Ag doses impacts T cell memory formation. Of clinical relevance, it would be very interesting to perform a meta-analysis of different vaccine studies in people to compare the duration of Ag presentation and the activation status of

APC, specifically CD25 expression, following immunization and see if either increased duration of Ag presentation or APC CD25 expression correlated with improved vaccine efficacy or more T cell memory.

## CHAPTER V: References

1. Crotty, S. 2019. T Follicular Helper Cell Biology: A Decade of Discovery and Diseases. *Immunity* 50: 1132-1148.
2. Laidlaw, B. J., J. E. Craft, and S. M. Kaech. 2016. The multifaceted role of CD4(+) T cells in CD8(+) T cell memory. *Nat Rev Immunol* 16: 102-111.
3. Laidlaw, B. J., N. Zhang, H. D. Marshall, M. M. Staron, T. Guan, Y. Hu, L. S. Cauley, J. Craft, and S. M. Kaech. 2014. CD4+ T cell help guides formation of CD103+ lung-resident memory CD8+ T cells during influenza viral infection. *Immunity* 41: 633-645.
4. Cullen, J. G., H. A. McQuilten, K. M. Quinn, M. Olshansky, B. E. Russ, A. Morey, S. Wei, J. E. Prier, N. L. La Gruta, P. C. Doherty, and S. J. Turner. 2019. CD4(+) T help promotes influenza virus-specific CD8(+) T cell memory by limiting metabolic dysfunction. *Proc Natl Acad Sci USA*.
5. McKinstry, K. K., T. M. Strutt, Y. Kuang, D. M. Brown, S. Sell, R. W. Dutton, and S. L. Swain. 2012. Memory CD4+ T cells protect against influenza through multiple synergizing mechanisms. *J Clin Invest* 122: 2847-2856.
6. Brown, D. M., A. M. Dilzer, D. L. Meents, and S. L. Swain. 2006. CD4 T cell-mediated protection from lethal influenza: perforin and antibody-mediated mechanisms give a one-two punch. *J Immunol* 177: 2888-2898.
7. Teijaro, J. R., D. Verhoeven, C. A. Page, D. Turner, and D. L. Farber. 2010. Memory CD4 T cells direct protective responses to influenza virus in the lungs through helper-independent mechanisms. *J Virol* 84: 9217-9226.
8. Krammer, F., G. J. D. Smith, R. A. M. Fouchier, M. Peiris, K. Kedzierska, P. C. Doherty, P. Palese, M. L. Shaw, J. Treanor, R. G. Webster, and A. Garcia-Sastre. 2018. Influenza. *Nat Rev Dis Primers* 4: 3.
9. Sederdahl, B. K., and J. V. Williams. 2020. Epidemiology and Clinical Characteristics of Influenza C Virus. *Viruses* 12.
10. Asha, K., and B. Kumar. 2019. Emerging Influenza D Virus Threat: What We Know so Far! *J Clin Med* 8.
11. 1980. A revision of the system of nomenclature for influenza viruses: a WHO memorandum. *Bull World Health Organ* 58: 585-591.
12. Baum LG, P. J. 1990. Sialyloligosaccharides of the respiratory epithelium in the selection of human influenza virus receptor specificity. *Acta Histochem Suppl.* 40: 35-38.
13. Kuchipudi, S. V., R. K. Nelli, A. Gontu, R. Satyakumar, M. Surendran Nair, and M. Subbiah. 2021. Sialic Acid Receptors: The Key to Solving the Enigma of Zoonotic Virus Spillover. *Viruses* 13.
14. Helft, J., B. Manicassamy, P. Guernonprez, D. Hashimoto, A. Silvin, J. Agudo, B. D. Brown, M. Schmolke, J. C. Miller, M. Leboeuf, K. M. Murphy, A. Garcia-Sastre,

- and M. Merad. 2012. Cross-presenting CD103+ dendritic cells are protected from influenza virus infection. *J Clin Invest* 122: 4037-4047.
15. Manicassamy, B., S. Manicassamy, A. Belicha-Villanueva, G. Pisanelli, B. Pulendran, and A. Garcia-Sastre. 2010. Analysis of in vivo dynamics of influenza virus infection in mice using a GFP reporter virus. *Proc Natl Acad Sci U S A* 107: 11531-11536.
  16. Martin, K., and A. Helenius. 1991. Transport of incoming influenza virus nucleocapsids into the nucleus. *J Virol* 65: 232-244.
  17. Tarendeau, F., J. Boudet, D. Guilligay, P. J. Mas, C. M. Bougault, S. Boulo, F. Baudin, R. W. Ruigrok, N. Daigle, J. Ellenberg, S. Cusack, J. P. Simorre, and D. J. Hart. 2007. Structure and nuclear import function of the C-terminal domain of influenza virus polymerase PB2 subunit. *Nat Struct Mol Biol* 14: 229-233.
  18. Nath, S. T., and D. P. Nayak. 1990. Function of two discrete regions is required for nuclear localization of polymerase basic protein 1 of A/WSN/33 influenza virus (H1 N1). *Mol Cell Biol* 10: 4139-4145.
  19. Fodor, E., and M. Smith. 2004. The PA subunit is required for efficient nuclear accumulation of the PB1 subunit of the influenza A virus RNA polymerase complex. *J Virol* 78: 9144-9153.
  20. Neumann, G., M. R. Castrucci, and Y. Kawaoka. 1997. Nuclear import and export of influenza virus nucleoprotein. *J Virol* 71: 9690-9700.
  21. Engelhardt, O. G., M. Smith, and E. Fodor. 2005. Association of the influenza A virus RNA-dependent RNA polymerase with cellular RNA polymerase II. *J Virol* 79: 5812-5818.
  22. Plotch, S. J., M. Bouloy, I. Ulmanen, and R. M. Krug. 1981. A unique cap(m7GpppXm)-dependent influenza virion endonuclease cleaves capped RNAs to generate the primers that initiate viral RNA transcription. *Cell* 23: 847-858.
  23. Burgui, I., E. Yáñez, N. Sonenberg, and A. Nieto. 2007. Influenza virus mRNA translation revisited: is the eIF4E cap-binding factor required for viral mRNA translation? *J Virol* 81: 12427-12438.
  24. Iuliano, A. D., K. M. Roguski, H. H. Chang, D. J. Muscatello, R. Palekar, S. Tempia, C. Cohen, J. M. Gran, D. Schanzer, B. J. Cowling, P. Wu, J. Kyncl, L. W. Ang, M. Park, M. Redlberger-Fritz, H. Yu, L. Espenhain, A. Krishnan, G. Emukule, L. van Asten, S. Pereira da Silva, S. Aungkananon, U. Buchholz, M. A. Widdowson, and J. S. Bresee. 2018. Estimates of global seasonal influenza-associated respiratory mortality: a modelling study. *Lancet* 391: 1285-1300.
  25. Uyeki, T. M. 2021. Influenza. *Ann Intern Med* 174: ITC161-ITC176.
  26. Putri, W., D. J. Muscatello, M. S. Stockwell, and A. T. Newall. 2018. Economic burden of seasonal influenza in the United States. *Vaccine* 36: 3960-3966.
  27. Olsen, S. J., A. K. Winn, A. P. Budd, M. M. Prill, J. Steel, C. M. Midgley, K. Kniss, E. Burns, T. Rowe, A. Foust, G. Jasso, A. Merced-Morales, C. T. Davis, Y. Jang, J. Jones, P. Daly, L. Gubareva, J. Barnes, R. Kondor, W. Sessions, C. Smith, D. E.

- Wentworth, S. Garg, F. P. Havers, A. M. Fry, A. J. Hall, L. Brammer, and B. J. Silk. 2021. Changes in influenza and other respiratory virus activity during the COVID-19 pandemic-United States, 2020-2021. *Am J Transplant* 21: 3481-3486.
28. Johnson, N. P., and J. Mueller. 2002. Updating the accounts: global mortality of the 1918-1920 "Spanish" influenza pandemic. *Bull Hist Med* 76: 105-115.
  29. Smith, W., C. H. Andrewes, and P. P. Laidlaw. 1933. A virus obtained from influenza patients. *Lancet* 222: 66-68.
  30. Smorodintseff, A. A., M. D. Tushinsky, A. I. Drobyshevskaya, A. A. Korovin, and A. I. Osetroff. 1937. Investigation on volunteers infected with the influenza virus. *American Journal of Medical Sciences* 194: 159-170.
  31. Chen, R., and E. C. Holmes. 2006. Avian influenza virus exhibits rapid evolutionary dynamics. *Mol Biol Evol* 23: 2336-2341.
  32. Nobusawa, E., and K. Sato. 2006. Comparison of the mutation rates of human influenza A and B viruses. *J Virol* 80: 3675-3678.
  33. Kash, J. C., and J. K. Taubenberger. 2015. The role of viral, host, and secondary bacterial factors in influenza pathogenesis. *Am J Pathol* 185: 1528-1536.
  34. Gatherer, D. 2009. The 2009 H1N1 influenza outbreak in its historical context. *J Clin Virol* 45: 174-178.
  35. Dugan, V. G., R. Chen, D. J. Spiro, N. Sengamalay, J. Zaborsky, E. Ghedin, J. Nolting, D. E. Swayne, J. A. Runstadler, G. M. Happ, D. A. Senne, R. Wang, R. D. Slemons, E. C. Holmes, and J. K. Taubenberger. 2008. The evolutionary genetics and emergence of avian influenza viruses in wild birds. *PLoS Pathog* 4: e1000076.
  36. Dawood, F. S., S. Jain, L. Finelli, M. W. Shaw, S. Lindstrom, R. J. Garten, L. V. Gubareva, X. Xu, C. B. Bridges, and T. M. Uyeki. 2009. Emergence of a novel swine-origin influenza A (H1N1) virus in humans. *N Engl J Med* 360: 2605-2615.
  37. Wong, S. S., and R. J. Webby. 2013. Traditional and new influenza vaccines. *Clin Microbiol Rev* 26: 476-492.
  38. Kon, T. C., A. Onu, L. Berbecila, E. Lupulescu, A. Ghiorgisor, G. F. Kersten, Y. Q. Cui, J. P. Amorij, and L. Van der Pol. 2016. Influenza Vaccine Manufacturing: Effect of Inactivation, Splitting and Site of Manufacturing. Comparison of Influenza Vaccine Production Processes. *PLoS One* 11: e0150700.
  39. Zhang, N., B. J. Zheng, L. Lu, Y. Zhou, S. Jiang, and L. Du. 2015. Advancements in the development of subunit influenza vaccines. *Microbes Infect* 17: 123-134.
  40. Keitel, W. A., R. B. Couch, T. R. Cate, K. R. Hess, B. Baxter, J. M. Quarles, R. L. Atmar, and H. R. Six. 1994. High doses of purified influenza A virus hemagglutinin significantly augment serum and nasal secretion antibody responses in healthy young adults. *J Clin Microbiol* 32: 2468-2473.
  41. Cox, M. M., P. A. Patriarca, and J. Treanor. 2008. FluBlok, a recombinant hemagglutinin influenza vaccine. *Influenza Other Respir Viruses* 2: 211-219.
  42. Keitel, W. A., T. R. Cate, R. L. Atmar, C. S. Turner, D. Nino, C. M. Dukes, H. R. Six, and R. B. Couch. 1996. Increasing doses of purified influenza virus hemagglutinin

- and subvirion vaccines enhance antibody responses in the elderly. *Clin Diagn Lab Immunol* 3: 507-510.
43. Richards, K. A., S. Moritzky, I. Shannon, T. Fitzgerald, H. Yang, A. Branche, D. J. Topham, J. J. Treanor, J. Nayak, and A. J. Sant. 2020. Recombinant HA-based vaccine outperforms split and subunit vaccines in elicitation of influenza-specific CD4 T cells and CD4 T cell-dependent antibody responses in humans. *NPJ Vaccines* 5: 77.
  44. Minozzi, S., T. Lytras, S. Gianola, M. Gonzalez-Lorenzo, G. Castellini, C. Galli, D. Cereda, S. Bonovas, E. Pariani, and L. Moja. 2022. Comparative efficacy and safety of vaccines to prevent seasonal influenza: A systematic review and network meta-analysis. *EClinicalMedicine* 46: 101331.
  45. Tregoning, J. S., R. F. Russell, and E. Kinnear. 2018. Adjuvanted influenza vaccines. *Hum Vaccin Immunother* 14: 550-564.
  46. Fischetti, L., Z. Zhong, C. L. Pinder, J. S. Tregoning, and R. J. Shattock. 2017. The synergistic effects of combining TLR ligand based adjuvants on the cytokine response are dependent upon p38/JNK signalling. *Cytokine* 99: 287-296.
  47. Mosca, F., E. Tritto, A. Muzzi, E. Monaci, F. Bagnoli, C. Iavarone, D. O'Hagan, R. Rappuoli, and E. De Gregorio. 2008. Molecular and cellular signatures of human vaccine adjuvants. *Proc Natl Acad Sci U S A* 105: 10501-10506.
  48. Martinon, F., S. Krishnan, G. Lenzen, R. Magné, E. Gomar, J. G. Guillet, J. P. Lévy, and P. Meulien. 1993. Induction of virus-specific cytotoxic T lymphocytes in vivo by liposome-entrapped mRNA. *Eur J Immunol* 23: 1719-1722.
  49. Martins, K. A., J. T. Steffens, S. A. van Tongeren, J. B. Wells, A. A. Bergeron, S. P. Dickson, J. M. Dye, A. M. Salazar, and S. Bavari. 2014. Toll-like receptor agonist augments virus-like particle-mediated protection from Ebola virus with transient immune activation. *PLoS One* 9: e89735.
  50. Zabaleta, N., W. Dai, U. Bhatt, C. Hérate, P. Maisonnasse, J. A. Chichester, J. Sanmiguel, R. Estelien, K. T. Michalson, C. Diop, D. Maciorowski, N. Dereuddre-Bosquet, M. Cavarelli, A. S. Gallouët, T. Naninck, N. Kahlaoui, J. Lemaitre, W. Qi, E. Hudspeth, A. Cucalon, C. D. Dyer, M. B. Pampena, J. J. Knox, R. C. LaRocque, R. C. Charles, D. Li, M. Kim, A. Sheridan, N. Storm, R. I. Johnson, J. Feldman, B. M. Hauser, V. Contreras, R. Marlin, R. H. Tsong Fang, C. Chapon, S. van der Werf, E. Zinn, A. Ryan, D. T. Kobayashi, R. Chauhan, M. McGlynn, E. T. Ryan, A. G. Schmidt, B. Price, A. Honko, A. Griffiths, S. Yaghmour, R. Hodge, M. R. Betts, M. W. Freeman, J. M. Wilson, R. Le Grand, and L. H. Vandenberghe. 2021. An AAV-based, room-temperature-stable, single-dose COVID-19 vaccine provides durable immunogenicity and protection in non-human primates. *Cell Host Microbe* 29: 1437-1453.e1438.
  51. Mateus, J., J. M. Dan, Z. Zhang, C. Rydyznski Moderbacher, M. Lammers, B. Goodwin, A. Sette, S. Crotty, and D. Weiskopf. 2021. Low-dose mRNA-1273

- COVID-19 vaccine generates durable memory enhanced by cross-reactive T cells. *Science* 374: eabj9853.
52. Xia, J., Y. Kuang, J. Liang, M. Jones, and S. L. Swain. 2020. Influenza Vaccine-Induced CD4 Effectors Require Antigen Recognition at an Effector Checkpoint to Generate CD4 Lung Memory and Antibody Production. *J Immunol* 205: 2077-2090.
  53. Pardi, N., M. J. Hogan, M. S. Naradikian, K. Parkhouse, D. W. Cain, L. Jones, M. A. Moody, H. P. Verkerke, A. Myles, E. Willis, C. C. LaBranche, D. C. Montefiori, J. L. Lobby, K. O. Saunders, H. X. Liao, B. T. Korber, L. L. Sutherland, R. M. Scearce, P. T. Hraber, I. Tombácz, H. Muramatsu, H. Ni, D. A. Balikov, C. Li, B. L. Mui, Y. K. Tam, F. Krammer, K. Karikó, P. Polacino, L. C. Eisenlohr, T. D. Madden, M. J. Hope, M. G. Lewis, K. K. Lee, S. L. Hu, S. E. Hensley, M. P. Cancro, B. F. Haynes, and D. Weissman. 2018. Nucleoside-modified mRNA vaccines induce potent T follicular helper and germinal center B cell responses. *J Exp Med* 215: 1571-1588.
  54. Ndeupen, S., Z. Qin, S. Jacobsen, A. Bouteau, H. Estantbouli, and B. Z. Igyártó. 2021. The mRNA-LNP platform's lipid nanoparticle component used in preclinical vaccine studies is highly inflammatory. *iScience* 24: 103479.
  55. Iwasaki, A., and P. S. Pillai. 2014. Innate immunity to influenza virus infection. *Nat Rev Immunol* 14: 315-328.
  56. Pang, I. K., P. S. Pillai, and A. Iwasaki. 2013. Efficient influenza A virus replication in the respiratory tract requires signals from TLR7 and RIG-I. *Proc Natl Acad Sci U S A* 110: 13910-13915.
  57. Le Goffic, R., J. Pothlichet, D. Vitour, T. Fujita, E. Meurs, M. Chignard, and M. Si-Tahar. 2007. Cutting Edge: Influenza A virus activates TLR3-dependent inflammatory and RIG-I-dependent antiviral responses in human lung epithelial cells. *J Immunol* 178: 3368-3372.
  58. Lund, J. M., L. Alexopoulou, A. Sato, M. Karow, N. C. Adams, N. W. Gale, A. Iwasaki, and R. A. Flavell. 2004. Recognition of single-stranded RNA viruses by Toll-like receptor 7. *Proc Natl Acad Sci U S A* 101: 5598-5603.
  59. Diebold, S. S., T. Kaisho, H. Hemmi, S. Akira, and C. Reis e Sousa. 2004. Innate antiviral responses by means of TLR7-mediated recognition of single-stranded RNA. *Science* 303: 1529-1531.
  60. Heer, A. K., A. Shamshiev, A. Donda, S. Uematsu, S. Akira, M. Kopf, and B. J. Marsland. 2007. TLR signaling fine-tunes anti-influenza B cell responses without regulating effector T cell responses. *J Immunol* 178: 2182-2191.
  61. Hornung, V., J. Ellegast, S. Kim, K. Brzózka, A. Jung, H. Kato, H. Poeck, S. Akira, K. K. Conzelmann, M. Schlee, S. Endres, and G. Hartmann. 2006. 5'-Triphosphate RNA is the ligand for RIG-I. *Science* 314: 994-997.
  62. Rehwinkel, J., C. P. Tan, D. Goubau, O. Schulz, A. Pichlmair, K. Bier, N. Robb, F. Vreede, W. Barclay, E. Fodor, and C. Reis e Sousa. 2010. RIG-I detects viral genomic RNA during negative-strand RNA virus infection. *Cell* 140: 397-408.

63. Seth, R. B., L. Sun, C. K. Ea, and Z. J. Chen. 2005. Identification and characterization of MAVS, a mitochondrial antiviral signaling protein that activates NF-kappaB and IRF 3. *Cell* 122: 669-682.
64. Jiang, F., A. Ramanathan, M. T. Miller, G. Q. Tang, M. Gale, Jr., S. S. Patel, and J. Marcotrigiano. 2011. Structural basis of RNA recognition and activation by innate immune receptor RIG-I. *Nature* 479: 423-427.
65. Allen, I. C., M. A. Scull, C. B. Moore, E. K. Holl, E. McElvania-TeKippe, D. J. Taxman, E. H. Guthrie, R. J. Pickles, and J. P. Ting. 2009. The NLRP3 inflammasome mediates in vivo innate immunity to influenza A virus through recognition of viral RNA. *Immunity* 30: 556-565.
66. Ichinohe, T., I. K. Pang, and A. Iwasaki. 2010. Influenza virus activates inflammasomes via its intracellular M2 ion channel. *Nat Immunol* 11: 404-410.
67. McAuley, J. L., M. D. Tate, C. J. MacKenzie-Kludas, A. Pinar, W. Zeng, A. Stutz, E. Latz, L. E. Brown, and A. Mansell. 2013. Activation of the NLRP3 inflammasome by IAV virulence protein PB1-F2 contributes to severe pathophysiology and disease. *PLoS Pathog* 9: e1003392.
68. Seo, S. U., H. J. Kwon, J. H. Song, Y. H. Byun, B. L. Seong, T. Kawai, S. Akira, and M. N. Kweon. 2010. MyD88 signaling is indispensable for primary influenza A virus infection but dispensable for secondary infection. *J Virol* 84: 12713-12722.
69. Thomas, P. G., P. Dash, J. R. Aldridge, Jr., A. H. Ellebedy, C. Reynolds, A. J. Funk, W. J. Martin, M. Lamkanfi, R. J. Webby, K. L. Boyd, P. C. Doherty, and T. D. Kanneganti. 2009. The intracellular sensor NLRP3 mediates key innate and healing responses to influenza A virus via the regulation of caspase-1. *Immunity* 30: 566-575.
70. Denton, A. E., P. C. Doherty, S. J. Turner, and N. L. La Gruta. 2007. IL-18, but not IL-12, is required for optimal cytokine production by influenza virus-specific CD8+ T cells. *Eur J Immunol* 37: 368-375.
71. Koyama, S., K. J. Ishii, H. Kumar, T. Tanimoto, C. Coban, S. Uematsu, T. Kawai, and S. Akira. 2007. Differential role of TLR- and RLR-signaling in the immune responses to influenza A virus infection and vaccination. *J Immunol* 179: 4711-4720.
72. Geeraedts, F., N. Goutagny, V. Hornung, M. Severa, A. de Haan, J. Pool, J. Wilschut, K. A. Fitzgerald, and A. Huckriede. 2008. Superior immunogenicity of inactivated whole virus H5N1 influenza vaccine is primarily controlled by Toll-like receptor signalling. *PLoS Pathog* 4: e1000138.
73. Clingan, J. M., and M. Matloubian. 2013. B Cell-intrinsic TLR7 signaling is required for optimal B cell responses during chronic viral infection. *J Immunol* 191: 810-818.
74. Hashimoto, Y., T. Moki, T. Takizawa, A. Shiratsuchi, and Y. Nakanishi. 2007. Evidence for phagocytosis of influenza virus-infected, apoptotic cells by neutrophils and macrophages in mice. *J Immunol* 178: 2448-2457.

75. Ho, A. W., N. Prabhu, R. J. Betts, M. Q. Ge, X. Dai, P. E. Hutchinson, F. C. Lew, K. L. Wong, B. J. Hanson, P. A. Macary, and D. M. Kemeny. 2011. Lung CD103+ dendritic cells efficiently transport influenza virus to the lymph node and load viral antigen onto MHC class I for presentation to CD8 T cells. *J Immunol* 187: 6011-6021.
76. Eichelberger, M., W. Allan, M. Zijlstra, R. Jaenisch, and P. C. Doherty. 1991. Clearance of influenza virus respiratory infection in mice lacking class I major histocompatibility complex-restricted CD8+ T cells. *J Exp Med* 174: 875-880.
77. Tripp, R. A., S. R. Sarawar, and P. C. Doherty. 1995. Characteristics of the influenza virus-specific CD8+ T cell response in mice homozygous for disruption of the H-2IAb gene. *J Immunol* 155: 2955-2959.
78. Mozdzanowska, K., M. Furchner, G. Washko, J. Mozdzanowski, and W. Gerhard. 1997. A pulmonary influenza virus infection in SCID mice can be cured by treatment with hemagglutinin-specific antibodies that display very low virus-neutralizing activity in vitro. *J Virol* 71: 4347-4355.
79. Bender, B. S., T. Croghan, L. Zhang, and P. A. Small, Jr. 1992. Transgenic mice lacking class I major histocompatibility complex-restricted T cells have delayed viral clearance and increased mortality after influenza virus challenge. *J Exp Med* 175: 1143-1145.
80. Jenkins, M. R., J. A. Trapani, P. C. Doherty, and S. J. Turner. 2008. Granzyme K expressing cytotoxic T lymphocytes protects against influenza virus in granzyme AB-/- mice. *Viral Immunol* 21: 341-346.
81. Topham, D. J., and P. C. Doherty. 1998. Clearance of an influenza A virus by CD4+ T cells is inefficient in the absence of B cells. *J Virol* 72: 882-885.
82. Hargadon, K. M., H. Zhou, R. A. Albrecht, H. A. Dodd, A. García-Sastre, and T. J. Braciale. 2011. Major histocompatibility complex class II expression and hemagglutinin subtype influence the infectivity of type A influenza virus for respiratory dendritic cells. *J Virol* 85: 11955-11963.
83. Miller, M. A., A. P. Ganesan, N. Luckashenak, M. Mendonca, and L. C. Eisenlohr. 2015. Endogenous antigen processing drives the primary CD4+ T cell response to influenza. *Nat Med* 21: 1216-1222.
84. Belz, G. T., C. M. Smith, L. Kleinert, P. Reading, A. Brooks, K. Shortman, F. R. Carbone, and W. R. Heath. 2004. Distinct migrating and nonmigrating dendritic cell populations are involved in MHC class I-restricted antigen presentation after lung infection with virus. *Proc Natl Acad Sci U S A* 101: 8670-8675.
85. Nakano, H., K. L. Lin, M. Yanagita, C. Charbonneau, D. N. Cook, T. Kakiuchi, and M. D. Gunn. 2009. Blood-derived inflammatory dendritic cells in lymph nodes stimulate acute T helper type 1 immune responses. *Nat Immunol* 10: 394-402.
86. Kim, T. S., and T. J. Braciale. 2009. Respiratory dendritic cell subsets differ in their capacity to support the induction of virus-specific cytotoxic CD8+ T cell responses. *PLoS One* 4: e4204.

87. Ballesteros-Tato, A., B. León, F. E. Lund, and T. D. Randall. 2010. Temporal changes in dendritic cell subsets, cross-priming and costimulation via CD70 control CD8(+) T cell responses to influenza. *Nat Immunol* 11: 216-224.
88. Román, E., E. Miller, A. Harmsen, J. Wiley, U. H. Von Andrian, G. Huston, and S. L. Swain. 2002. CD4 effector T cell subsets in the response to influenza: heterogeneity, migration, and function. *J Exp Med* 196: 957-968.
89. Swain, S. L., R. W. Dutton, and D. L. Woodland. 2004. T Cell Responses to Influenza Virus Infection: Effector and Memory Cells. *Viral Immunology* 17: 197-209.
90. Powell, T. J., D. M. Brown, J. A. Hollenbaugh, T. Charbonneau, R. A. Kemp, S. L. Swain, and R. W. Dutton. 2004. CD8+ T cells responding to influenza infection reach and persist at higher numbers than CD4+ T cells independently of precursor frequency. *Clin Immunol* 113: 89-100.
91. Brown, D. M., S. Lee, L. Garcia-Hernandez Mde, and S. L. Swain. 2012. Multifunctional CD4 cells expressing gamma interferon and perforin mediate protection against lethal influenza virus infection. *J Virol* 86: 6792-6803.
92. Jelley-Gibbs, D. M., D. M. Brown, J. P. Dibble, L. Haynes, S. M. Eaton, and S. L. Swain. 2005. Unexpected prolonged presentation of influenza antigens promotes CD4 T cell memory generation. *J Exp Med* 202: 697-706.
93. Lukacher, A. E., V. L. Braciale, and T. J. Braciale. 1984. In vivo effector function of influenza virus-specific cytotoxic T lymphocyte clones is highly specific. *J Exp Med* 160: 814-826.
94. Topham, D. J., R. A. Tripp, and P. C. Doherty. 1997. CD8+ T cells clear influenza virus by perforin or Fas-dependent processes. *J Immunol* 159: 5197-5200.
95. Hamada, H., E. Bassity, A. Flies, T. M. Strutt, L. Garcia-Hernandez Mde, K. K. McKinstry, T. Zou, S. L. Swain, and R. W. Dutton. 2013. Multiple redundant effector mechanisms of CD8+ T cells protect against influenza infection. *J Immunol* 190: 296-306.
96. Marshall, N. B., A. M. Vong, P. Devarajan, M. D. Brauner, Y. Kuang, R. Nayar, E. A. Schutten, C. H. Castonguay, L. J. Berg, S. L. Nutt, and S. L. Swain. 2017. NKG2C/E Marks the Unique Cytotoxic CD4 T Cell Subset, ThCTL, Generated by Influenza Infection. *J Immunol* 198: 1142-1155.
97. Kamperschroer, C., J. P. Dibble, D. L. Meents, P. L. Schwartzberg, and S. L. Swain. 2006. SAP is required for Th cell function and for immunity to influenza. *J Immunol* 177: 5317-5327.
98. Devarajan, P., A. M. Vong, C. H. Castonguay, O. Kugler-Umana, B. L. Bautista, M. C. Jones, K. A. Kelly, J. Xia, and S. L. Swain. 2022. Strong influenza-induced TFH generation requires CD4 effectors to recognize antigen locally and receive signals from continuing infection. *Proc Natl Acad Sci USA* 119.
99. McKinstry, K. K., T. M. Strutt, A. Buck, J. D. Curtis, J. P. Dibble, G. Huston, M. Tighe, H. Hamada, S. Sell, R. W. Dutton, and S. L. Swain. 2009. IL-10 deficiency

- unleashes an influenza-specific Th17 response and enhances survival against high-dose challenge. *J Immunol* 182: 7353-7363.
100. Betts, R. J., N. Prabhu, A. W. Ho, F. C. Lew, P. E. Hutchinson, O. Rotzschke, P. A. Macary, and D. M. Kemeny. 2012. Influenza A virus infection results in a robust, antigen-responsive, and widely disseminated Foxp3<sup>+</sup> regulatory T cell response. *J Virol* 86: 2817-2825.
  101. Bedoya, F., G. S. Cheng, A. Leibow, N. Zakhary, K. Weissler, V. Garcia, M. Aitken, E. Kropf, D. S. Garlick, E. J. Wherry, J. Erikson, and A. J. Caton. 2013. Viral antigen induces differentiation of Foxp3<sup>+</sup> natural regulatory T cells in influenza virus-infected mice. *J Immunol* 190: 6115-6125.
  102. Belz, G. T., D. Wodarz, G. Diaz, M. A. Nowak, and P. C. Doherty. 2002. Compromised influenza virus-specific CD8(+)-T-cell memory in CD4(+)-T-cell-deficient mice. *J Virol* 76: 12388-12393.
  103. Sun, J., H. Dodd, E. K. Moser, R. Sharma, and T. J. Braciale. 2011. CD4<sup>+</sup> T cell help and innate-derived IL-27 induce Blimp-1-dependent IL-10 production by antiviral CTLs. *Nat Immunol* 12: 327-334.
  104. Ballesteros-Tato, A., B. León, F. E. Lund, and T. D. Randall. 2013. CD4<sup>+</sup> T helper cells use CD154-CD40 interactions to counteract T reg cell-mediated suppression of CD8<sup>+</sup> T cell responses to influenza. *J Exp Med* 210: 1591-1601.
  105. Dhume, K., C. M. Finn, T. M. Strutt, S. Sell, and K. K. McKinstry. 2019. T-bet optimizes CD4 T-cell responses against influenza through CXCR3-dependent lung trafficking but not functional programming. *Mucosal Immunol* 12: 1220-1230.
  106. McKinstry, K. K., S. Golech, W. H. Lee, G. Huston, N. P. Weng, and S. L. Swain. 2007. Rapid default transition of CD4 T cell effectors to functional memory cells. *J Exp Med* 204: 2199-2211.
  107. Weinstein, J. S., E. I. Herman, B. Lainez, P. Licona-Limón, E. Esplugues, R. Flavell, and J. Craft. 2016. TFH cells progressively differentiate to regulate the germinal center response. *Nat Immunol* 17: 1197-1205.
  108. Yusuf, I., R. Kageyama, L. Monticelli, R. J. Johnston, D. Ditoro, K. Hansen, B. Barnett, and S. Crotty. 2010. Germinal center T follicular helper cell IL-4 production is dependent on signaling lymphocytic activation molecule receptor (CD150). *J Immunol* 185: 190-202.
  109. Zhang, J., T. Bárdos, Q. Shao, J. Tschopp, K. Mikecz, T. T. Glant, and A. Finnegan. 2003. IL-4 potentiates activated T cell apoptosis via an IL-2-dependent mechanism. *J Immunol* 170: 3495-3503.
  110. Lenardo, M. J. 1991. Interleukin-2 programs mouse alpha beta T lymphocytes for apoptosis. *Nature* 353: 858-861.
  111. Stranges, P. B., J. Watson, C. J. Cooper, C. M. Choisy-Rossi, A. C. Stonebraker, R. A. Beighton, H. Hartig, J. P. Sundberg, S. Servick, G. Kaufmann, P. J. Fink, and A. V. Chervonsky. 2007. Elimination of antigen-presenting cells and autoreactive T cells by Fas contributes to prevention of autoimmunity. *Immunity* 26: 629-641.

112. Nguyen, L. T., K. McKall-Faienza, A. Zakarian, D. E. Speiser, T. W. Mak, and P. S. Ohashi. 2000. TNF receptor 1 (TNFR1) and CD95 are not required for T cell deletion after virus infection but contribute to peptide-induced deletion under limited conditions. *Eur J Immunol* 30: 683-688.
113. Lohman, B. L., E. S. Razvi, and R. M. Welsh. 1996. T-lymphocyte downregulation after acute viral infection is not dependent on CD95 (Fas) receptor-ligand interactions. *J Virol* 70: 8199-8203.
114. Zhou, S., R. Ou, L. Huang, and D. Moskophidis. 2002. Critical role for perforin-, Fas/FasL-, and TNFR1-mediated cytotoxic pathways in down-regulation of antigen-specific T cells during persistent viral infection. *J Virol* 76: 829-840.
115. Bonfoco, E., P. M. Stuart, T. Brunner, T. Lin, T. S. Griffith, Y. Gao, H. Nakajima, P. A. Henkart, T. A. Ferguson, and D. R. Green. 1998. Inducible nonlymphoid expression of Fas ligand is responsible for superantigen-induced peripheral deletion of T cells. *Immunity* 9: 711-720.
116. Hale, J. S., B. Youngblood, D. R. Latner, A. U. Mohammed, L. Ye, R. S. Akondy, T. Wu, S. S. Iyer, and R. Ahmed. 2013. Distinct memory CD4+ T cells with commitment to T follicular helper- and T helper 1-cell lineages are generated after acute viral infection. *Immunity* 38: 805-817.
117. Russ, B. E., M. Olshanksy, H. S. Smallwood, J. Li, A. E. Denton, J. E. Prier, A. T. Stock, H. A. Croom, J. G. Cullen, M. L. Nguyen, S. Rowe, M. R. Olson, D. B. Finkelstein, A. Kelso, P. G. Thomas, T. P. Speed, S. Rao, and S. J. Turner. 2014. Distinct epigenetic signatures delineate transcriptional programs during virus-specific CD8(+) T cell differentiation. *Immunity* 41: 853-865.
118. Yu, B., K. Zhang, J. J. Milner, C. Toma, R. Chen, J. P. Scott-Browne, R. M. Pereira, S. Crotty, J. T. Chang, M. E. Pipkin, W. Wang, and A. W. Goldrath. 2017. Epigenetic landscapes reveal transcription factors that regulate CD8(+) T cell differentiation. *Nat Immunol* 18: 573-582.
119. Bevington, S. L., R. Fiancette, D. W. Gajdasik, P. Keane, J. K. Soley, C. M. Willis, D. J. L. Coleman, D. R. Withers, and P. N. Cockerill. 2021. Stable Epigenetic Programming of Effector and Central Memory CD4 T Cells Occurs Within 7 Days of Antigen Exposure In Vivo. *Front Immunol* 12: 642807.
120. Swain, S. L., M. C. Jones, P. Devarajan, J. Xia, R. W. Dutton, T. M. Strutt, and K. K. McKinstry. 2021. Durable CD4 T-Cell Memory Generation Depends on Persistence of High Levels of Infection at an Effector Checkpoint that Determines Multiple Fates. *Cold Spring Harb Perspect Biol* 13.
121. Swain, S. L., K. K. McKinstry, and T. M. Strutt. 2012. Expanding roles for CD4(+) T cells in immunity to viruses. *Nat Rev Immunol* 12: 136-148.
122. Strutt, T. M., K. K. McKinstry, N. B. Marshall, A. M. Vong, R. W. Dutton, and S. L. Swain. 2013. Multipronged CD4(+) T-cell effector and memory responses cooperate to provide potent immunity against respiratory virus. *Immunol Rev* 255: 149-164.

123. Strutt, T. M., K. K. McKinstry, Y. Kuang, L. M. Bradley, and S. L. Swain. 2012. Memory CD4+ T-cell-mediated protection depends on secondary effectors that are distinct from and superior to primary effectors. *Proc Natl Acad Sci USA* 109: E2551-2560.
124. Strutt, T. M., K. K. McKinstry, J. P. Dibble, C. Winchell, Y. Kuang, J. D. Curtis, G. Huston, R. W. Dutton, and S. L. Swain. 2010. Memory CD4+ T cells induce innate responses independently of pathogen. *Nat Med* 16: 558-564, 551p following 564.
125. Sallusto, F., D. Lenig, R. Förster, M. Lipp, and A. Lanzavecchia. 1999. Two subsets of memory T lymphocytes with distinct homing potentials and effector functions. *Nature* 401: 708-712.
126. Zaph, C., J. Uzonna, S. M. Beverley, and P. Scott. 2004. Central memory T cells mediate long-term immunity to *Leishmania major* in the absence of persistent parasites. *Nat Med* 10: 1104-1110.
127. Reinhardt, R. L., A. Khoruts, R. Merica, T. Zell, and M. K. Jenkins. 2001. Visualizing the generation of memory CD4 T cells in the whole body. *Nature* 410: 101-105.
128. Unsoeld, H., S. Krautwald, D. Voehringer, U. Kunzendorf, and H. Pircher. 2002. Cutting edge: CCR7+ and CCR7- memory T cells do not differ in immediate effector cell function. *J Immunol* 169: 638-641.
129. Wolint, P., M. R. Betts, R. A. Koup, and A. Oxenius. 2004. Immediate cytotoxicity but not degranulation distinguishes effector and memory subsets of CD8+ T cells. *J Exp Med* 199: 925-936.
130. Wherry, E. J., V. Teichgräber, T. C. Becker, D. Masopust, S. M. Kaech, R. Antia, U. H. von Andrian, and R. Ahmed. 2003. Lineage relationship and protective immunity of memory CD8 T cell subsets. *Nat Immunol* 4: 225-234.
131. Masopust, D., V. Vezys, A. L. Marzo, and L. Lefrançois. 2001. Preferential localization of effector memory cells in nonlymphoid tissue. *Science* 291: 2413-2417.
132. Roberts, A. D., K. H. Ely, and D. L. Woodland. 2005. Differential contributions of central and effector memory T cells to recall responses. *J Exp Med* 202: 123-133.
133. Wherry, E. J., and R. Ahmed. 2004. Memory CD8 T-cell differentiation during viral infection. *J Virol* 78: 5535-5545.
134. Ibraghimov, A. R., and R. G. Lynch. 1994. T cell specialization at environmental interfaces: T cells from the lung and the female genital tract of *Ipr* and *gld* mice differ from their splenic and lymph node counterparts. *Eur J Immunol* 24: 1848-1852.
135. Sathaliyawala, T., M. Kubota, N. Yudanin, D. Turner, P. Camp, J. J. Thome, K. L. Bickham, H. Lerner, M. Goldstein, M. Sykes, T. Kato, and D. L. Farber. 2013. Distribution and compartmentalization of human circulating and tissue-resident memory T cell subsets. *Immunity* 38: 187-197.

136. Klonowski, K. D., K. J. Williams, A. L. Marzo, D. A. Blair, E. G. Lingenheld, and L. Lefrançois. 2004. Dynamics of blood-borne CD8 memory T cell migration in vivo. *Immunity* 20: 551-562.
137. Turner, D. L., K. L. Bickham, J. J. Thome, C. Y. Kim, F. D'Ovidio, E. J. Wherry, and D. L. Farber. 2014. Lung niches for the generation and maintenance of tissue-resident memory T cells. *Mucosal Immunol* 7: 501-510.
138. Teijaro, J. R., D. Turner, Q. Pham, E. J. Wherry, L. Lefrançois, and D. L. Farber. 2011. Cutting edge: Tissue-retentive lung memory CD4 T cells mediate optimal protection to respiratory virus infection. *J Immunol* 187: 5510-5514.
139. Gebhardt, T., L. M. Wakim, L. Eidsmo, P. C. Reading, W. R. Heath, and F. R. Carbone. 2009. Memory T cells in nonlymphoid tissue that provide enhanced local immunity during infection with herpes simplex virus. *Nat Immunol* 10: 524-530.
140. Iijima, N., and A. Iwasaki. 2014. T cell memory. A local macrophage chemokine network sustains protective tissue-resident memory CD4 T cells. *Science* 346: 93-98.
141. Jiang, X., R. A. Clark, L. Liu, A. J. Wagers, R. C. Fuhlbrigge, and T. S. Kupper. 2012. Skin infection generates non-migratory memory CD8+ T(RM) cells providing global skin immunity. *Nature* 483: 227-231.
142. Schenkel, J. M., K. A. Fraser, L. K. Beura, K. E. Pauken, V. Vezys, and D. Masopust. 2014. T cell memory. Resident memory CD8 T cells trigger protective innate and adaptive immune responses. *Science* 346: 98-101.
143. Strydom, G., A. Olive, A. F. Radovic-Moreno, D. Gondek, D. Alvarez, P. A. Basto, M. Perro, V. D. Vrbanc, A. M. Tager, J. Shi, J. A. Yethon, O. C. Farokhzad, R. Langer, M. N. Starnbach, and U. H. von Andrian. 2015. VACCINES. A mucosal vaccine against *Chlamydia trachomatis* generates two waves of protective memory T cells. *Science* 348: aaa8205.
144. Dijkman, K., N. Aguilo, C. Boot, S. O. Hofman, C. C. Sombroek, R. A. W. Vervenne, C. H. M. Kocken, D. Marinova, J. Thole, E. Rodríguez, M. P. M. Vierboom, K. G. Haanstra, E. Puentes, C. Martin, and F. A. W. Verreck. 2021. Pulmonary MTBVAC vaccination induces immune signatures previously correlated with prevention of tuberculosis infection. *Cell Rep Med* 2: 100187.
145. Glennie, N. D., V. A. Yeramilli, D. P. Beiting, S. W. Volk, C. T. Weaver, and P. Scott. 2015. Skin-resident memory CD4+ T cells enhance protection against *Leishmania major* infection. *J Exp Med* 212: 1405-1414.
146. Lakhani, S. A., A. Masud, K. Kuida, G. A. Porter, Jr., C. J. Booth, W. Z. Mehal, I. Inayat, and R. A. Flavell. 2006. Caspases 3 and 7: key mediators of mitochondrial events of apoptosis. *Science* 311: 847-851.
147. Kuida, K., T. S. Zheng, S. Na, C. Kuan, D. Yang, H. Karasuyama, P. Rakic, and R. A. Flavell. 1996. Decreased apoptosis in the brain and premature lethality in CPP32-deficient mice. *Nature* 384: 368-372.

148. Pellegrini, M., G. Belz, P. Bouillet, and A. Strasser. 2003. Shutdown of an acute T cell immune response to viral infection is mediated by the proapoptotic Bcl-2 homology 3-only protein Bim. *Proc Natl Acad Sci U S A* 100: 14175-14180.
149. Wojciechowski, S., M. B. Jordan, Y. Zhu, J. White, A. J. Zajac, and D. A. Hildeman. 2006. Bim mediates apoptosis of CD127(lo) effector T cells and limits T cell memory. *Eur J Immunol* 36: 1694-1706.
150. Petschner, F., C. Zimmerman, A. Strasser, D. Grillot, G. Nunez, and H. Pircher. 1998. Constitutive expression of Bcl-xL or Bcl-2 prevents peptide antigen-induced T cell deletion but does not influence T cell homeostasis after a viral infection. *Eur J Immunol* 28: 560-569.
151. Alam, A., L. Y. Cohen, S. Aouad, and R. P. Sékaly. 1999. Early activation of caspases during T lymphocyte stimulation results in selective substrate cleavage in nonapoptotic cells. *J Exp Med* 190: 1879-1890.
152. Doms, H., E. Kahn, B. Knoechel, and A. K. Abbas. 2004. IL-2 induces a competitive survival advantage in T lymphocytes. *J Immunol* 172: 5973-5979.
153. Marrack, P., J. Kappler, and T. Mitchell. 1999. Type I interferons keep activated T cells alive. *J Exp Med* 189: 521-530.
154. Curtsinger, J. M., C. S. Schmidt, A. Mondino, D. C. Lins, R. M. Kedl, M. K. Jenkins, and M. F. Mescher. 1999. Inflammatory cytokines provide a third signal for activation of naive CD4+ and CD8+ T cells. *J Immunol* 162: 3256-3262.
155. Kondrack, R. M., J. Harbertson, J. T. Tan, M. E. McBreen, C. D. Surh, and L. M. Bradley. 2003. Interleukin 7 regulates the survival and generation of memory CD4 cells. *J Exp Med* 198: 1797-1806.
156. Li, J., G. Huston, and S. L. Swain. 2003. IL-7 promotes the transition of CD4 effectors to persistent memory cells. *J Exp Med* 198: 1807-1815.
157. Schluns, K. S., W. C. Kieper, S. C. Jameson, and L. Lefrançois. 2000. Interleukin-7 mediates the homeostasis of naïve and memory CD8 T cells in vivo. *Nat Immunol* 1: 426-432.
158. Goldrath, A. W., P. V. Sivakumar, M. Glaccum, M. K. Kennedy, M. J. Bevan, C. Benoist, D. Mathis, and E. A. Butz. 2002. Cytokine requirements for acute and Basal homeostatic proliferation of naive and memory CD8+ T cells. *J Exp Med* 195: 1515-1522.
159. Hashimoto, M., S. J. Im, K. Araki, and R. Ahmed. 2019. Cytokine-Mediated Regulation of CD8 T-Cell Responses During Acute and Chronic Viral Infection. *Cold Spring Harbor Perspectives in Biology* 11.
160. Judge, A. D., X. Zhang, H. Fujii, C. D. Surh, and J. Sprent. 2002. Interleukin 15 controls both proliferation and survival of a subset of memory-phenotype CD8(+) T cells. *J Exp Med* 196: 935-946.
161. Becker, T. C., E. J. Wherry, D. Boone, K. Murali-Krishna, R. Antia, A. Ma, and R. Ahmed. 2002. Interleukin 15 is required for proliferative renewal of virus-specific memory CD8 T cells. *J Exp Med* 195: 1541-1548.

162. Tan, J. T., B. Ernst, W. C. Kieper, E. LeRoy, J. Sprent, and C. D. Surh. 2002. Interleukin (IL)-15 and IL-7 jointly regulate homeostatic proliferation of memory phenotype CD8<sup>+</sup> cells but are not required for memory phenotype CD4<sup>+</sup> cells. *J Exp Med* 195: 1523-1532.
163. Kaech, S. M., J. T. Tan, E. J. Wherry, B. T. Konieczny, C. D. Surh, and R. Ahmed. 2003. Selective expression of the interleukin 7 receptor identifies effector CD8 T cells that give rise to long-lived memory cells. *Nat Immunol* 4: 1191-1198.
164. Williams, M. A., and M. J. Bevan. 2004. Shortening the infectious period does not alter expansion of CD8 T cells but diminishes their capacity to differentiate into memory cells. *J Immunol* 173: 6694-6702.
165. Rabenstein, H., A. C. Behrendt, J. W. Ellwart, R. Naumann, M. Horsch, J. Beckers, and R. Obst. 2014. Differential kinetics of antigen dependency of CD4<sup>+</sup> and CD8<sup>+</sup> T cells. *J Immunol* 192: 3507-3517.
166. Prlic, M., G. Hernandez-Hoyos, and M. J. Bevan. 2006. Duration of the initial TCR stimulus controls the magnitude but not functionality of the CD8<sup>+</sup> T cell response. *J Exp Med* 203: 2135-2143.
167. Zehn, D., S. Y. Lee, and M. J. Bevan. 2009. Complete but curtailed T-cell response to very low-affinity antigen. *Nature* 458: 211-214.
168. Obst, R., H.-M. van Santen, D. Mathis, and C. Benoist. 2005. Antigen persistence is required throughout the expansion phase of a CD4<sup>+</sup> T cell response. *J Exp Med* 201: 1555-1565.
169. Corse, E., R. A. Gottschalk, and J. P. Allison. 2011. Strength of TCR–Peptide/MHC Interactions and In Vivo T Cell Responses. *J Immunol* 186: 5039-5045.
170. Hosken, B. N. A., K. Shibuya, A. W. Heath, K. M. Murphy, and A. O. Garra. 1995. The effect of antigen dose on CD4<sup>+</sup> T helper cell phenotype development in a T cell receptor-alpha beta-transgenic model. *J Exp Med* 182: 1579-1584.
171. Brogdon, J. L., D. Leitenberg, and K. Bottomly. 2002. The Potency of TCR Signaling Differentially Regulates NFATc/p Activity and Early IL-4 Transcription in Naive CD4<sup>+</sup> T Cells. *J Immunol* 168: 3825-3832.
172. Constant, B. S., C. Pfeiffer, A. Woodard, T. Pasqualini, and K. Bottomly. 1995. Extent of T cell receptor ligation can determine the functional differentiation of naive CD4<sup>+</sup> T cells. *J Exp Med* 182: 1591-1596.
173. Tubo, N. J., A. J. Pagán, J. J. Taylor, R. W. Nelson, J. L. Linehan, J. M. Ertelt, E. S. Huseby, S. S. Way, and M. K. Jenkins. 2013. Single Naive CD4<sup>+</sup> T Cells from a Diverse Repertoire Produce Different Effector Cell Types during Infection. *Cell* 153: 785-796.
174. Fazilleau, N., L. J. McHeyzer-Williams, H. Rosen, and M. G. McHeyzer-Williams. 2009. The function of follicular helper T cells is regulated by the strength of T cell antigen receptor binding. *Nat Immunol* 10: 375.

175. Baumjohann, D., S. Preite, A. Reboldi, F. Ronchi, K. M. Ansel, A. Lanzavecchia, and F. Sallusto. 2013. Persistent antigen and germinal center B cells sustain T follicular helper cell responses and phenotype. *Immunity* 38: 596-605.
176. Kotov, D. I., J. S. Mitchell, T. Pengo, C. Ruedl, S. S. Way, R. A. Langlois, B. T. Fife, and M. K. Jenkins. 2019. TCR Affinity Biases Th Cell Differentiation by Regulating CD25, Eef1e1, and Gbp2. *J Immunol* 202: 2535-2545.
177. Keck, S., M. Schmalzer, S. Ganter, L. Wyss, S. Oberle, E. S. Huseby, D. Zehn, and C. G. King. 2014. Antigen affinity and antigen dose exert distinct influences on CD4 T-cell differentiation. *Proc Natl Acad Sci USA* 111: 14852-14857.
178. Ploquin, M. J., U. Eksmond, and G. Kassiotis. 2011. B cells and TCR avidity determine distinct functions of CD4+ T cells in retroviral infection. *J Immunol* 187: 3321-3330.
179. Khatun, A., M. Y. Kasmani, R. Zander, D. M. Schauder, J. P. Snook, J. Shen, X. Wu, R. Burns, Y. G. Chen, C. W. Lin, M. A. Williams, and W. Cui. 2021. Single-cell lineage mapping of a diverse virus-specific naive CD4 T cell repertoire. *J Exp Med* 218.
180. Vanguri, V., C. C. Govern, R. Smith, and E. S. Huseby. 2013. Viral antigen density and confinement time regulate the reactivity pattern of CD4 T-cell responses to vaccinia virus infection. *Proc Natl Acad Sci USA* 110: 288-293.
181. Persaud, S. P., C. R. Parker, W. L. Lo, K. S. Weber, and P. M. Allen. 2014. Intrinsic CD4+ T cell sensitivity and response to a pathogen are set and sustained by avidity for thymic and peripheral complexes of self peptide and MHC. *Nat Immunol* 15: 266-274.
182. Bartleson, J. M., A. A. Viehmann Milam, D. L. Donermeyer, S. Horvath, Y. Xia, T. Egawa, and P. M. Allen. 2020. Strength of tonic T cell receptor signaling instructs T follicular helper cell-fate decisions. *Nat Immunol* 21: 1384-1396.
183. Devarajan, P., A. M. Vong, C. H. Castonguay, B. L. Bautista, M. C. Jones, O. Kugler-Umana, K. A. Kelly, and S. L. Swain. 2020. CD4 Effectors Need to Recognize Antigen Locally to Become Cytotoxic CD4 and Follicular Helper T Cells. *bioRxiv*.
184. Stemberger, C., K. M. Huster, M. Koffler, F. Anderl, M. Schiemann, H. Wagner, and D. H. Busch. 2007. A single naive CD8+ T cell precursor can develop into diverse effector and memory subsets. *Immunity* 27: 985-997.
185. Gerlach, C., J. W. van Heijst, E. Swart, D. Sie, N. Armstrong, R. M. Kerkhoven, D. Zehn, M. J. Bevan, K. Schepers, and T. N. Schumacher. 2010. One naive T cell, multiple fates in CD8+ T cell differentiation. *J Exp Med* 207: 1235-1246.
186. Cho, Y. L., M. Flossdorf, L. Kretschmer, T. Hofer, D. H. Busch, and V. R. Buchholz. 2017. TCR Signal Quality Modulates Fate Decisions of Single CD4(+) T Cells in a Probabilistic Manner. *Cell Rep* 20: 806-818.
187. Weber, K. S., Q. J. Li, S. P. Persaud, J. D. Campbell, M. M. Davis, and P. M. Allen. 2012. Distinct CD4+ helper T cells involved in primary and secondary responses to infection. *Proc Natl Acad Sci U S A* 109: 9511-9516.

188. Badovinac, V. P., B. B. Porter, and J. T. Harty. 2002. Programmed contraction of CD8(+) T cells after infection. *Nat Immunol* 3: 619-626.
189. Badovinac, V. P., B. B. Porter, and J. T. Harty. 2004. CD8+ T cell contraction is controlled by early inflammation. *Nat Immunol* 5: 809-817.
190. Slifka, M. K., and J. L. Whitton. 2001. Functional avidity maturation of CD8(+) T cells without selection of higher affinity TCR. *Nat Immunol* 2: 711-717.
191. Busch, D. H., and E. G. Pamer. 1999. T cell affinity maturation by selective expansion during infection. *J Exp Med* 189: 701-709.
192. Masopust, D., S. J. Ha, V. Vezys, and R. Ahmed. 2006. Stimulation history dictates memory CD8 T cell phenotype: implications for prime-boost vaccination. *J Immunol* 177: 831-839.
193. Fiege, J. K., I. A. Stone, E. J. Fay, M. W. Markman, S. Wijeyesinghe, M. G. Macchietto, S. Shen, D. Masopust, and R. A. Langlois. 2019. The Impact of TCR Signal Strength on Resident Memory T Cell Formation during Influenza Virus Infection. *J Immunol* 203: 936-945.
194. León, B., A. Ballesteros-Tato, T. D. Randall, and F. E. Lund. 2014. Prolonged antigen presentation by immune complex-binding dendritic cells programs the proliferative capacity of memory CD8 T cells. *J Exp Med* 211: 1637-1655.
195. Ballesteros-Tato, A., B. Leon, B. O. Lee, F. E. Lund, and T. D. Randall. 2014. Epitope-specific regulation of memory programming by differential duration of antigen presentation to influenza-specific CD8(+) T cells. *Immunity* 41: 127-140.
196. Williams, M. A., E. V. Ravkov, and M. J. Bevan. 2008. Rapid culling of the CD4+ T cell repertoire in the transition from effector to memory. *Immunity* 28: 533-545.
197. Snook, J. P., C. Kim, and M. A. Williams. 2018. TCR signal strength controls the differentiation of CD4+ effector and memory T cells. *Sci Immunol* 3: 1-13.
198. Johnston, R. J., Y. S. Choi, J. A. Diamond, J. A. Yang, and S. Crotty. 2012. STAT5 is a potent negative regulator of TFH cell differentiation. *J Exp Med* 209: 243-250.
199. Powell, T. J., T. Strutt, J. Reome, J. A. Hollenbaugh, A. D. Roberts, D. L. Woodland, S. L. Swain, and R. W. Dutton. 2007. Priming with cold-adapted influenza A does not prevent infection but elicits long-lived protection against supralethal challenge with heterosubtypic virus. *J Immunol* 178: 1030-1038.
200. Bautista, B. L., P. Devarajan, K. K. McKinstry, T. M. Strutt, A. M. Vong, M. C. Jones, Y. Kuang, D. Mott, and S. L. Swain. 2016. Short-Lived Antigen Recognition but Not Viral Infection at a Defined Checkpoint Programs Effector CD4 T Cells To Become Protective Memory. *J Immunol* 197: 3936-3949.
201. McKinstry, K. K., T. M. Strutt, B. Bautista, W. Zhang, Y. Kuang, A. M. Cooper, and S. L. Swain. 2014. Effector CD4 T-cell transition to memory requires late cognate interactions that induce autocrine IL-2. *Nat Commun* 5: 5377.
202. Zhang, B. X., L. Giangreco, H. E. Broome, C. M. Dargan, and S. L. Swain. 1995. Control of CD4 effector fate: transforming growth factor beta 1 and interleukin 2

- synergize to prevent apoptosis and promote effector expansion. *J Exp Med* 182: 699-709.
203. Moran, A. E., K. L. Holzapfel, Y. Xing, N. R. Cunningham, J. S. Maltzman, J. Punt, and K. A. Hogquist. 2011. T cell receptor signal strength in Treg and iNKT cell development demonstrated by a novel fluorescent reporter mouse. *J Exp Med* 208: 1279-1289.
  204. Stadinski, B. D., P. Trenh, R. L. Smith, B. Bautista, P. G. Huseby, G. Li, L. J. Stern, and E. S. Huseby. 2011. A role for differential variable gene pairing in creating T cell receptors specific for unique major histocompatibility ligands. *Immunity* 35: 694-704.
  205. Huseby, E. S., B. Sather, P. G. Huseby, and J. Goverman. 2001. Age-dependent T cell tolerance and autoimmunity to myelin basic protein. *Immunity* 14: 471-481.
  206. Zhumabekov, T., P. Corbella, M. Tolaini, and D. Kioussis. 1995. Improved version of a human CD2 minigene based vector for T cell-specific expression in transgenic mice. *Journal of Immunological Methods* 185: 133-140.
  207. Brahmakshatriya, V., Y. Kuang, P. Devarajan, J. Xia, W. Zhang, A. M. Vong, and S. L. Swain. 2017. IL-6 Production by TLR-Activated APC Broadly Enhances Aged Cognate CD4 Helper and B Cell Antibody Responses In Vivo. *J Immunol* 198: 2819-2833.
  208. McKinstry, K. K., T. M. Strutt, and S. L. Swain. 2010. Regulation of CD4+ T-cell contraction during pathogen challenge. *Immunological Reviews* 236: 110-124.
  209. Nanaware, P. P., M. M. Jurewicz, C. C. Clement, L. Lu, L. Santambrogio, and L. J. Stern. 2021. Distinguishing Signal From Noise in Immunopeptidome Studies of Limiting-Abundance Biological Samples: Peptides Presented by I-A(b) in C57BL/6 Mouse Thymus. *Front Immunol* 12: 658601.
  210. Itoh, Y., K. Kajino, K. Ogasawara, A. Takahashi, K. Namba, I. Negishi, N. Matsuki, K. Iwabuchi, M. Kakinuma, R. A. Good, and K. Onoé. 1997. Interaction of pigeon cytochrome c-(43-58) peptide analogs with either T cell antigen receptor or I-Ab molecule. *Proc Natl Acad Sci U S A* 94: 12047-12052.
  211. Zhu, Y., A. Y. Rudensky, A. L. Corper, L. Teyton, and I. A. Wilson. 2003. Crystal structure of MHC class II I-Ab in complex with a human CLIP peptide: prediction of an I-Ab peptide-binding motif. *J Mol Biol* 326: 1157-1174.
  212. Groom, J. R., and A. D. Luster. 2011. CXCR3 ligands: redundant, collaborative and antagonistic functions. *Immunol Cell Biol* 89: 207-215.
  213. Kohlmeier, J. E., T. Cookenham, S. C. Miller, A. D. Roberts, J. P. Christensen, A. R. Thomsen, and D. L. Woodland. 2009. CXCR3 directs antigen-specific effector CD4+ T cell migration to the lung during parainfluenza virus infection. *J Immunol* 183: 4378-4384.
  214. Groom, J. R., J. Richmond, T. T. Murooka, E. W. Sorensen, J. H. Sung, K. Bankert, U. H. von Andrian, J. J. Moon, T. R. Mempel, and A. D. Luster. 2012. CXCR3

- chemokine receptor-ligand interactions in the lymph node optimize CD4+ T helper 1 cell differentiation. *Immunity* 37: 1091-1103.
215. Conley, J. M., M. P. Gallagher, and L. J. Berg. 2016. T Cells and Gene Regulation: The Switching On and Turning Up of Genes after T Cell Receptor Stimulation in CD8 T Cells. *Front Immunol* 7: 76.
  216. Bradly, L. M., D. D. Duncan, S. Tonkonogy, and S. L. Swain. 1991. Characterization of antigen-specific CD4+ effector T cells in vivo: immunization results in a transient population of MEL-14-, CD45RB- helper cells that secretes interleukin 2 (IL-2), IL-3, IL-4, and interferon gamma. *J Exp Med* 174: 547-559.
  217. Lodolce, J. P., P. R. Burkett, D. L. Boone, M. Chien, and A. Ma. 2001. T cell-independent interleukin 15R $\alpha$  signals are required for bystander proliferation. *J Exp Med* 194: 1187-1193.
  218. Dubois, S., J. Mariner, T. A. Waldmann, and Y. Tagaya. 2002. IL-15R $\alpha$  Recycles and Presents IL-15 In trans to Neighboring Cells. *Immunity* 17: 537-547.
  219. Stonier, S. W., and K. S. Schluns. 2010. Trans-presentation: a novel mechanism regulating IL-15 delivery and responses. *Immunol Lett* 127: 85-92.
  220. Wuest, S. C., J. H. Edwan, J. F. Martin, S. Han, J. S. Perry, C. M. Cartagena, E. Matsuura, D. Maric, T. A. Waldmann, and B. Bielekova. 2011. A role for interleukin-2 trans-presentation in dendritic cell-mediated T cell activation in humans, as revealed by daclizumab therapy. *Nat Med* 17: 604-609.
  221. Eicher, D. M., and T. A. Waldmann. 1998. IL-2R $\alpha$  on one cell can present IL-2 to IL-2R $\beta$ / $\gamma$ c on another cell to augment IL-2 signaling. *J Immunol* 161: 5430-5437.
  222. Kim, M., T. J. Kim, H. M. Kim, J. Doh, and K. M. Lee. 2017. Multi-cellular natural killer (NK) cell clusters enhance NK cell activation through localizing IL-2 within the cluster. *Sci Rep* 7: 40623.
  223. Dubey, C., M. Croft, and S. L. Swain. 1995. Costimulatory requirements of naive CD4+ T cells. ICAM-1 or B7-1 can costimulate naive CD4 T cell activation but both are required for optimum response. *J Immunol* 155: 45-57.
  224. Beura, L. K., S. E. Hamilton, K. Bi, J. M. Schenkel, O. A. Odumade, K. A. Casey, E. A. Thompson, K. A. Fraser, P. C. Rosato, A. Filali-Mouhim, R. P. Sekaly, M. K. Jenkins, V. Vezys, W. N. Haining, S. C. Jameson, and D. Masopust. 2016. Normalizing the environment recapitulates adult human immune traits in laboratory mice. *Nature* 532: 512-516.
  225. Reese, T. A., K. Bi, A. Kambal, A. Filali-Mouhim, L. K. Beura, M. C. Burger, B. Pulendran, R. P. Sekaly, S. C. Jameson, D. Masopust, W. N. Haining, and H. W. Virgin. 2016. Sequential Infection with Common Pathogens Promotes Human-like Immune Gene Expression and Altered Vaccine Response. *Cell Host Microbe* 19: 713-719.
  226. Herati, R. S., A. Muselman, L. Vella, B. Bengsch, K. Parkhouse, D. Del Alcazar, J. Kotzin, S. A. Doyle, P. Tebas, S. E. Hensley, L. F. Su, K. E. Schmader, and E. J. Wherry. 2017. Successive annual influenza vaccination induces a recurrent

- oligoclonotypic memory response in circulating T follicular helper cells. *Sci Immunol* 2.
227. Joshi, N. S., W. Cui, A. Chandele, H. K. Lee, D. R. Urso, J. Hagman, L. Gapin, and S. M. Kaech. 2007. Inflammation directs memory precursor and short-lived effector CD8(+) T cell fates via the graded expression of T-bet transcription factor. *Immunity* 27: 281-295.
  228. Kaech, S. M., and E. J. Wherry. 2007. Heterogeneity and cell-fate decisions in effector and memory CD8+ T cell differentiation during viral infection. *Immunity* 27: 393-405.
  229. Devarajan, P., B. Bautista, A. M. Vong, K. K. McKinstry, T. M. Strutt, and S. L. Swain. 2016. New Insights into the Generation of CD4 Memory May Shape Future Vaccine Strategies for Influenza. *Frontiers in Immunology* 7.
  230. Kim, C., T. Wilson, K. F. Fischer, and M. A. Williams. 2013. Sustained interactions between T cell receptors and antigens promote the differentiation of CD4(+) memory T cells. *Immunity* 39: 508-520.
  231. Blattman, J. N., R. Antia, D. J. Sourdive, X. Wang, S. M. Kaech, K. Murali-Krishna, J. D. Altman, and R. Ahmed. 2002. Estimating the precursor frequency of naive antigen-specific CD8 T cells. *J Exp Med* 195: 657-664.
  232. Jenkins, M. K., and J. J. Moon. 2012. The role of naive T cell precursor frequency and recruitment in dictating immune response magnitude. *J Immunol* 188: 4135-4140.
  233. Geiger, R., T. Duhon, A. Lanzavecchia, and F. Sallusto. 2009. Human naive and memory CD4+ T cell repertoires specific for naturally processed antigens analyzed using libraries of amplified T cells. *J Exp Med* 206: 1525-1534.
  234. Wang, S., T. Q. Le, N. Kurihara, J. Chida, Y. Cisse, M. Yano, and H. Kido. 2010. Influenza virus-cytokine-protease cycle in the pathogenesis of vascular hyperpermeability in severe influenza. *J Infect Dis* 202: 991-1001.
  235. Xu, L., H. Yoon, M. Q. Zhao, J. Liu, C. V. Ramana, and R. I. Enelow. 2004. Cutting edge: pulmonary immunopathology mediated by antigen-specific expression of TNF-alpha by antiviral CD8+ T cells. *J Immunol* 173: 721-725.
  236. DeBerge, M. P., K. H. Ely, G. S. Cheng, and R. I. Enelow. 2013. ADAM17-mediated processing of TNF- $\alpha$  expressed by antiviral effector CD8+ T cells is required for severe T-cell-mediated lung injury. *PLoS One* 8: e79340.
  237. Liu, A. N., A. Z. Mohammed, W. R. Rice, D. T. Fiedeldej, J. S. Liebermann, J. A. Whitsett, T. J. Braciale, and R. I. Enelow. 1999. Perforin-independent CD8(+) T-cell-mediated cytotoxicity of alveolar epithelial cells is preferentially mediated by tumor necrosis factor-alpha: relative insensitivity to Fas ligand. *Am J Respir Cell Mol Biol* 20: 849-858.
  238. van de Sandt, C. E., M. Bárcena, A. J. Koster, J. Kasper, C. J. Kirkpatrick, D. P. Scott, R. D. de Vries, S. Herold, G. F. Rimmelzwaan, T. Kuiken, and K. R. Short.

2017. Human CD8(+) T Cells Damage Noninfected Epithelial Cells during Influenza Virus Infection In Vitro. *Am J Respir Cell Mol Biol* 57: 536-546.
239. Srikiatkachorn, A., J. Chintapalli, J. Liu, M. Jamaluddin, K. S. Harrod, J. A. Whitsett, R. I. Enelow, and C. V. Ramana. 2010. Interference with intraepithelial TNF- $\alpha$  signaling inhibits CD8(+) T-cell-mediated lung injury in influenza infection. *Viral Immunol* 23: 639-645.
240. Teshigawara, K., H. M. Wang, K. Kato, and K. A. Smith. 1987. Interleukin 2 high-affinity receptor expression requires two distinct binding proteins. *J Exp Med* 165: 223-238.
241. Myszka, D. G., P. R. Arulanantham, T. Sana, Z. Wu, T. A. Morton, and T. L. Ciardelli. 1996. Kinetic analysis of ligand binding to interleukin-2 receptor complexes created on an optical biosensor surface. *Protein Sci* 5: 2468-2478.
242. Damjanovich, S., L. Bene, J. Matkó, A. Alileche, C. K. Goldman, S. Sharrow, and T. A. Waldmann. 1997. Preassembly of interleukin 2 (IL-2) receptor subunits on resting Kit 225 K6 T cells and their modulation by IL-2, IL-7, and IL-15: a fluorescence resonance energy transfer study. *Proc Natl Acad Sci U S A* 94: 13134-13139.
243. Takeshita, T., H. Asao, K. Ohtani, N. Ishii, S. Kumaki, N. Tanaka, H. Munakata, M. Nakamura, and K. Sugamura. 1992. Cloning of the gamma chain of the human IL-2 receptor. *Science* 257: 379-382.
244. Nakamura, Y., S. M. Russell, S. A. Mess, M. Friedmann, M. Erdos, C. Francois, Y. Jacques, S. Adelstein, and W. J. Leonard. 1994. Heterodimerization of the IL-2 receptor beta- and gamma-chain cytoplasmic domains is required for signalling. *Nature* 369: 330-333.
245. Nelson, B. H., J. D. Lord, and P. D. Greenberg. 1994. Cytoplasmic domains of the interleukin-2 receptor beta and gamma chains mediate the signal for T-cell proliferation. *Nature* 369: 333-336.
246. Ross, S. H., and D. A. Cantrell. 2018. Signaling and Function of Interleukin-2 in T Lymphocytes. *Annu Rev Immunol* 36: 411-433.
247. Wang, X., M. Rickert, and K. C. Garcia. 2005. Structure of the quaternary complex of interleukin-2 with its alpha, beta, and gammac receptors. *Science* 310: 1159-1163.
248. Stauber, D. J., E. W. Debler, P. A. Horton, K. A. Smith, and I. A. Wilson. 2006. Crystal structure of the IL-2 signaling complex: paradigm for a heterotrimeric cytokine receptor. *Proc Natl Acad Sci U S A* 103: 2788-2793.
249. Giri, J. G., S. Kumaki, M. Ahdieh, D. J. Friend, A. Loomis, K. Shanebeck, R. DuBose, D. Cosman, L. S. Park, and D. M. Anderson. 1995. Identification and cloning of a novel IL-15 binding protein that is structurally related to the alpha chain of the IL-2 receptor. *Embo j* 14: 3654-3663.
250. Anderson, D. M., S. Kumaki, M. Ahdieh, J. Bertles, M. Tometsko, A. Loomis, J. Giri, N. G. Copeland, D. J. Gilbert, N. A. Jenkins, and et al. 1995. Functional

- characterization of the human interleukin-15 receptor alpha chain and close linkage of IL15RA and IL2RA genes. *J Biol Chem* 270: 29862-29869.
251. Bernard, J., C. Harb, E. Mortier, A. Quéméner, R. H. Meloen, C. Vermot-Desroches, J. Wijdeness, P. van Dijken, J. Grötzinger, J. W. Sloatstra, A. Plet, and Y. Jacques. 2004. Identification of an interleukin-15alpha receptor-binding site on human interleukin-15. *J Biol Chem* 279: 24313-24322.
  252. Mortier, E., A. Quéméner, P. Vusio, I. Lorenzen, Y. Boublik, J. Grötzinger, A. Plet, and Y. Jacques. 2006. Soluble interleukin-15 receptor alpha (IL-15R alpha)-sushi as a selective and potent agonist of IL-15 action through IL-15R beta/gamma. Hyperagonist IL-15 x IL-15R alpha fusion proteins. *J Biol Chem* 281: 1612-1619.
  253. Eisenman, J., M. Ahdieh, C. Beers, K. Brasel, M. K. Kennedy, T. Le, T. P. Bonnert, R. J. Paxton, and L. S. Park. 2002. Interleukin-15 interactions with interleukin-15 receptor complexes: characterization and species specificity. *Cytokine* 20: 121-129.
  254. Li, J., E. Lu, T. Yi, and J. G. Cyster. 2016. EB12 augments Tfh cell fate by promoting interaction with IL-2-quenching dendritic cells. *Nature* 533: 110-114.